Geology and Geohydrology of the East Texas Basin

A Report on the Progress of Nuclear Waste Isolation Feasibility Studies (1979)

C. W. Kreitler, O. K. Agagu, J. M. Basciano, E. W. Collins, O. Dix, S. P. Dutton, G. E. Fogg, A. B. Giles, E. H. Guevara, D. W. Harris, D. K. Hobday, M. K. McGowen, D. Pass, and D. H. Wood

1980

Geological Circular 80-12

GEOLOGY AND GEOHYDROLOGY OF THE EAST TEXAS BASIN

A Report on the Progress of Nuclear Waste Isolation
Feasibility Studies (1979)

by

C. W. Kreitler, O. K. Agagu, J. M. Basciano,
E. W. Collins, O. Dix, S. P. Dutton, G. E. Fogg,
A. B. Giles, E. H. Guevara, D. W. Harris,
D. K. Hobday, M. K. McGowen, D. Pass, and D. H. Wood

Bureau of Economic Geology
W. L. Fisher, Director
The University of Texas at Austin
University Station, P. O. Box X
Austin, Texas 78712

1980

CONTENTS

FIGURES

iv
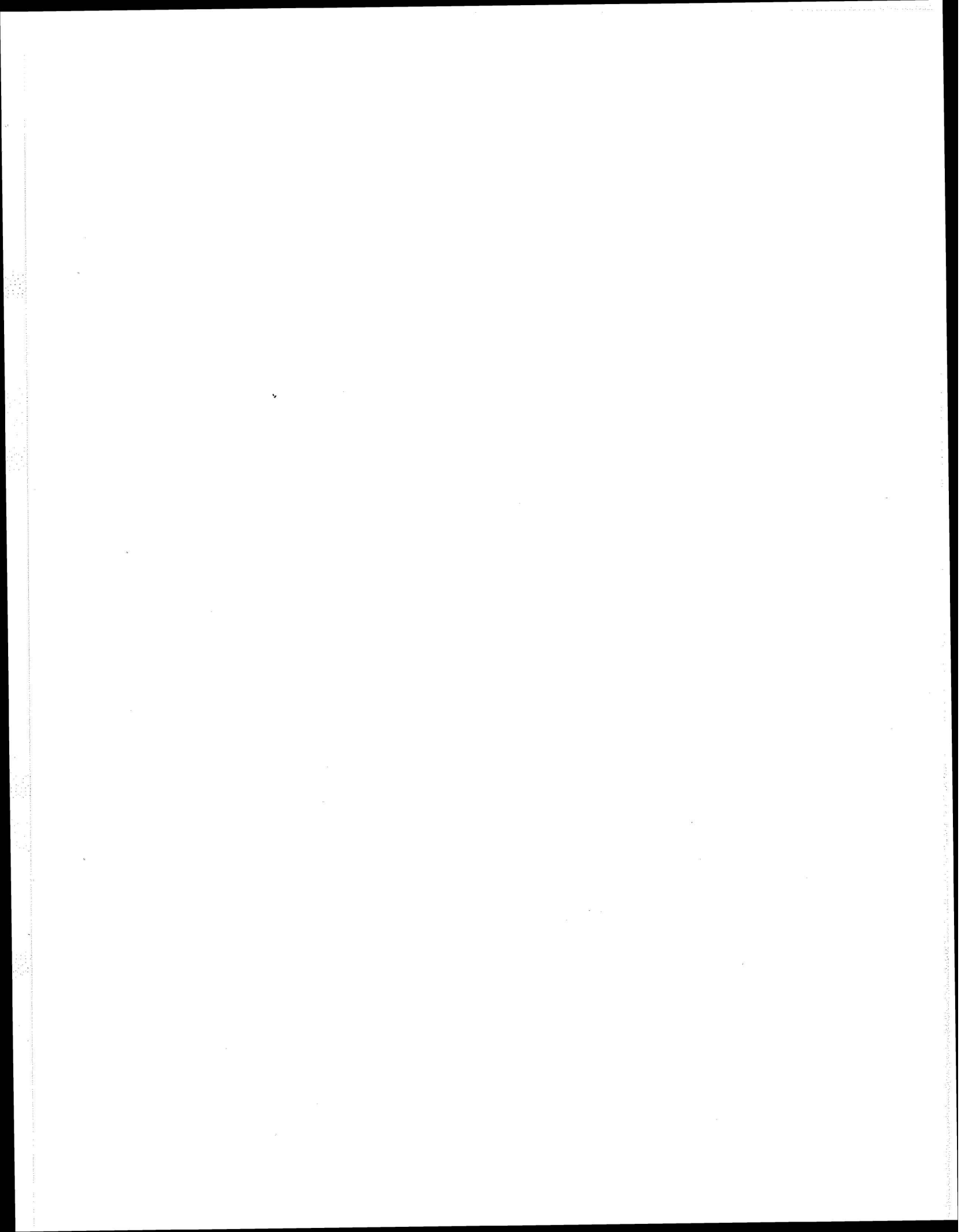
TABLES

EAST TEXAS SALT DOME STUDIES -- A SUMMARY OF SECOND-YEAR RESEARCH ACTIVITIES

Research Staff

Analysis during the second year was highlighted by a historical characterization of East Texas Basin infilling, the development of a model to explain the growth history of the domes, the continued studies of the Quaternary in East Texas, and a better understanding of the near-dome and regional hydrology of the basin. Each advancement represents a part of the larger integrated program addressing the critical problems of geologic and hydrologic stabilities of salt domes in the East Texas Basin.

During the second year of the East Texas salt dome studies, significant advances in understanding the hydrologic and geologic stabilities of salt domes were based on the acquisition of much new data. Among these new sources of data are (1) 400 km (250 mi) of seismic reflection data that are both regional and site specific, (2) gravity data for the East Texas Basin, (3) 20 shallow boreholes over Oakwood Dome, (4) 1 hydrologic test hole downdip from Oakwood Dome, and (5) a complete core of the anhydrite-gypsum cap rock over Gyp Hill Dome in South Texas.

The acquisition of seismic, gravity, and electric log data provided new understanding of the sedimentary infilling of the East Texas Basin and how it caused salt migration and dome growth. Deposition of the Travis Peak-Schuler sediments caused the first differential loading of the underlying Louann Salt and the migration of the salt into anticlinal ridges. Subsequent clastic depocenters occurred laterally to Travis Peak depocenters and caused further migration of the salt into diapirs. The greater the sediment loading, the further the salt anticline advanced through Trusheim's (1960) growth sequence: pillow structure to immature diapir and finally to a mature diapir. Most domes in the basin can be placed within this dome growth sequence.

Analysis of the Gyp Hill cap rock showed that the cap rock was the result of salt dome dissolution and the accumulation of the insoluble residuum, anhydrite.

Work completed on the Carrizo-Wilcox aquifer, the major fresh-water aquifer in the basin, shows that this aquifer has the greatest potential for causing dome dissolution leading to radionuclide transport. Ground-water circulation is controlled primarily by topography and structure. Fluid movement is generally downward because of the structural dip and leakage from overlying units. Chemical composition of the water evolves from a low-pH, oxidizing, calcium bicarbonate water in the outcrop to a high-pH, reducing, sodium bicarbonate water deeper in the aquifer. This chemical change has important implications for radionuclide transport.

The Palestine Salt Dome is no longer under consideration as a potential repository for nuclear waste because of the occurrence of numerous collapse sinks that resulted from an earlier brining operation.

To date, studies of Quaternary strata have not found evidence of salt dome growth during the Pleistocene or Recent.
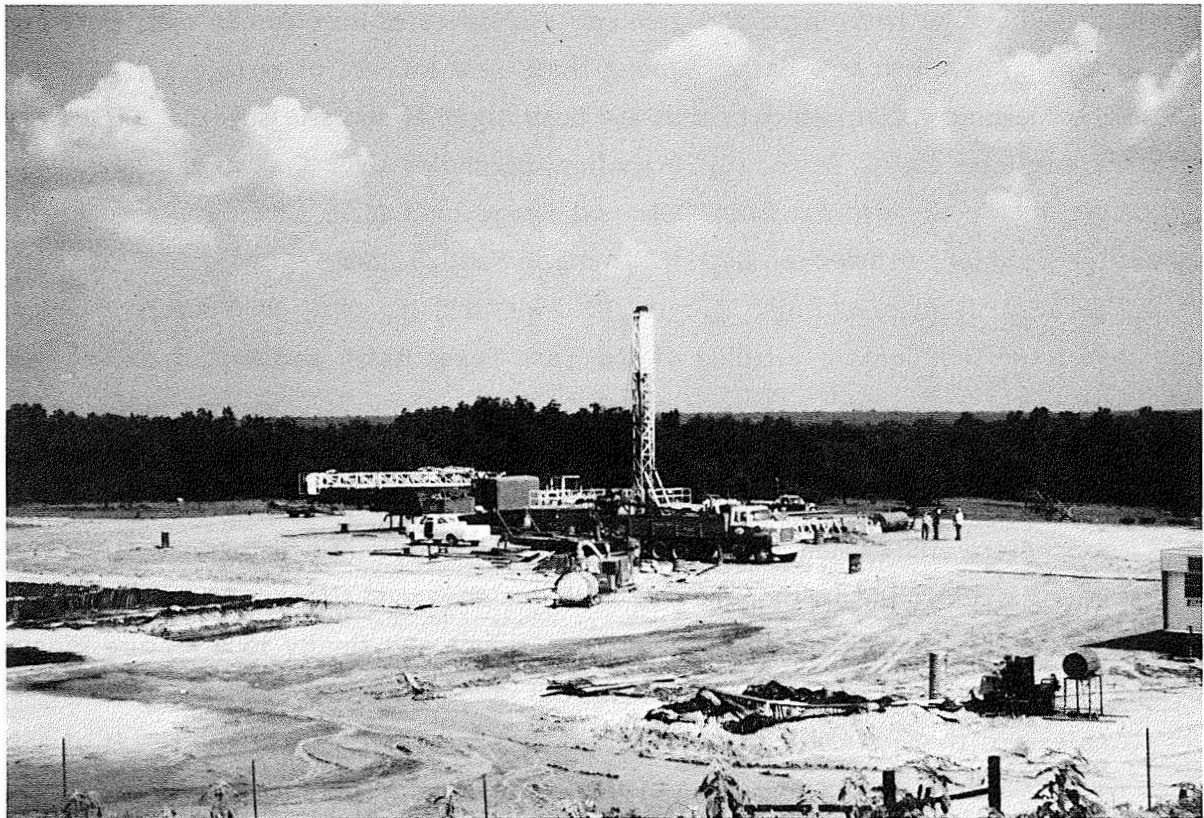
Drilling of hydrologic monitoring well south of Oakwood Dome.

PURPOSE AND SCOPE

Research Staff

The program to investigate the suitability of salt domes in the East Texas Basin for long-term nuclear waste repositories addresses the stability of specific domes for potential repositories and evaluates generically the geologic and hydrogeologic stability of all the domes in the region.

East Texas Basin studies are part of salt dome studies of those interior basins of Texas, Louisiana, and Mississippi that compose the Gulf Coast Interior Salt Basin. The East Texas Basin study is one regional element of the National Nuclear Waste Isolation Program. The U.S. Department of Energy (DOE) intends to choose one salt dome from the Gulf Coast Interior Basin for a nuclear waste repository. This report concerns the salt dome program in East Texas and presents some preliminary conclusions reached during 1979 on dome suitability.

The 1979 program to investigate the stability of salt domes in the East Texas Basin was divided into three subprograms: (1) subsurface geology; (2) surficial geology, remote sensing, and geomorphology; and (3) hydrogeology. The integration of the results of these three subprograms will (1) determine the general suitability of salt domes in the East Texas Basin for a nuclear waste repository; and (2) identify candidate salt domes for further, more detailed studies.

The subsurface program was designed to (1) identify pre-Pleistocene growth histories for domes in the East Texas Basin; (2) explain the relationship of basin infilling and salt dome growth; (3) map detailed subsurface geology around the salt domes; and (4) delineate size and shape of salt domes, depth to cap rock, and depth to salt.

The surficial geology and geomorphology program was designed to (1) determine if the domes have grown during the Quaternary; (2) describe detailed surface geology over the domes; (3) evaluate the structure of the basin to discover whether any structural activity has occurred during the Quaternary; and (4) map surface Tertiary formations and ascertain how they relate to dome and tectonic history.

The primary purposes of the hydrogeology program were to (1) examine regional ground-water flow paths and (2) assess the potential impacts of salt dissolution on domes. Studies included regional hydrogeology in fresh-water aquifers, regional hydrogeology in the deeper saline aquifers, and hydrogeology around domes.

This paper, a summary progress report, reviews principal conclusions and illustrates the methodologies used and the types of data and displays generated. Several topical reports, presenting details of various geological aspects of salt domes in the East Texas Basin, will be forthcoming as phases of the study are completed.

STRATIGRAPHIC FRAMEWORK AND DEPOSITIONAL SEQUENCES OF THE EAST TEXAS BASIN

O. K. Agagu, E. H. Guevara, and D. H. Wood

The stratigraphic succession in the East Texas Basin is composed of sequences of transgressive limestones, chalks, and shale, alternating with regressive fluvio-deltaic sandstones and shales. Six such sequences can be recognized regionally in the basin, but each may contain one or more minor sequences. The first transgressive episode also deposited a thick layer of salt, which was buried beneath 5,547 m (18,200 ft) of sediments deposited in the five other sequences.

Regional subsurface stratigraphy of the East Texas Basin is being studied to explain basin evolution, tectonic stability, depositional patterns, and local dome growth and dome stability. The region includes approximately 43,570 km^2 (16,800 mi^2) extending from the Mexia-Talco Fault Zone in the north and west, to the Sabine Uplift in the east, and to the vicinity of Angelina County in the south (fig. 1).

Stratigraphic analysis is based primarily on correlation of electric log stratigraphic markers in about 2,600 wells in the basin. Forty-nine cross sections were constructed, and about 50 stratigraphic units were correlated. These cross sections provide the basis for correlating other wells in the basin. Well log interpretation was supplemented by about 400 km (250 mi) of regional, sixfold, conventional CDP reflection seismic data and both Bouguer and residual gravity maps, which cover the entire basin.

About 5,791 m (19,000 ft) of Mesozoic and Tertiary strata are preserved in the central parts of the East Texas Basin. These rocks overlie metamorphosed Paleozoic Ouachita strata, which are probably a continuation of the Appalachian foldbelt (Lyons, 1957; Wood and Walper, 1974; McGookey, 1975). Stratigraphy of the Mesozoic and Tertiary strata has been discussed by several authors, notably Waters and others (1955), Eaton (1956), Nichols (1964), and Nichols and others (1968). A comprehensive summary of basin stratigraphy is presented in figures 2, 3, and 4. The present investigations involve six pairs of repetitive, regional depositional sequences in the basin. Each couplet consists of a lower, dominantly fluvio-deltaic unit of sandstones and shales that is overlain by shelf carbonates and shales.

The Eagle Mills-Louann sequence (Upper Triassic-Middle Jurassic).--This sequence was initiated by deposition of the undated continental Eagle Mills red beds. The Eagle Mills red beds are composed of red-brown shales, sandstones, and unfossiliferous limestones, which are unconformably overlain by the Werner Formation.

Lower sections of the Werner consist of conglomerates and fine- to coarse-grained sandstones that grade upward into finer clastics and evaporites in the upper part of the formation. Halite interbeds in the Werner progressively increase volumetrically toward the top of the formation and are transitional into the conformably overlying Louann Salt (Nichols and others, 1968).

The Louann Salt consists of white, gray to blue halite with minor amounts of anhydrite. Upper parts of the formation exhibit some red plastic shales transitional into the conformably overlying Norphlet Formation (Nichols and others, 1968). The partially restricted nature of the East Texas Basin during its initial stages of formation (Wood and Walper, 1974) provided an ideal setting for large-scale evaporitic processes, which have not been repeated in the basin.

Norphlet-Bossier sequence (Upper Jurassic).--The Norphlet Formation consists of sandstones, siltstones, and red shales. The basal part contains halite, anhydrite, and dolomite transitional into the subjacent Louann evaporites (Nichols and others, 1968). The relatively thin Norphlet Formation is conformably overlain by the Smackover Formation, which documents a regressive phase between deposition of the Louann Salt and the Smackover Limestone.

The Smackover Limestone here consists of a basal laminated micrite that grades upward into a pelletal micrite and ultimately into a coated grainstone. The Smackover Limestone is overlain by and is in part correlative with the Buckner Formation, which contains red sandstones in the western and northern margins of the basin and grades basinward into evaporites, shales, dolomites, and limestones (Nichols and others, 1968). The Smackover-Buckner strata document a shoaling sequence from subtidal in the lower Smackover Limestone to supratidal conditions in the Buckner Formation. The Cotton Valley Limestone and Bossier Formation are deeper water, gray, micritic limestones and gray to black shales (Nichols and others, 1968) that onlap the Buckner supratidal facies, an indication of a minor sequence boundary above the Smackover Formation.

Schuler-Glen Rose sequence (Upper Jurassic-Lower Cretaceous).--The Schuler and Travis Peak Formations attest to the high rate of terrigenous clastic influx during Late Jurassic and the Early Cretaceous. They compose a thick sequence (900 m, 3,000 ft) predominantly of sandstones interbedded with dull red and green-gray shales (Nichols and others, 1968). The Schuler-Travis Peak sequence onlaps the subjacent marine units despite its strongly terrigenous character and is probably an example of coastal onlap, which was most likely related to the globally rising sea level during the Late Jurassic and the Early Cretaceous (Vail and others, 1977).

The Glen Rose Group consists of a thick (750 m, 2,500 ft) sequence of shallow marine, micritic, pelletal, oolitic, and shelly limestones interbedded with dark-gray shales and anhydrites (Nichols and others, 1968). The predominantly calcareous units, such as the Pettet, James, and Rodessa Members and much of the Upper Glen Rose Formation, are deeper water facies. Sandy shale units, such as the Pine Island Shale, and evaporites, such as the Massive Anhydrite, were deposited during minor influxes of fine, terrigenous sediment and deposition in supratidal environments, respectively. Terrigenous facies dominate, especially along the north and northwestern flanks of the basin.

Paluxy-Washita sequence (Lower Cretaceous).--The Paluxy Formation consists of interbeds of sandstones and shales, and rare conglomerates lie in the northern half of the East Texas Basin. Basinward, toward the south, the Paluxy gradually changes into dark-gray shales and micritic limestones (Nichols and others, 1968). The volume of terrigenous clastic sediment (up to 135 m, 450 ft) and the high rate of deposition indicate that a major though short-lived phase of fluvial-deltaic clastic influx occurred. Limestone and shales of the Fredericksburg and Washita Groups in East Texas document the Early Cretaceous sea-level high that drowned the Paluxy deltas.

Woodbine-Midway sequence (Upper Cretaceous-Paleocene).--Spasmodic uplift of the marginal areas of the East Texas Basin during Late Cretaceous to Paleocene times, accompanied by lowering of relative sea level, resulted in the terrigenous clastic influx marked by the Woodbine and Eagle Ford Groups. The Woodbine Group, composed mainly of fluvial and deltaic sandstone and subordinate shales, marks the peak of clastic sedimentation during this phase. The Eagle Ford Group, consisting primarily of shelf and slope shales and minor sandstones, documents the waning phase of clastic deposition.

The Austin Group initiated the transgressive and submergent phase that terminated in the Paleocene. During this depositional phase, up to 244 m (800 ft) of shelf chalks, shales, and marls were deposited with rare clastic facies that define minor variations in this sequence.

Tertiary clastics.--The Tertiary stratigraphic sequence in the East Texas Basin is a complex unit mainly composed of fluvio-deltaic sandstones and shales. The Wilcox Group is a thick (up to 900 m, 3,000 ft) unit of fluvial and deltaic sands, clays, lignites, and marls that has not yet been regionally subdivided. The Claiborne Group is similar to the Wilcox Group, but it displays some shaly, glauconitic, fossiliferous shelf/embayment units (Reklaw Formation, Weches Formation, and Cook Mountain) that alternate regionally with more sandy fluvial-deltaic units (Carrizo, Queen City, Sparta, and Yegua Formations). The entire Tertiary section constitutes the major regressive phase of the sixth depositional sequence.

6
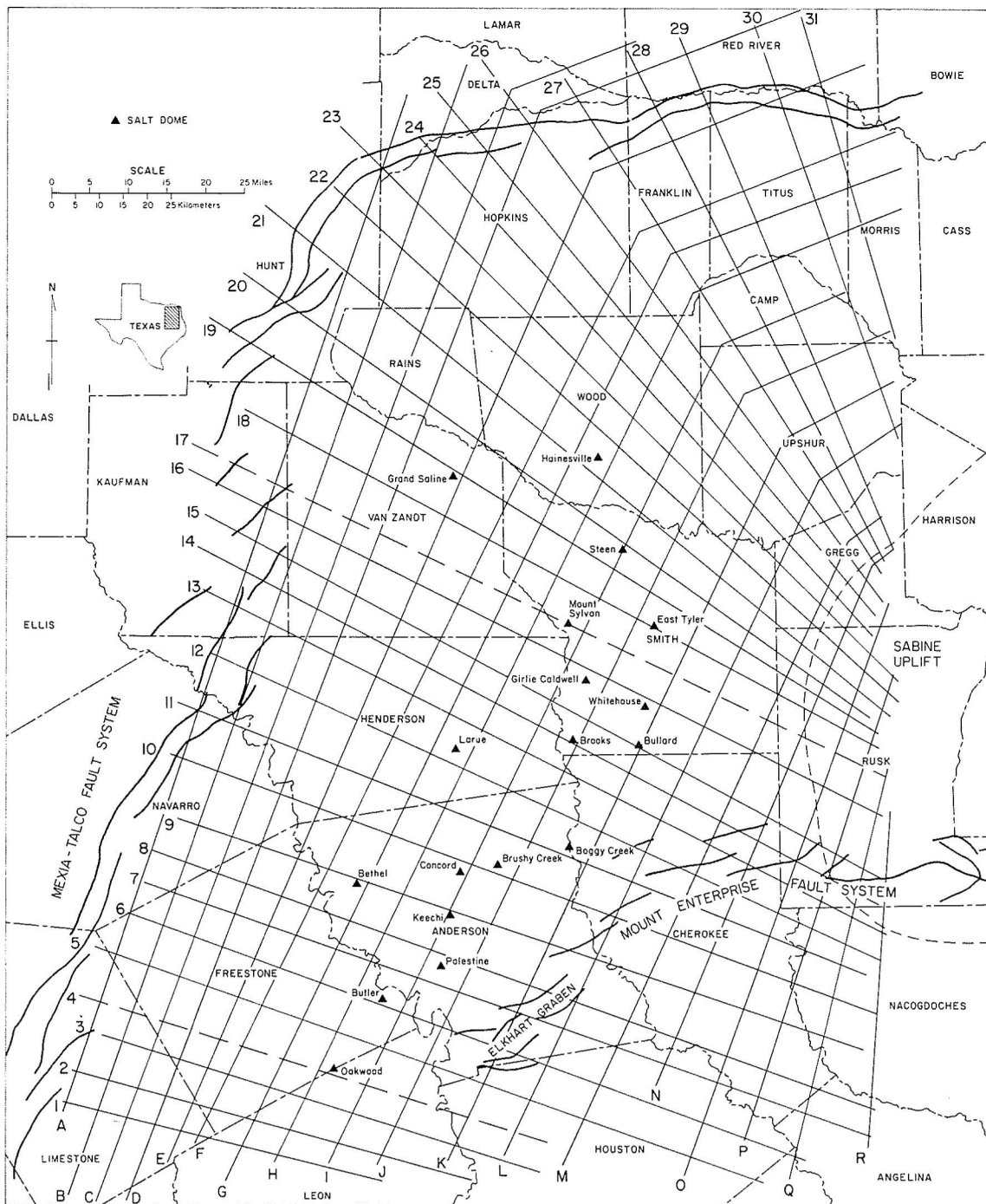
Figure 1. Location map of salt dome province, East Texas Basin. Stratigraphic cross sections are arranged parallel to regional strike and dip. Dashed sections are presented in this report.

7

ERA	SYSTEM	SERIES	GROUP	FORMATION	MEMBER
CENOZOIC	TERTIARY	EOCENE	CLAIBORNE	YEGUA	
				COOK MOUNTAIN	
				SPARTA	
				WECHES	
				QUEEN CITY	
				REKLAW	
				CARRIZO	
			WILCOX	UNDIFFERENTIATED	
		PALEOCENE	MIDWAY	UNDIFFERENTIATED	
MESOZOIC	CRETACEOUS	UPPER CRETACEOUS	NAVARRO	UPPER NAVARRO CLAY	
				UPPER NAVARRO MARL	
				NACATOCH SAND	
				LOWER NAVARRO	
			TAYLOR	UPPER	
				PECAN GAP CHALK (LOWER)	
				WOLF CITY SAND (LOWER)	
			AUSTIN	GOBER CHALK	
				AUSTIN CHALK	
				ECTOR CHALK	
			EAGLE FORD	EAGLE FORD	SUBCLARKSVILLE SAND
			WOODBINE	LEWISVILLE	
				DEXTER	
		LOWER CRETACEOUS	WASHITA	MANESS SHALE	
				BUDA LIMESTONE	
				GRAYSON SHALE	
				MAIN STREET LS. (GEORGETOWN)	
				WENO-PAW PAW LS. (GEORGETOWN)	
				DENTON SHALE (GEORGETOWN)	
				FORT WORTH LS. (GEORGETOWN)	
				DUCK CREEK SHALE (GEORGETOWN)	
				DUCK CREEK LS. (GEORGETOWN)	
			FREDERICKSBURG	KIAMICHI SHALE	
				GOODLAND LIMESTONE	
				PALUXY	
			TRINITY	UPPER GLEN ROSE (GLEN ROSE)	
				MASSIVE ANHYDRITE (GLEN ROSE)	RODESSA
				LOWER GLEN ROSE (GLEN ROSE)	JAMES LIMESTONE
					PINE ISLAND SHALE
					PETTET (SLIGO)
				TRAVIS PEAK	
	JURASSIC	UPPER JURASSIC	COTTON VALLEY	SCHULER	
				BOSSIER	
				COTTON VALLEY LS.	
				BUCKNER	
				SMACKOVER	
				NORPHLET	
		MIDDLE JURASSIC		LOUANN SALT	
				WERNER	
		Triassic ?		EAGLE MILLS	
PALEOZOIC				OUACHITA	

Figure 2. Stratigraphic succession and nomenclature in East Texas Basin (adapted from Nichols and others, 1968).
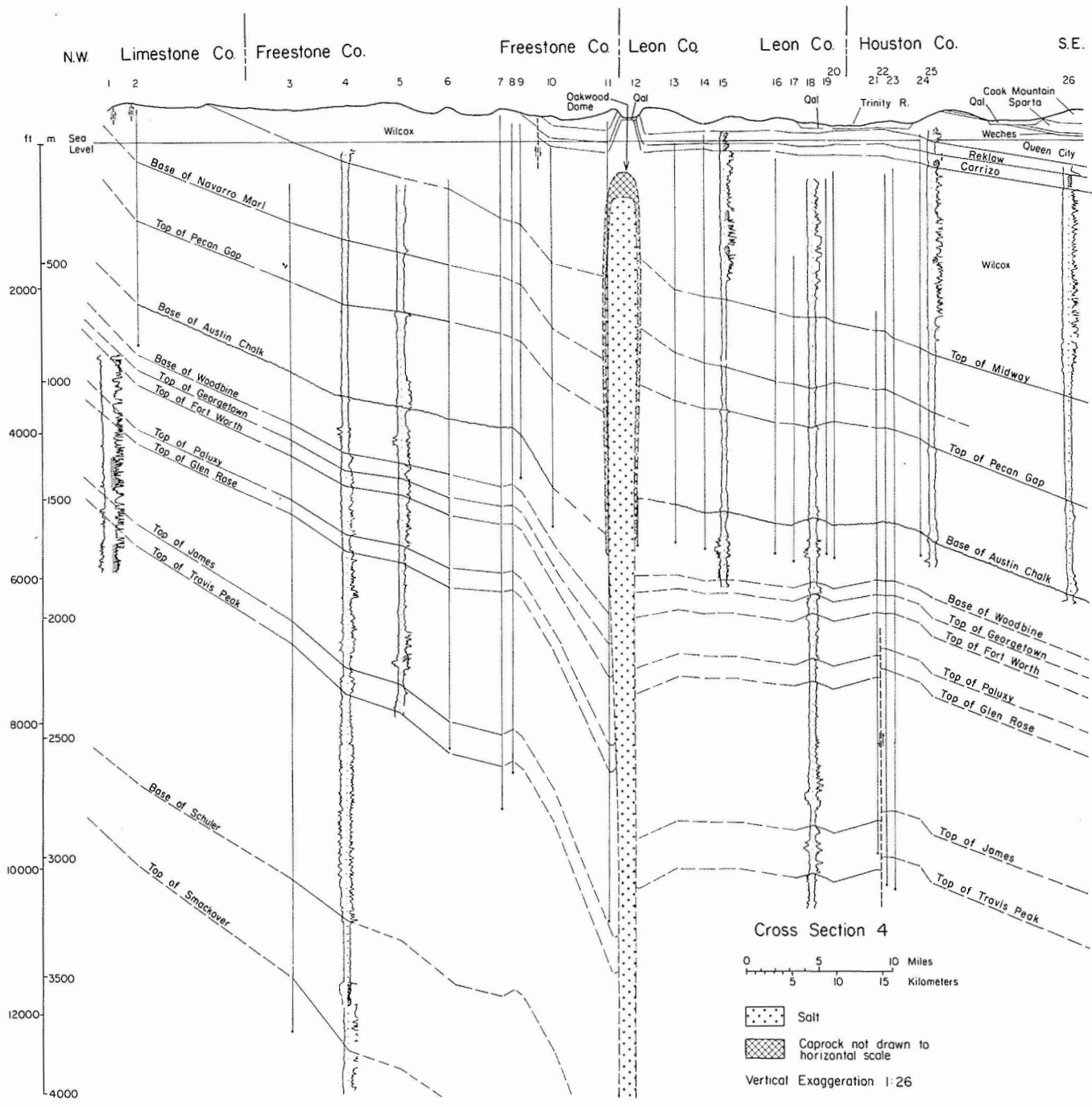
Figure 3. Dip structure cross section through Freestone, Leon, and Houston Counties.
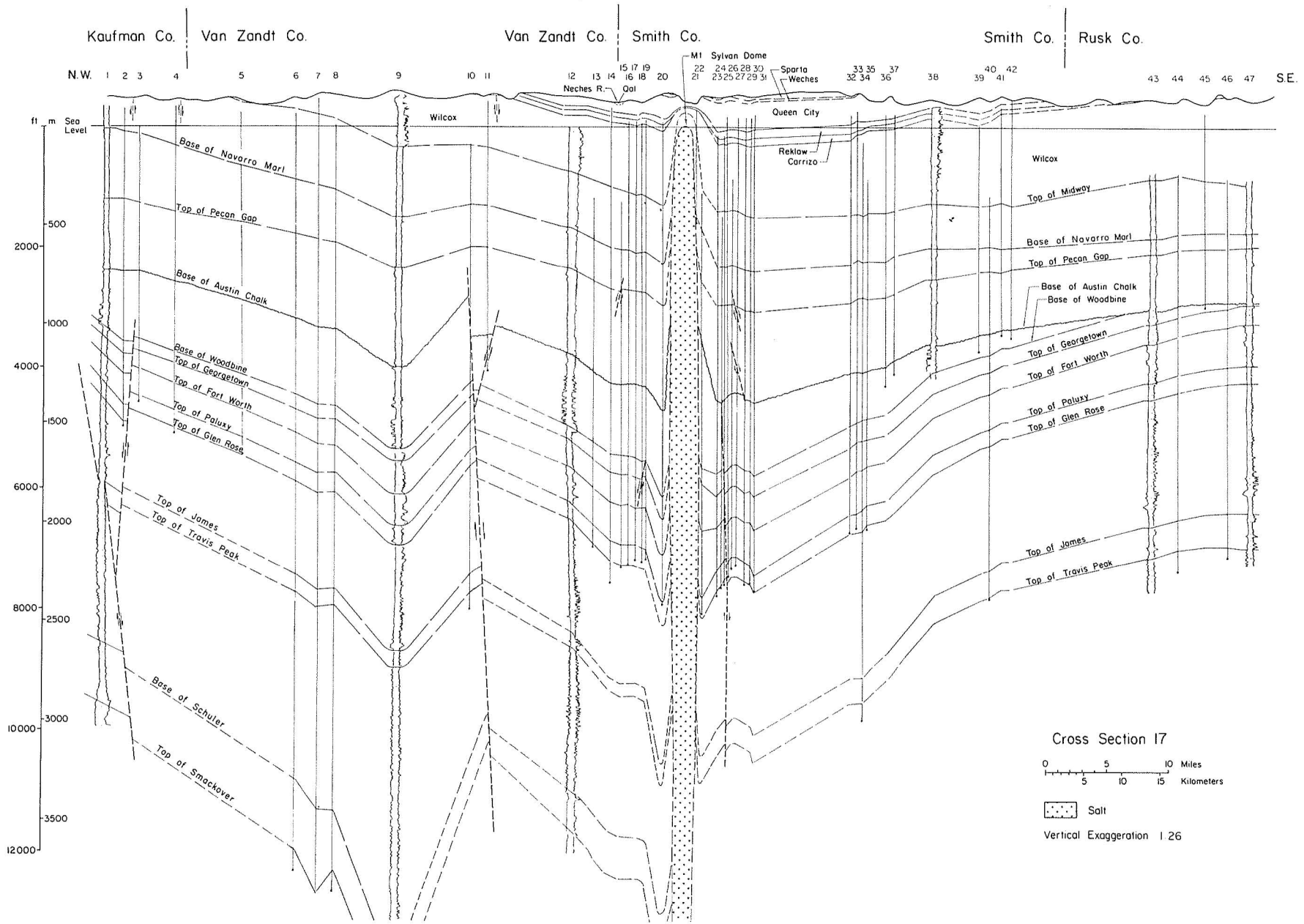
Figure 4. Dip structure cross section through Van Zandt, Smith, and Rusk Counties.

REGIONAL TECTONIC FRAMEWORK OF THE EAST TEXAS BASIN

O. K. Agagu, M. K. McGowen, D. H. Wood, J. M. Basciano, and D. W. Harris

The East Texas Basin is framed by basement elements that have persisted since inception of the basin (Late Triassic). Pre-Louann strata in the basin are only slightly deformed in contrast to post-Louann strata, which are complexly folded and faulted by salt tectonics. Salt diapirism in the central part of the basin was probably initiated during Late Jurassic by differential loading from Schuler-Travis Peak strata. Salt deformation appears, to have started earlier near the basin margin. Structures created by salt movement remained active into the Tertiary. Salt-induced regional structures later influenced rates of deposition, thicknesses of strata, and volume of available salt.

Regional subsurface structures in the East Texas Basin are currently being mapped to determine the tectonic evolution of the basin. Mapping covers the southern two-thirds of the basin from the Sabine River south to the Angelina flexure. From well data, structure-contour maps for 6 stratigraphic horizons and isopachous maps for 10 stratigraphic units have been constructed. Later, these maps will be extended to depict the entire region, and, possibly, additional horizons will be mapped. Well log information is supplemented by about 400 km (250 mi) of regional, sixfold, conventional CDP reflection seismic data; Bouguer gravity and residual gravity maps are available for the entire region.

Tectonic elements.--The pre-Mesozoic record in the East Texas Basin is speculative. Available evidence, however, points to a Late Triassic or Early Jurassic origin when the postulated rifting of Pangea separated North and South America to form the Gulf of Mexico (Lyons, 1957; Wood and Walper, 1974; McGookey, 1975). The locus of subsidence that produced the East Texas Basin may also be related to pre-rifting lineaments associated with the Appalachian-Ouachita-Marathon orogeny.

Basement-related tectonic elements in and around the East Texas Basin were formed early in basin history (fig. 5). Except for some speculated gentle downwarping caused by sediment loading (Turk, Kehle, and Associates, 1978) and some uplift in the Sabine area (Granata, 1963), the basement has remained fairly stable. Structural complexity in the central parts of the basin is, therefore, due primarily to halokinetic movements. Some tectonic elements peripheral to the basin exhibit both diastrophic and halokinetic origins.

Boundary elements.--The Mexia-Talco Fault Zone (fig. 5) bounds the East Texas Basin on the west and north. It is a series of en echelon faults and grabens that coincide with the updip limits of the Louann Salt. The fault system extensively displaces Mesozoic and lower Tertiary strata, is also coincident with a subdued scarp in the basement, and has locally associated volcanism (Turk, Kehle, and Associates, 1978). These evidences suggest that the fault system probably originated as part of a series of step faults bounding the northern frontiers of the Gulf of Mexico Basin. Possible downdip flow of salt and subsidence resulting from sediment load accentuated the Mexia-Talco Faults (more than others) in post-Louann times.

The Sabine Uplift (fig. 5) separates the East Texas Basin from the North Louisiana Basin. The uplift has been a positive feature probably since the inception of these basins, as indicated by thinning of the Louann Salt (McGookey, 1975). The area has also been spasmodically uplifted, especially during early Late Cretaceous times (Granata, 1963). No direct relationship appears between activation of the Sabine Uplift and salt tectonics. The isopachous map for the Maness, Woodbine, and Eagle Ford sequence (fig. 6) suggests that the Sabine Uplift was not a source of clastics even during development of the pronounced post-Eagle Ford erosional unconformity.

The Elkhart Graben-Mount Enterprise Fault System (fig. 5) is a zone of faulting that bounds the East Texas Basin on the south. The fault zone trends northeast-southwest through Rusk, Cherokee, Anderson, and possibly Leon Counties. This trend is coincident with a buried hinge line that is subparallel to and north of the Angelina-Caldwell flexure (Nichols, 1964) (figs. 5 and 7). This hinge line is the southern limit of the East Texas Salt Dome Province. Pre-Eocene sediments are thickest north of the hinge, whereas post-Eocene depocenters are thickest south of it.

The Elkhart Graben-Mount Enterprise hinge line probably is a structurally elevated, relict shelf edge. Post-Louann sediments have squeezed mobile salt from the East Texas Basin southward to produce a faulted uplift similar to the linear ridges on the slope and rise in the Gulf of Mexico (Antoine and others, 1967). This view is supported by the presence of a prominent gravity minimum along the graben. Two deep-seated salt uplifts, Elkhart and Slocum Domes, also occur along the system, probably as a result of second-order sediment thickness variations.

Basinal elements.--The entire East Texas Basin was underlain by the Louann Salt. The original tabular salt layer was initially deformed into a complex array of salt ridges, troughs, pillows, and piercement features. All post-Louann sediments are consequently affected; pre-Louann sediments are, however, relatively undeformed (fig. 8).

The East Texas Basin can be subdivided regionally into a western subbasin trending north-south and two eastern subbasins trending north-northeast - south-southwest (fig. 7). This basin structure is displayed on all the mapped horizons (Lower Cretaceous to Upper Cretaceous). Subsidiary elements, principally salt domes in Henderson and Anderson Counties, further subdivide the subbasins. Marginal areas of the basin are characterized by relatively consistent and more gentle basinward dips compared with the central parts of the basin, where the principal salt domes are concentrated.

In the southern part of the basin, regional thickness trends of Upper Cretaceous to Tertiary sedimentary units (figs. 7 and 9) conform closely to structures developed by salt movement. Generally, the main depocenters are the regional, halokinetic synclines; the flanks of the depocenters, which received thinner sediments, are sites of halokinetic anticlinal axes. As expected, the terrigenous clastic and chalk units conform to this salt distribution pattern, but in some areas, thick sequences of carbonates appear to have developed on paleotopographic highs (overlying salt anticlines) probably by reefal build-up and related processes (fig. 10). The western syncline was somewhat less active in Late Jurassic and Early Cretaceous times.

Salt mobilization started early in the history of the basin. In the central parts of the basin, salt-induced sedimentary thickness variations are noticeable only in the Cotton Valley Group and the younger strata (fig. 8). Before that time, post-Louann deposition in the central parts of the basin had been composed principally of marine limestones and shales that would have exhibited planar stratal geometry because of deposition on the undeformed substrate. Subsequent clastic influx during deposition of the Schuler and Travis Peak Formations, on the contrary, would have exhibited thick and sandy (denser) delta front facies -- a density imbalance that may have initiated salt movement. Burial of the Louann Salt by about 1,524 m (5,000 ft) of Norphlet-Cotton Valley Limestone sediments would also have created higher temperatures and pressures, which would have enhanced plastic deformation.
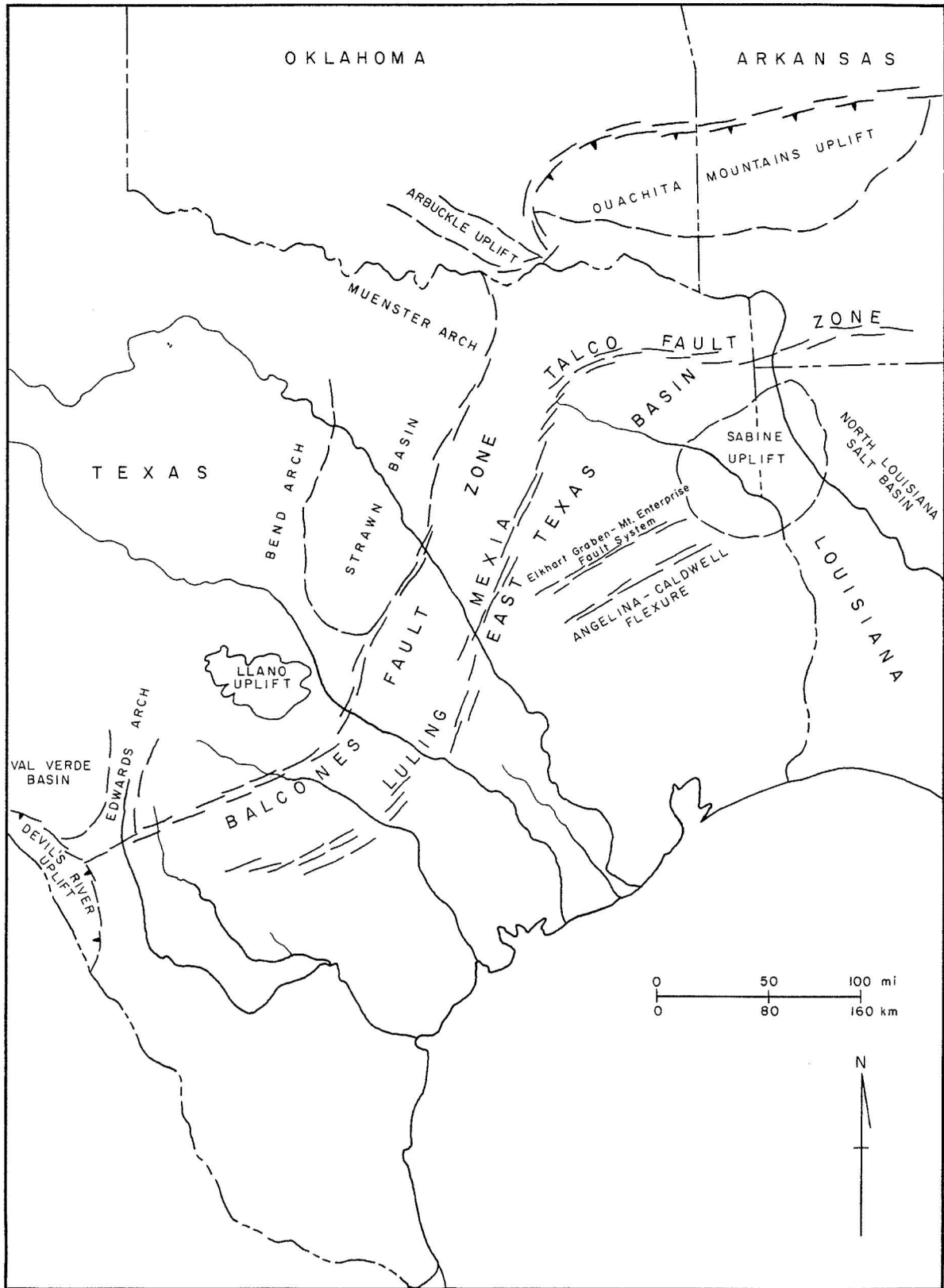
Figure 5. Megatectonic elements around the East Texas Basin.
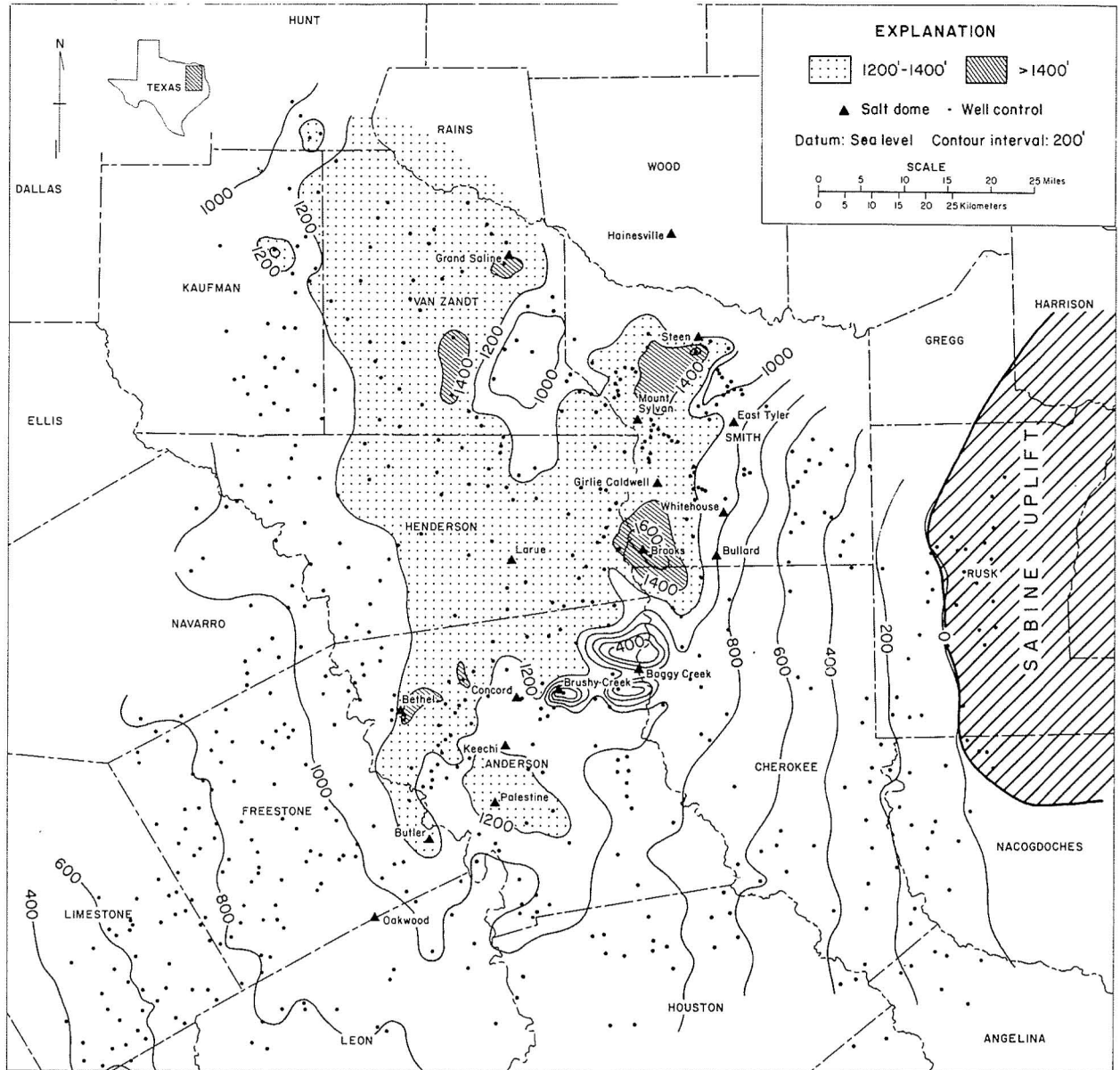
Figure 6. Isopach map of combined Eagle Ford, Woodbine, and Maness Formations. Stratigraphic pinch-out around the Sabine Uplift is not accompanied by any major clastic influx of eroded sediment.

Figure 7. Main structural trends in the East Texas Basin, indicated by structural configuration on top of the Pecan Gap Member of Taylor Formation.
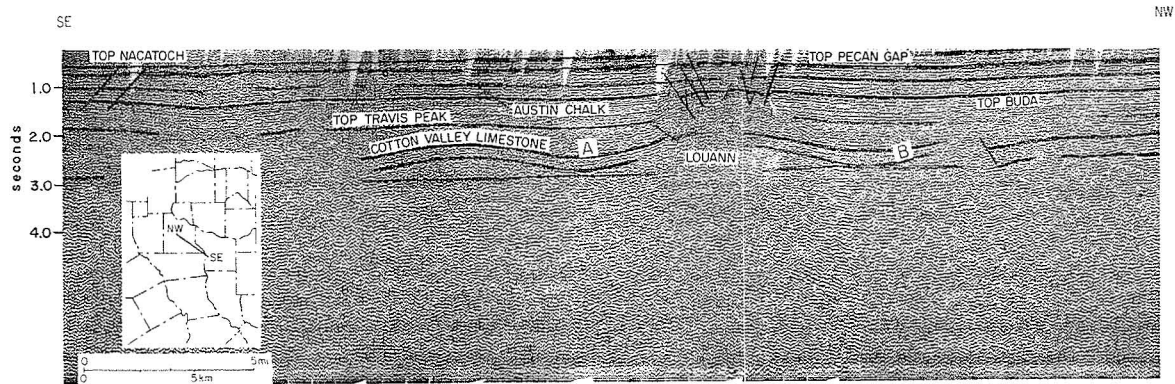
Figure 8. Seismic section through Van Zandt County. Main depositional axes define persistent structural troughs owing to salt withdrawal into intervening anticlinal area(s). Thickness variations indicating salt movement become evident in Schuler/Travis Peak time (A) in the central parts of the basin. Movement could have been initiated earlier near the margin of the basin (B). Seismic line courtesy of Teledyne Exploration Company.

Figure 9. Isopach map of Pecan Gap Member, Lower Taylor Formation, and Austin Group.
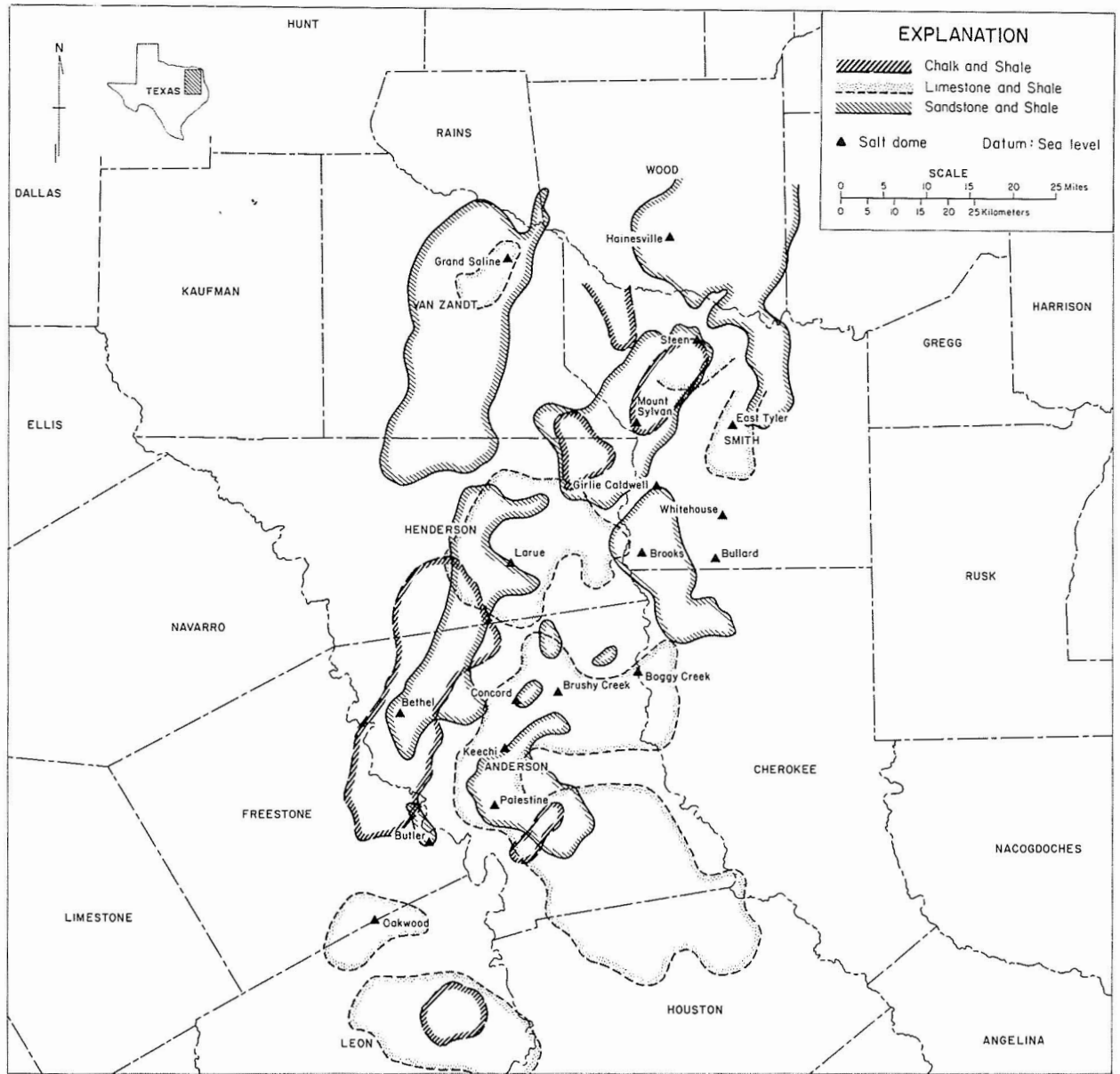
Figure 10. Major depositional axes in East Texas Basin. Depocenters coincide with positions of structural troughs in figure 7, especially in sand/shale and chalk/shale units.

EVOLUTION OF EAST TEXAS SALT DOMES

Alice B. Giles

Salt domes in various stages of maturity in the East Texas Basin can be recognized from analysis of the geometry of the domes and the strata surrounding them.

Salt dome evolution entails the domeward migration of the area of salt withdrawal (fig. 11) (Trusheim, 1960; Kupfer, 1970). The area of salt withdrawal is made apparent on cross sections by the thickening of sediments deposited during the time of withdrawal. The structure that accommodates the thickening is termed a *rim syncline*.

Immature salt domes are characterized by rim synclines that are relatively distant from the dome crest such that strata thin toward and dip away from the dome. The rim synclines of *mature salt domes* have migrated to the dome edge; therefore, younger strata thicken and dip toward the dome. Thickened beds adjacent to mature domes indicate substantial flow of salt into the dome and possible pinch-out of the salt source. Consequently, additional sediment loading should not promote further dome growth.

Numerous deep, nonpiercing salt pillows occur in the East Texas Basin and represent comparatively immature salt structures (fig. 9). Shallow salt domes in the basin, however, exhibit various degrees of maturity.

Keechi, Bullard, and Whitehouse Domes are in an intermediate stage of maturity. Although these domes have risen to shallow depths, surrounding strata thin toward and dip away from the domes (figs. 12, 13, and 14), an indication that more pillow salt is available for additional growth. The conical shape of these domes also indicates that more sediment loading of the flanks of the domes would cause additional dome growth (fig. 15).

Grand Saline, Bethel, and Hainesville Domes are more mature domes and are isolated from an additional supply of salt. The rim syncline has migrated to the edge of these domes, as indicated by the domeward thickening of strata (figs. 16, 17, and 18). The early (pillow) stage of dome growth at Bethel and Hainesville Domes is reflected in domeward thinning of Lower Cretaceous strata (figs. 17 and 18); the pillow stage at Grand Saline Dome must have ended by Fort Worth-Paluxy time (fig. 16). The cylindrical to mushroom shape of these domes also suggests that salt has been withdrawn from the area around the bases of the domes (fig. 19).
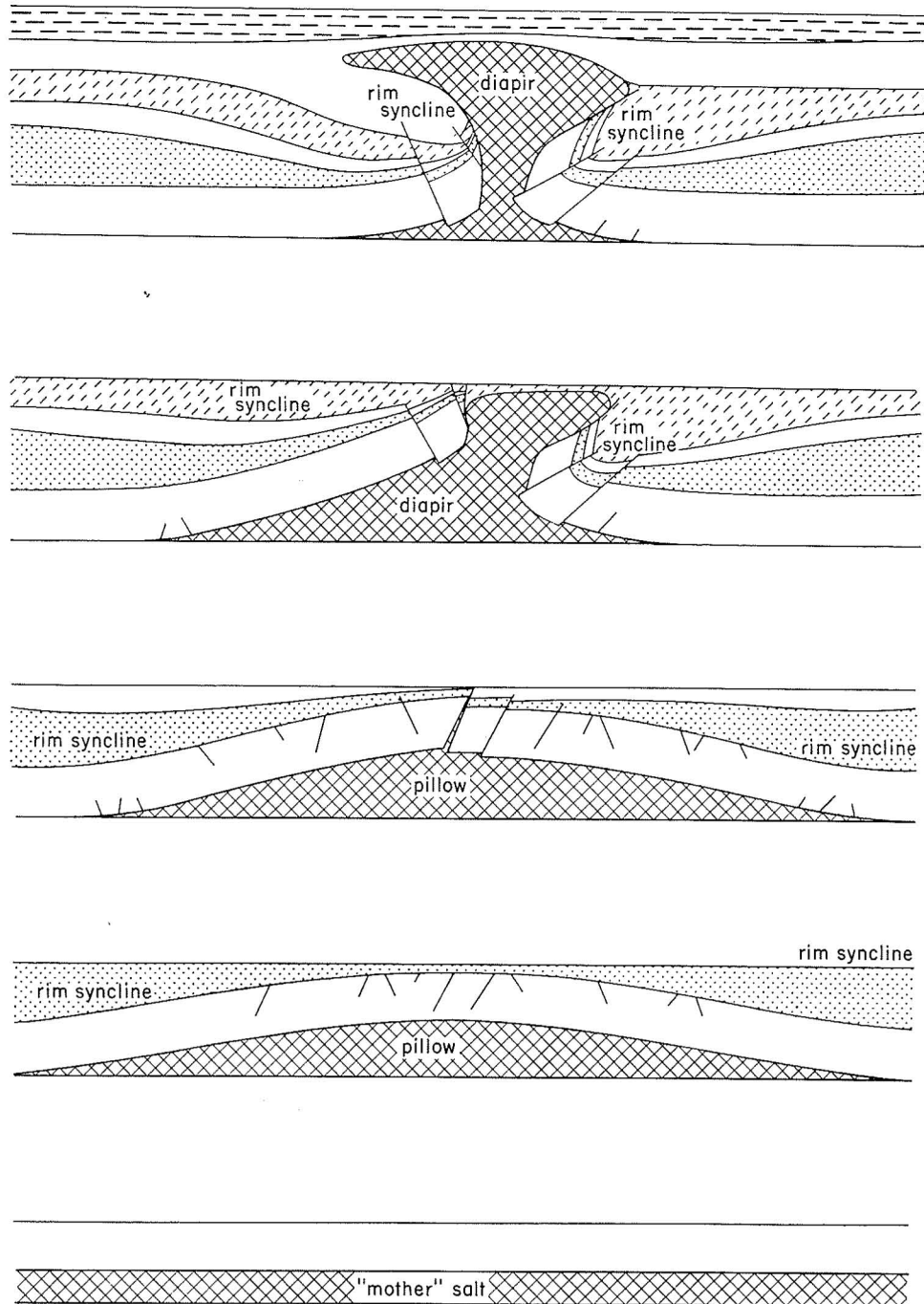
Figure 11. Schematic evolution of salt diapirs (modified from Trusheim, 1960).
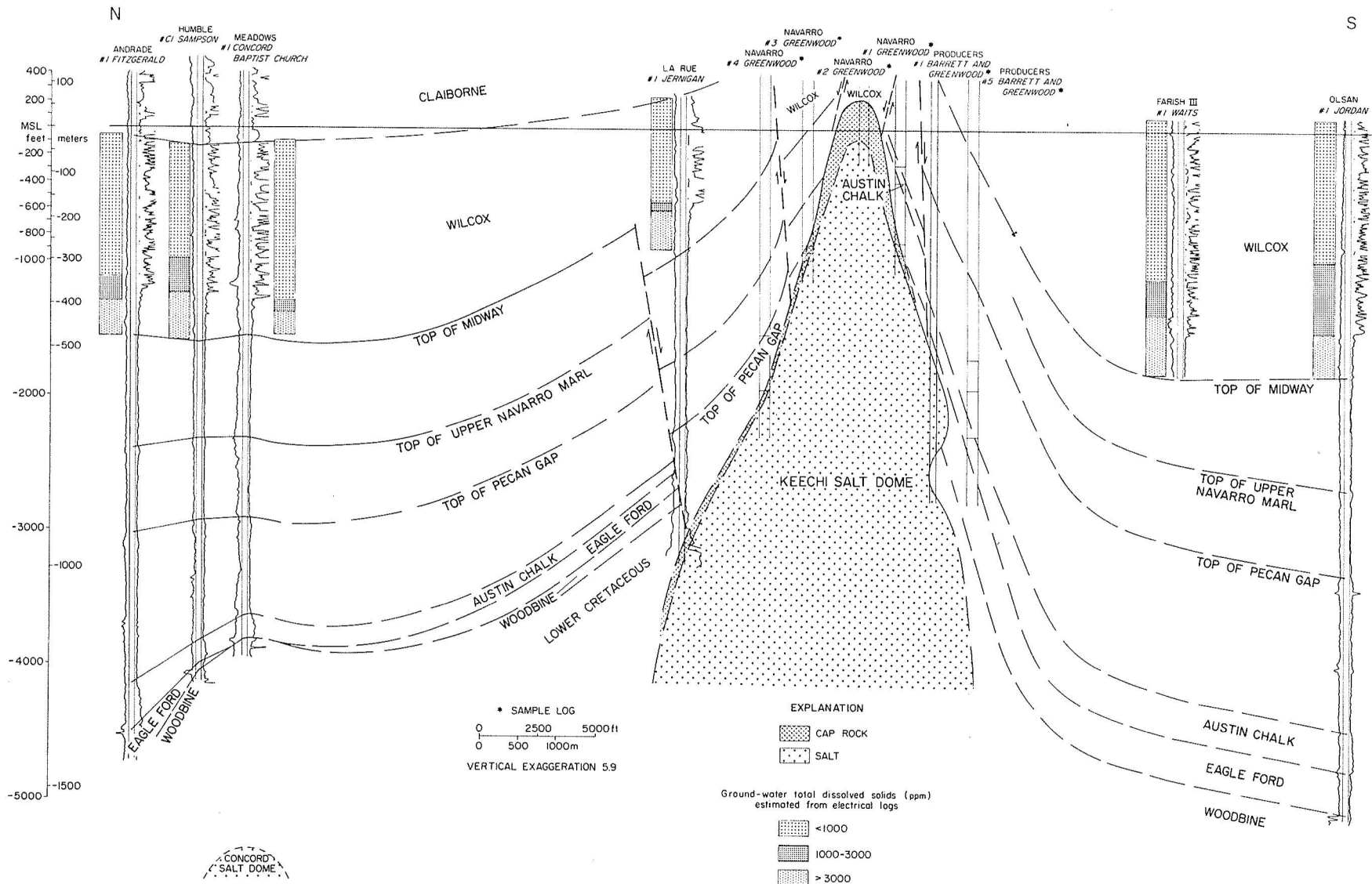
Figure 12. North-south structure section through Keechi Dome, Anderson County, Texas.
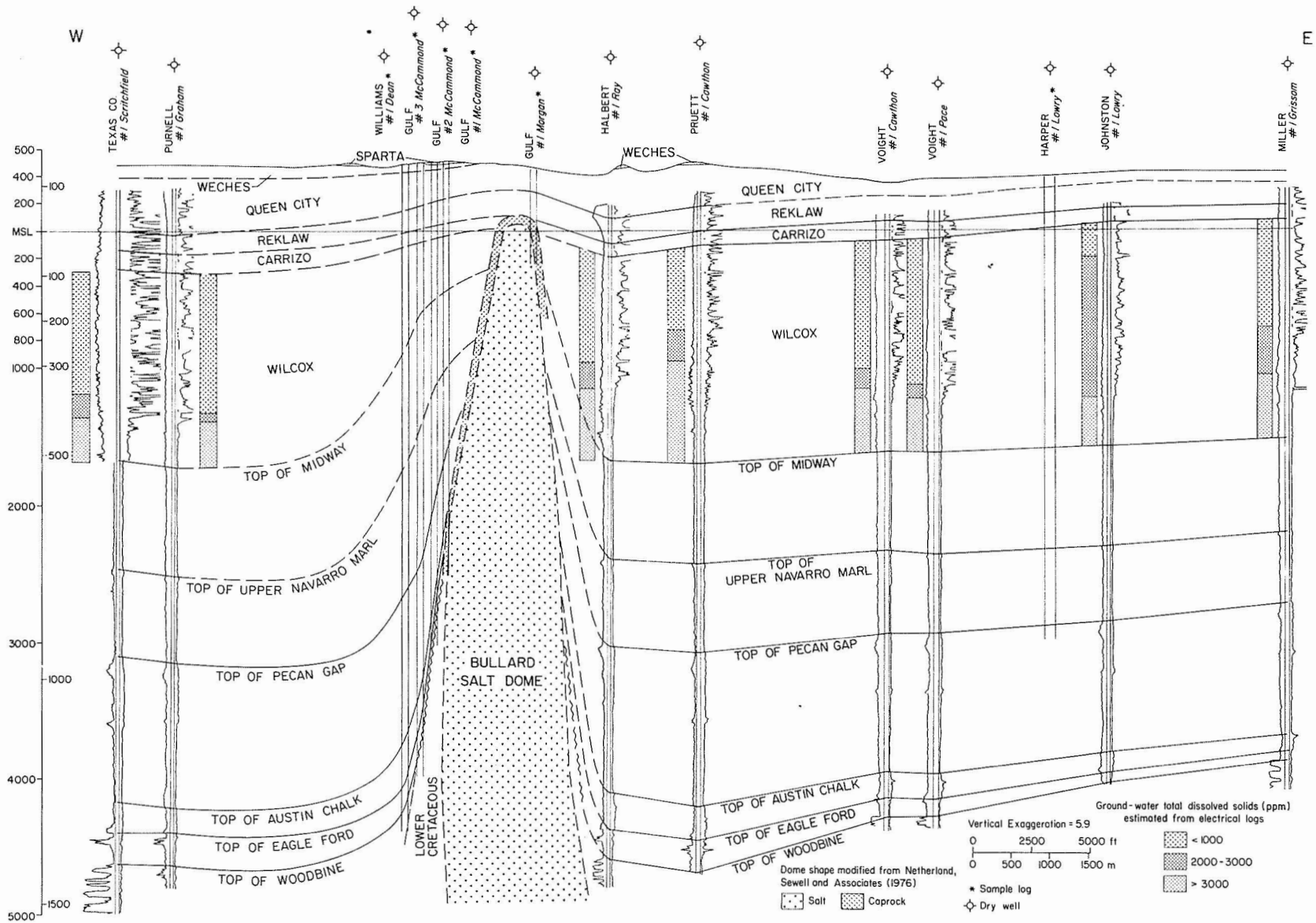
Figure 13. West-east structure section through Bullard Dome, Smith County, Texas.

23
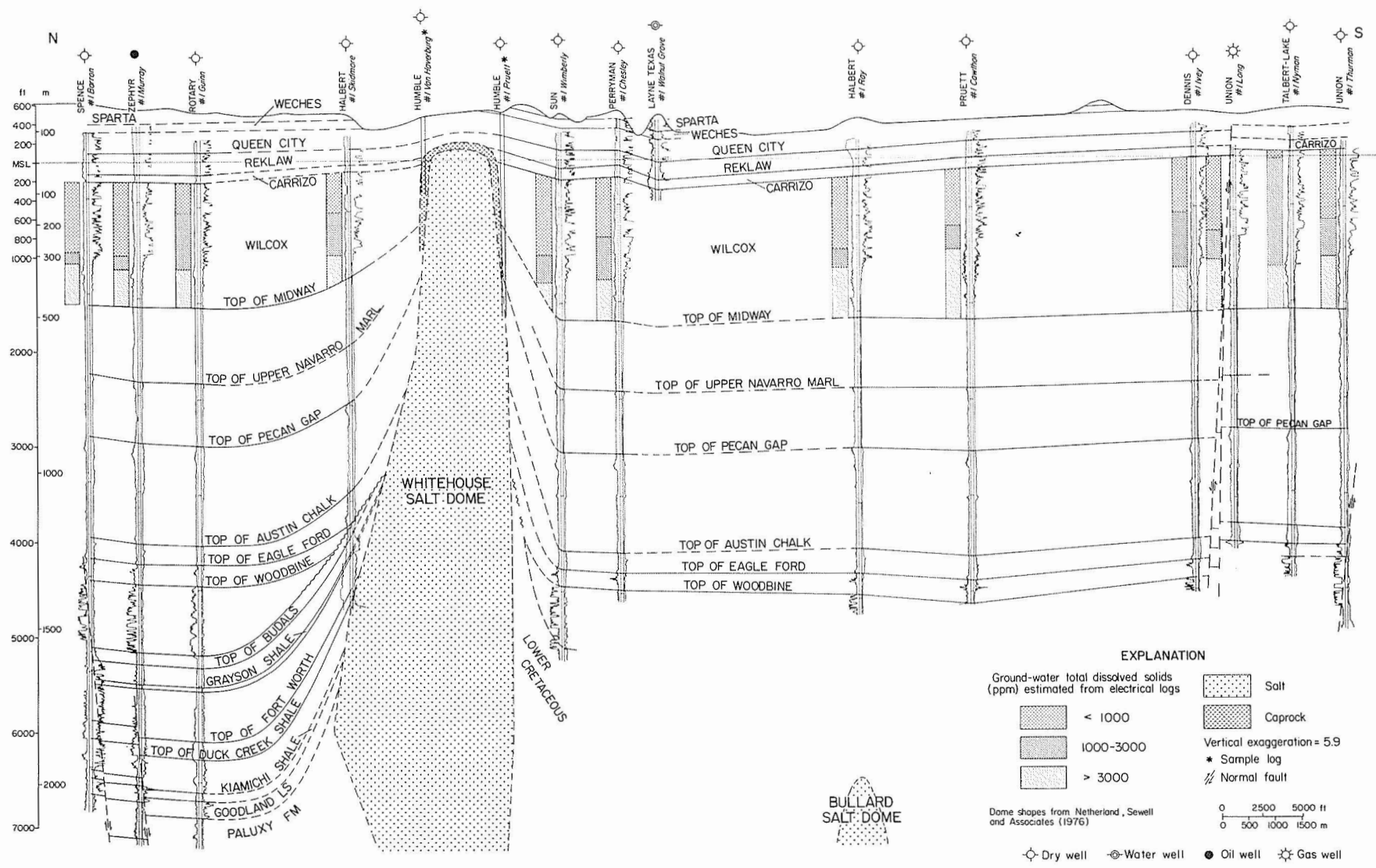
Figure 14. North-south structure section through Whitehouse Dome and the east flank of Bullard Dome, Smith County, Texas.
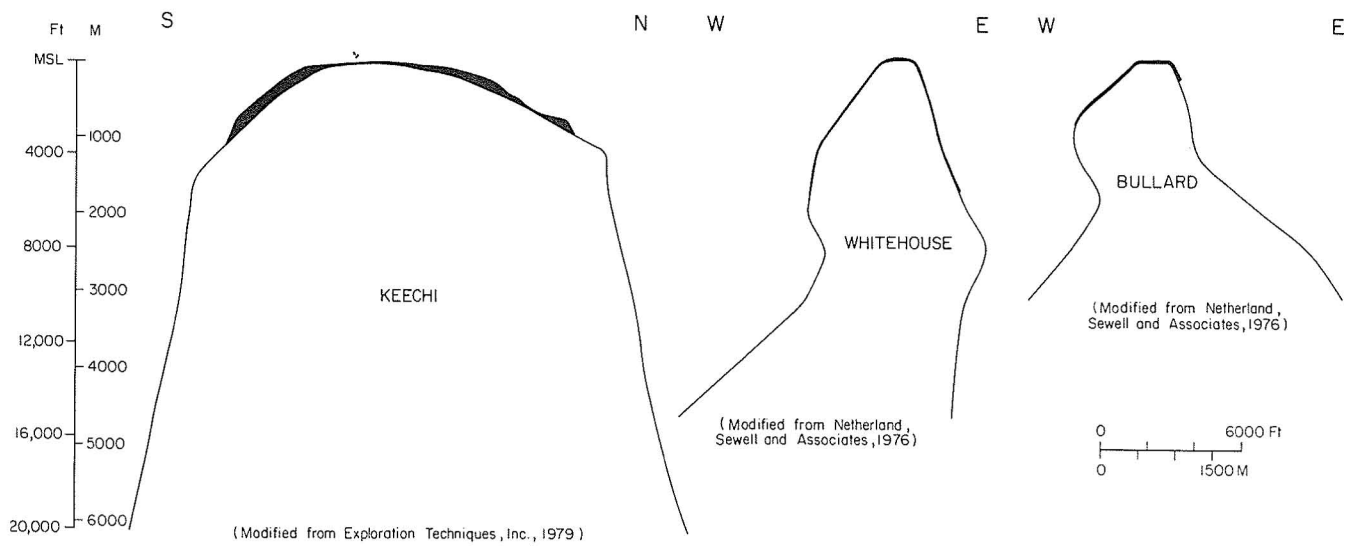
Figure 15. Domal sections with no vertical exaggeration. Black area indicates approximate cap rock. Cap rock on Whitehouse Dome is relatively thin.
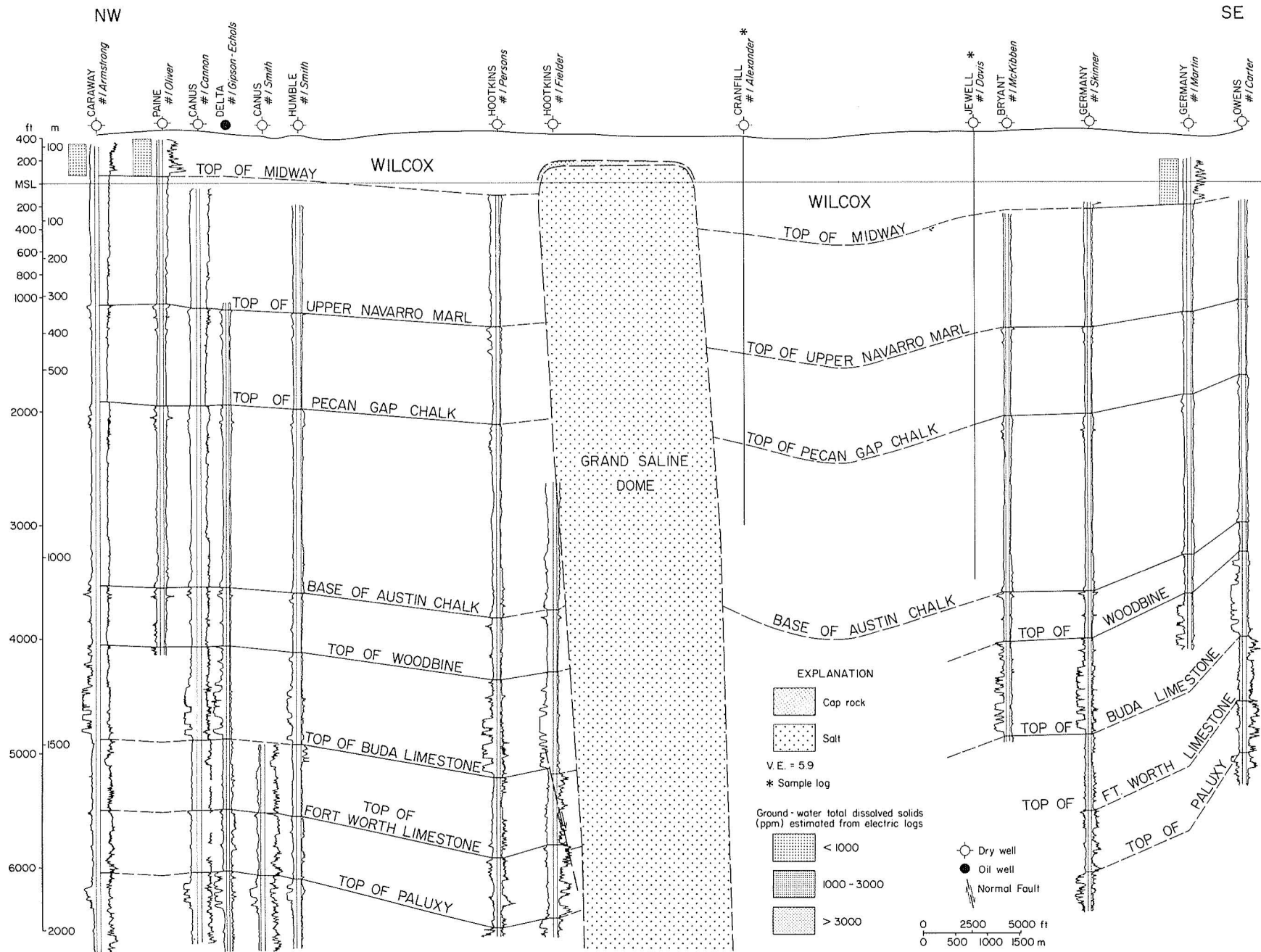
Figure 16. Northwest-southeast structure section through Grand Saline Dome, Van Zandt County, Texas.
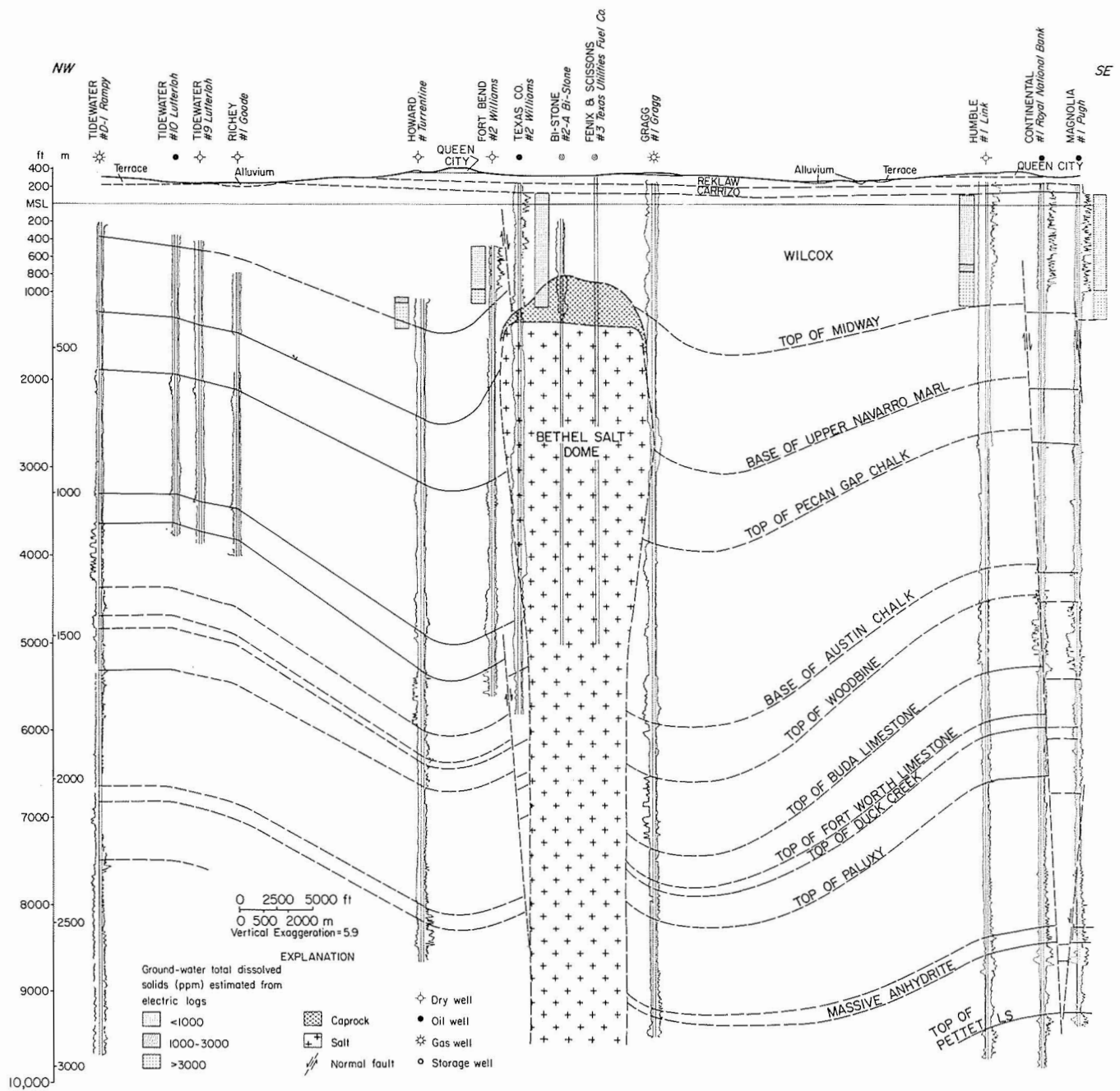
Figure 17. Northwest-southeast structure section through Bethel Dome, Anderson County, Texas.
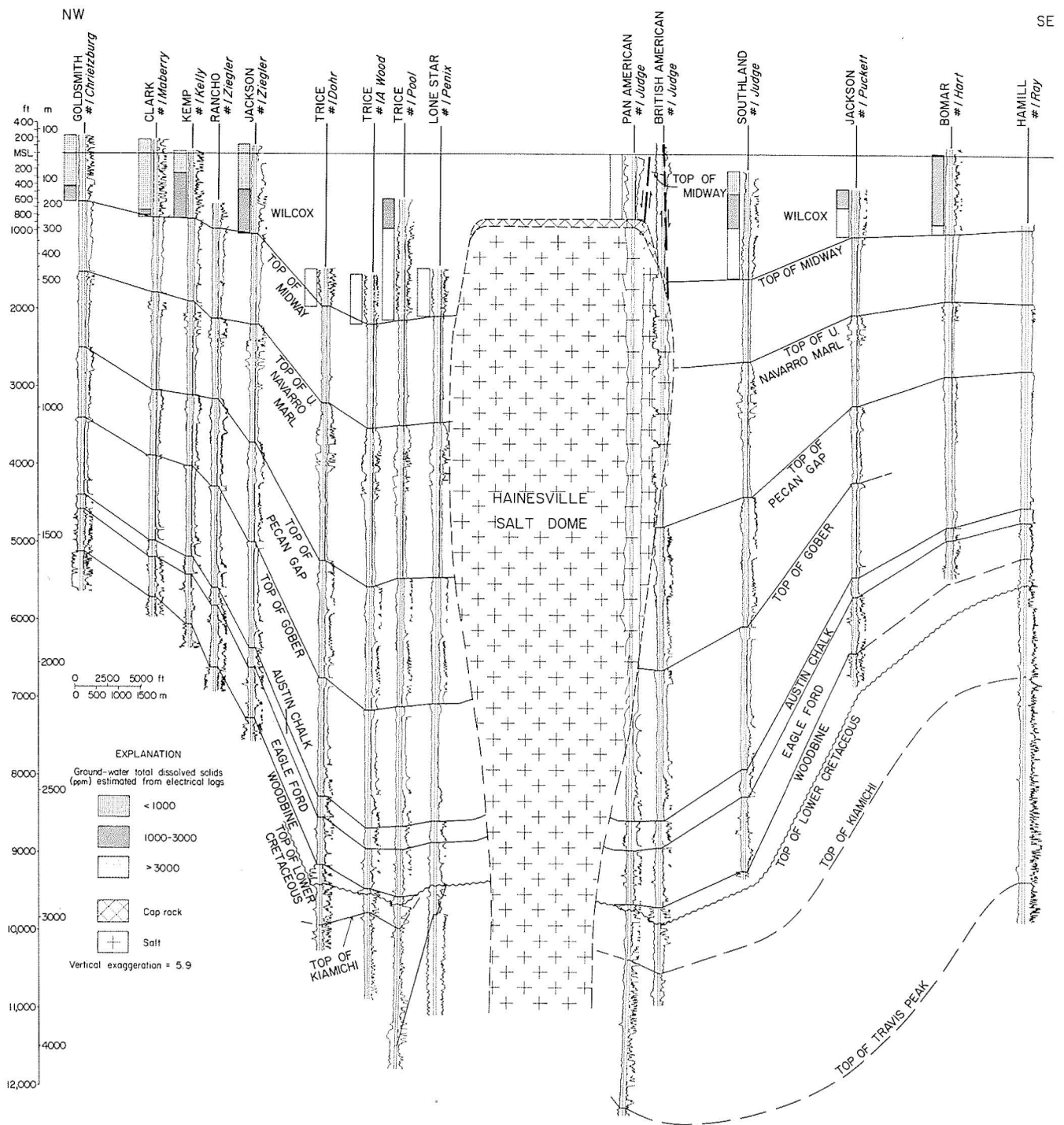
Figure 18. Northwest-southeast structure section through Hainesville Dome, Wood County, Texas.
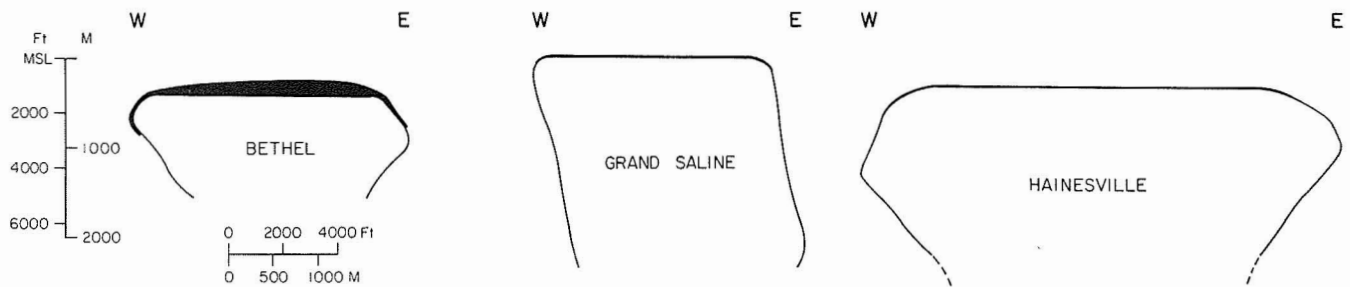
Figure 19. Domal sections with no vertical exaggeration. Black area indicates approximate cap rock. Grand Saline and Hainesville Domes have relatively thin cap rocks.

HYDROLOGIC STABILITY OF OAKWOOD DOME

Graham E. Fogg, Charles W. Kreitler, and Shirley P. Dutton

Oakwood Salt Dome apparently is in direct contact with the Wilcox aquifer. However, salinities observed around the dome do not indicate significant dome solution. Programs to evaluate dome solution include drilling, ground-water modeling, and petrographic studies of cap rock.

Oakwood Dome apparently is in direct contact with the Wilcox Group, a major fresh-water aquifer. The dome is probably vulnerable to salt dissolution, as suggested by Kreitler and others (1978, fig. 6), who noted that maximum salinities in the Wilcox aquifer increase from 2,000 to 8,000 ppm toward the dome. In every case, however, salinity anomalies occur in a thin, muddy sand layer near the base of the Wilcox Group. Because of low permeability and transmissivity in this muddy layer and its separation from upper, clean aquifer sands by 30 to 90 m (100 to 300 ft) of laterally continuous mudstone, the salinity values probably do not indicate significant dissolution rates.

Aquifers composed of clean sands higher in the Wilcox should have the greatest potential for dissolving salt, yet salinity values estimated from electric logs (fig. 20) and measured in water well samples from these sands document a general absence of salt dissolution. Figure 20 shows anomalously high salinities near the updip flanks of the dome and in an elongate plume that extends to the northeast and contains 2,000 to 4,000 ppm dissolved solids. If these sands are in contact with the dome, then the observed salinities are unexpectedly low, since water in such sands should be almost saturated with sodium and chloride (approximately 300,000 ppm) near the flank of the dome. Furthermore, according to the regional hydraulic gradient, any saline plume should extend down gradient to the southeast of the dome. Here, however, the Wilcox aquifer does contain such saline anomalies (fig. 20).

Three conditions may be responsible for the apparent lack of salt dissolution at Oakwood Dome. First, the cap rock may protect the salt from circulating ground water. Second, near-dome facies changes in the Wilcox may cause permeabilities to decrease toward the dome. Third, high salinities around Oakwood may be diluted by abundant recharge of fresh water over the dome and by subsequent mixing and solute dispersion.

If the dome formed a topographic high during Wilcox deposition (Agagu, 1979, personal communication), Wilcox facies may have become muddier near the flank of the dome, as several electric logs near the dome indicate. Although geophysical logs recently obtained from the drilling program in hole 2A (located about 610 m, 2,000 ft,

southeast of the dome flank) reinforce this idea by showing that the Wilcox is relatively muddy, the evidence is inconclusive.

Recharge directly over Oakwood Dome may be greater than in surrounding areas, as suggested by hydraulic heads that appear to increase toward the dome in both the Wilcox and the Carrizo aquifers. Such an increase in recharge could be caused by a combination of three factors: (1) the area over the dome is a regional, topographic high; (2) the Wilcox and Carrizo are uplifted slightly over the dome so that the aquifer crops out in a small recharge area over the dome; and (3) the uplift has produced faults and disrupted aquitards.

Three ongoing programs are designed to evaluate the causes for the absence of salinity anomalies around salt domes and Oakwood Dome in particular: (1) a drilling program at Oakwood Dome to evaluate distribution of hydraulic head, water chemistry, and aquifer/aquitard lithology and permeability; (2) a numerical ground-water modeling program to analyze the complexities of ground-water flow and solute dispersion induced by dome geometry and uplift, recharge over the dome, topographically controlled recharge and discharge, and aquifer/aquitard lithologies; and (3) cap rock evolution studies to determine characteristics of dome dissolution through geologic time and the ability of the cap rock to isolate the salt from circulating ground water.
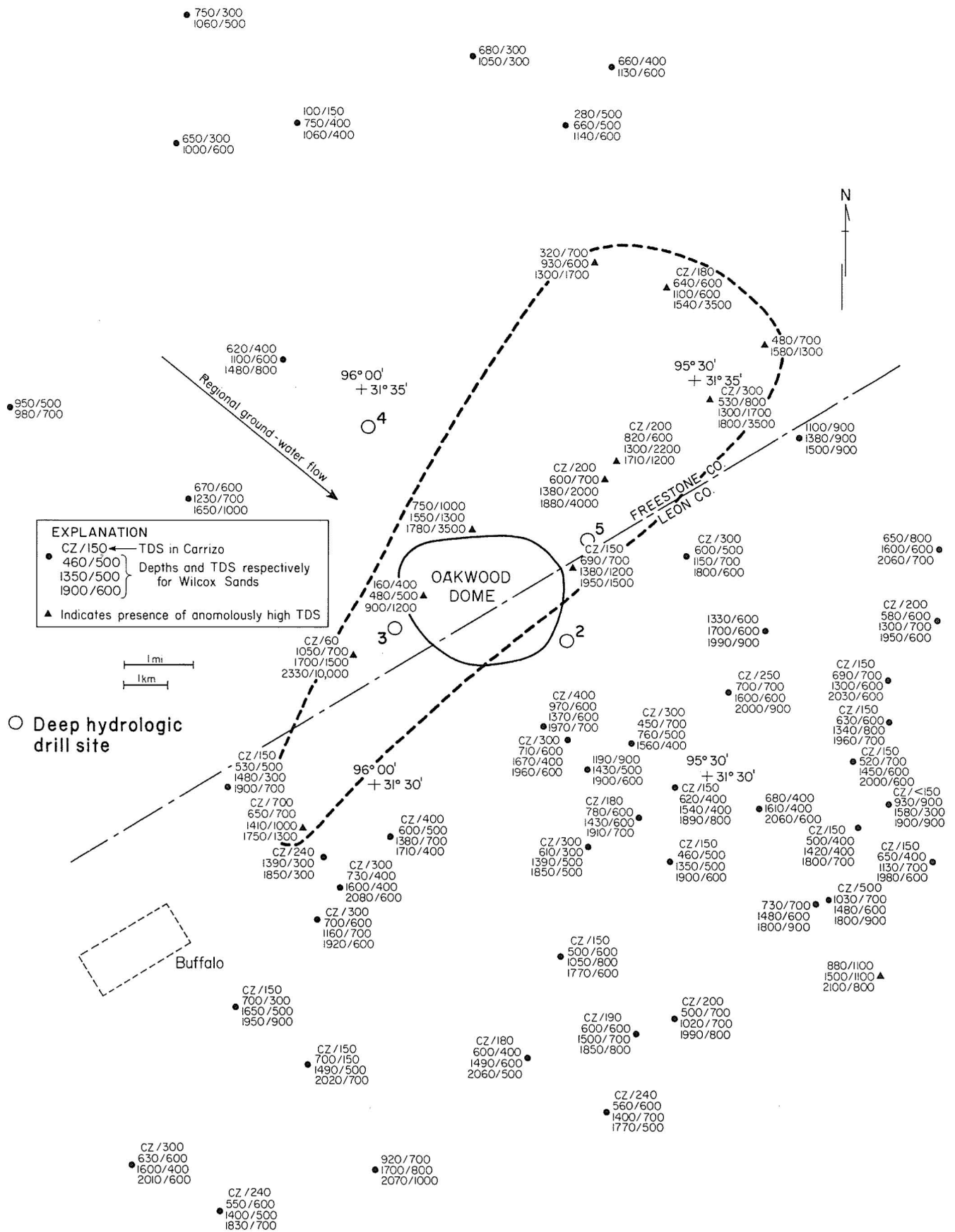
Figure 20. Ground-water salinity estimates in the Carrizo and major sands of the Wilcox. Anomalous salinities are found close to the updip flanks of the dome and in an elongate plume extending to the northeast.

DRILLING AND HYDROGEOLOGIC MONITORING AT OAK-WOOD SALT DOME

Graham E. Fogg

A hydrogeologic drilling program at Oakwood Dome was designed to evaluate the three-dimensional distribution of salinity and other chemical parameters, hydraulic gradient, aquifer/aquitard framework and permeability, and salt/cap rock characteristics.

On the basis of preliminary hydrogeologic studies at Oakwood Dome, a drilling program has been designed to provide the following information:

(1) Distribution of ground-water chemistry, including carbon-14 age dates;

(2) Hydraulic gradients and aquifer permeabilities needed to calculate ground-water velocity fields;

(3) Geologic framework, including distributions of aquifer heterogeneities and their associated heterogeneous permeabilities to provide an understanding of mass transport phenomena;

(4) Values of radionuclide adsorptive coefficients;

(5) Salt/cap rock characteristics;

(6) Fluctuation of long-term ground-water levels in response to recharge and vertical leakage across aquitards.

The drilling program was originally designed to include four well clusters located in each quadrant flanking the dome (sites 2, 3, 4, and 5) and a salt/cap rock core hole located directly over the dome (site 1) (see fig. 20). Sites 2 and 4 are located nearly parallel to the regional hydraulic gradient. Consequently, because of the regional hydraulic gradient, site 2 is located for sampling salinities immediately downdip of the dome. Well 2A, at site 2, which was completed in 1979, verifies existing electric log data documenting that, contrary to the regional hydraulic gradient, salinities immediately down-gradient from Oakwood Dome do not increase noticeably as a result of any salt dissolution. Site 4 is located so that it will provide background data that are unaffected by the dome. Site 3 is situated off the west flank of the dome where hydrologic data are sparse. Site 5 is positioned for an investigation of the saline/brackish ground-water plume that extends northeastward from the dome.

Each well cluster was designed to consist of eight wells: four production wells and four corresponding observation wells screened in various parts of the Wilcox-Carrizo system. The sequence of drilling at each site was as follows: (1) drill one deep-pilot hole through the Nacatoch Sand (at about 900 m or 3,000 ft), and core 30 m (100 ft) of Nacatoch Sand; (2) plug back to the Wilcox, and complete as a production or

observation well in a lower Wilcox Sand; and (3) drill the other seven wells at short spacings from the pilot hole, and complete in zones determined from geophysical logs, cores, and cuttings collected in the pilot hole.

Pumping tests lasting at least 24 hours were programmed to provide water samples and measurements of aquifer permeability and storativity in each production well. Maximum testing efficiency can be achieved by high-quality well construction, fully penetrating wells, and drawdown measurements in both production wells and observation wells.

The Wilcox aquifer was cored at site 2 in 1979. Analysis of the Wilcox core is intended to provide the following information: (1) nature of depositional environments and permeability of respective facies as related to dome growth history, (2) values of radionuclide adsorption coefficients, (3) sedimentary geochemistry and mineralogy, and (4) resource potential of deep lignite-bearing strata.

At site 2, monitoring wells at three different depths and the Wilcox core were completed. At site 5 and at the salt core site, wells in the Carrizo aquifer were completed. In addition to these wells, 10 shallow piezometers have been installed in the Carrizo and Queen City Formations.

Because of funding cutbacks from the Office of Nuclear Waste Isolation (ONWI), the number of wells in the monitoring program was significantly reduced. Funding cuts will greatly reduce the capability to interpret the hydrology around Oakwood Dome, or around any dome in the East Texas Basin. Available information will be used to develop the best, but an incomplete, picture of salt dome dissolution. Hydraulic heads in all wells, including those containing shallow piezometers in the Queen City and Carrizo aquifers, will be measured continuously over a 2-year period to provide boundary conditions needed to develop numerical ground-water models with which most of the hydrogeological data will be analyzed.

AQUIFER MODELING AT OAKWOOD DOME

Graham E. Fogg

Aquifer modeling by numerical methods is being used to analyze hydrogeologic conditions around Oakwood Salt Dome. A preliminary test model that considers only the effects of the dome itself on a three-dimensional flow field shows very local deflections of ground-water flow lines.

Aquifer modeling by numerical methods is being used to analyze the hydrogeologic system near Oakwood Salt Dome. Current efforts are addressed to construction of a detailed ground-water flow model. TERZAGI, the flow modeling program being used, employs an integrated finite difference, mixed explicit-implicit numerical scheme for solving problems of one-, two-, or three-dimensional fluid movement in fully or partially saturated porous media with vertical consolidation in the saturated zone. The theory behind TERZAGI, a description of its algorithm, and its applications to problems can be found in literature describing its two related programs, TRUST and FLUMP. TRUST, described by Narasimhan and Witherspoon (1977 and 1978) and Narasimhan and others (1978), is identical to TERZAGI, except that it includes vertical consolidation in both the fully and partially saturated zones. FLUMP, described by Fogg and others (1979), Narasimhan and others (1977), Neuman and Narasimhan (1977), and Narasimhan and others (1978), was developed from a version of TRUST by replacing the integrated finite difference matrix generator with a finite element matrix generator. TERZAGI was chosen because it is a flexible program which yields accurate answers to complex problems.

A preliminary simulation of flow through the Wilcox-Carrizo system, including the effects of the dome geometry on the three-dimensional flow field, has been completed. The purpose of this exercise was to discover how the dome itself affects flow patterns; consequently, it is a greatly simplified analysis. The three-dimensional, integrated finite difference (IFD) mesh is shown in figure 21. The radial node arrangement was chosen because it is an efficient, easy means of closely spacing nodes near the dome, where greater accuracy may be required because of abrupt changes in hydraulic gradient. Only half the dome area was modeled because the simple formulation of the problem makes it geometrically symmetric. The three layers used in the mesh do not represent lithologic layers, but are included to represent the vertical arrangement of the Wilcox-Carrizo aquifers around the dome and to allow vertical fluid movement. Transmissivity of each layer is one-third the total transmissivity of the Wilcox-Carrizo system, as estimated from pumping test esti-

mates of hydraulic conductivities in the East Texas Basin and average sand thicknesses estimated from electric logs located in the Oakwood Dome area. Regional dip of the aquifers is taken into account by tilting the mesh at an angle determined from electric log correlations. Boundary conditions are prescribed head on the updip and downdip margins and prescribed (zero) flux on the lateral boundaries.

Hydraulic heads computed by the model (fig. 22) show that the dome causes only a local deflection of ground-water flow lines, both vertically and horizontally. The general absence of vertical movement is shown by the fact that heads in each layer plot directly on top of one another except against the downdip flank of the dome, where heads in the upper layer (shown as dashed contours) are slightly higher than those in the lower two layers. Finer contour spacing would show a similar vertical gradient directed upward on the updip flank. Nevertheless, vertical flow rates computed by the model show vertical upward flow from the lower two layers to the upper layer along the northwestern flank of the dome to be 181 m^3 per day (53 acre-ft per year), or twice the value for the entire northern flank. Flow magnitude is exactly the same along the southern flank, but flow direction is reversed. Values are virtually unaffected by truncation errors induced by the numerical scheme, since the maximum error in mass balance at nodes surrounding the dome was only 0.5 m^3 per day (0.15 acre-ft per year).

Vertical flow rates are a small fraction of the lateral flow rates; however, they may be significant to solute transport. On the other hand, vertical upward movement may be nullified or reversed by recharge occurring over the dome and/or by permeabilities that are anisotropic with the maximum permeabilities oriented along the horizontal plane. The Wilcox aquifer, because of its mode of deposition, is most likely anisotropic on both lithologic and pore scales. Despite its lack of detail, the model provides information with which to plan test drilling and subsequent modeling.

The next step of the modeling program will incorporate all relevant aspects of the flow systems in the Oakwood Dome area. These aspects will be determined as the model is built and tested and more data are collected through drilling, testing, and monitoring. The following factors of potentially major importance will be included in the model:

(1) Three-dimensional permeability distributions, including effects of sedimentary facies patterns and the structural fabric;

(2) Variations in recharge and discharge caused by effects of topography; and

(3) Vertical fluid movement within aquifers and across aquitards.

Boundaries of the model will be extended to potentially important recharge and discharge areas in the region around Oakwood Dome.

Heterogeneous permeability distributions around Oakwood and Keechi Domes are being studied through graphic correlation of electric logs, as shown in figure 23. Sandbody distribution in the Wilcox Group is being used to subdivide the unit into hydrogeologic facies. On the basis of this work, maps of net sand, muddy sand, and clay/shale have been completed for three separate layers in the Wilcox within a 16-km (10-mi) radius of Oakwood Dome. Existing data provide the geologic framework, but can only be valid input into the model with good permeability estimates of the various facies. The drilling program is designed to provide this information through pumping tests and analysis of core samples. Core samples are also necessary for validating interpretations now being made solely from resistivity logs.

Macroscopic solute dispersion in the Wilcox aquifer is caused by the types of heterogeneities shown in figure 23. For years, hydrologists, through the use of a coefficient of dispersivity in a solute transport equation, have been attempting to describe the effects of aquifer heterogeneities on ground-water flow. However, the dispersivity is scale dependent and can seldom be measured on a scale that is representative of most solute transport problems. Existing methods for predicting dispersion are inadequate. Currently, research is being conducted to study ways of analyzing the dispersive qualities of the Wilcox by a statistical characterization of its heterogeneities as indicated by hydrogeological borehole data and depositional systems. Much of this effort is based on the work of Schwartz (1977), who uses deterministic flow models to analyze the effects of hypothetical aquifer heterogeneities on dispersivity, and Neuman (in press), who discusses the work of many authors on characterization of aquifer heterogeneities.

Plan   Cross-Section

Nodal point and associated nodal volume
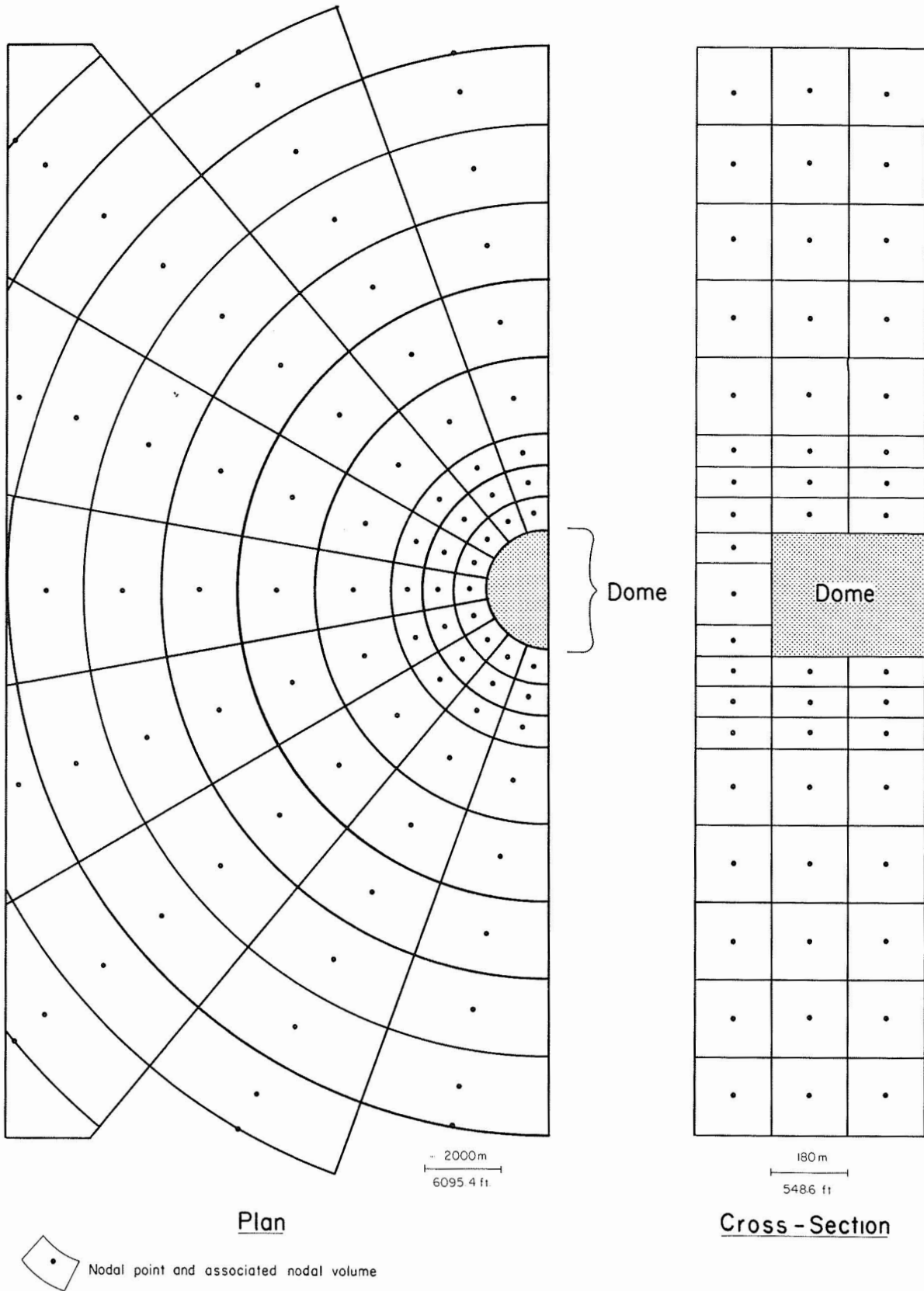
Figure 21. Integrated finite difference (IFD) mesh for preliminary model of flow around Oakwood Dome. One advantage of the IFD method is that it allows one to deform nodes into arbitrary shapes.
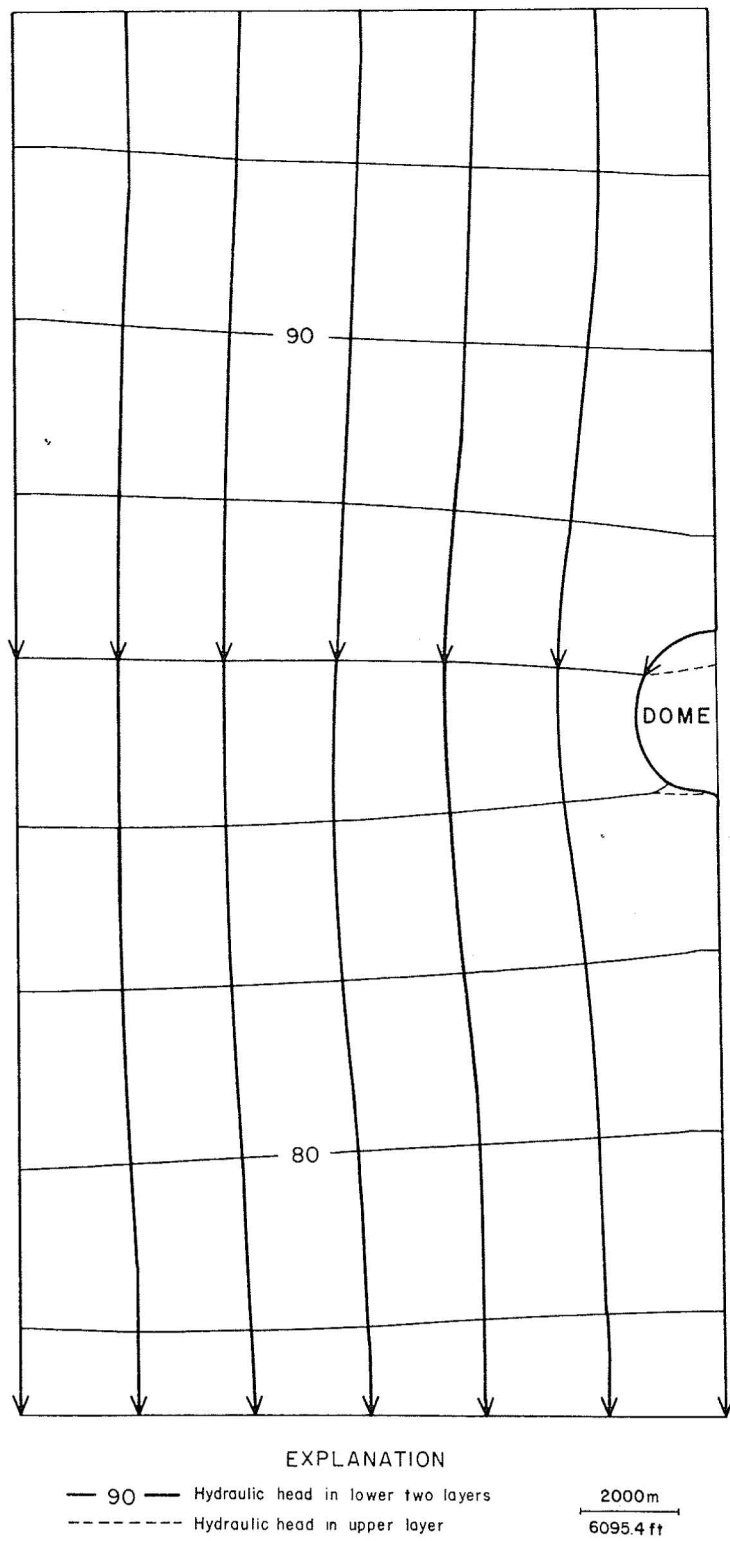
Figure 22.   Computed heads from preliminary model of flow around Oakwood Dome. The model indicates only a local perturbation of flow lines by the dome.
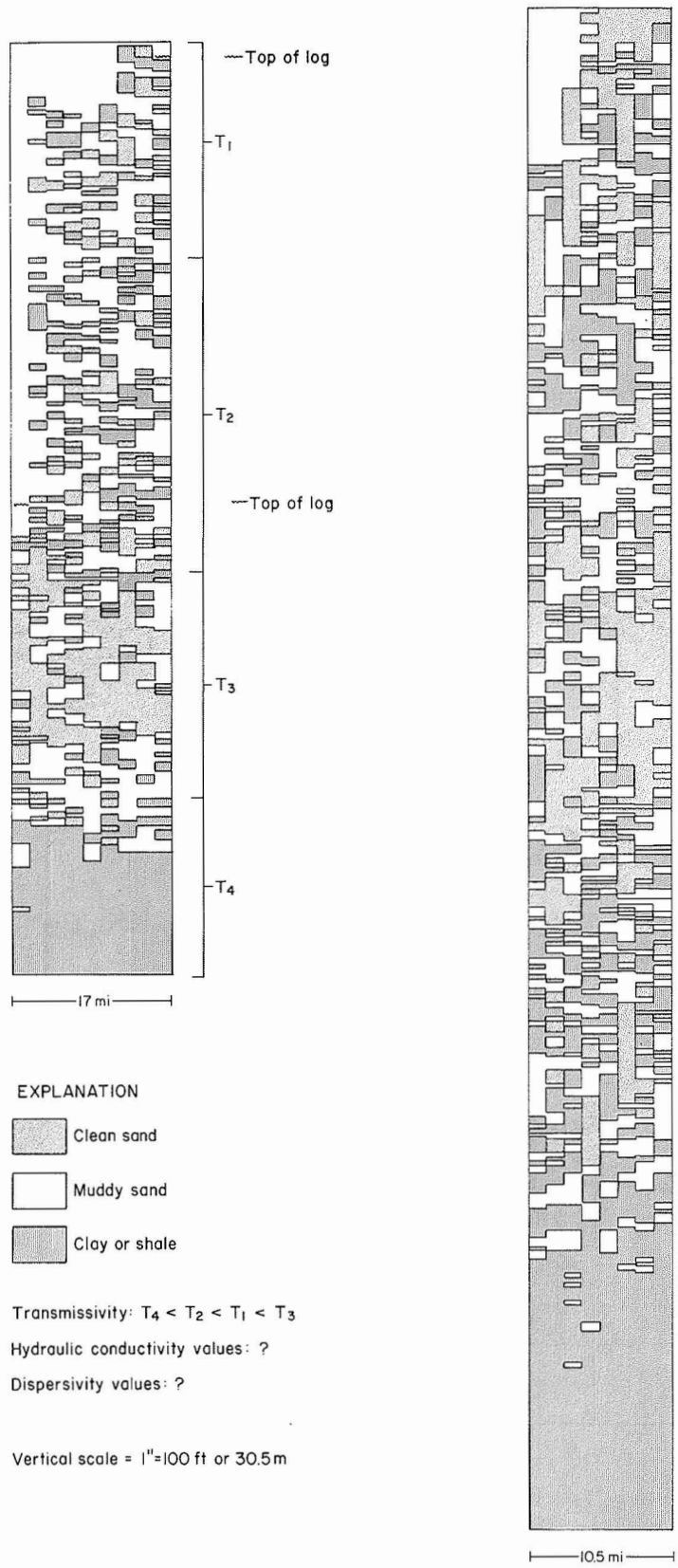
Figure 23. Graphic correlation of Wilcox Group heterogeneities using electric logs from Oakwood and Keechi Dome areas (left and right, respectively). Around Oakwood, the muddy layer labelled "T_2" may be an important aquitard, partially separating more transmissive zones above and below.

40

STUDIES OF CAP ROCK ON GYP HILL SALT DOME

Shirley P. Dutton and Charles W. Kreitler

The cap rock on Gyp Hill Salt Dome consists of gypsum near the surface (0 to 90 m, 0 to 300 ft) and gypsum-cemented anhydrite above the salt (90 to 273 m, 300 to 895 ft). The cap rock formed by concentration of insoluble anhydrite grains as the dome salt dissolved.

At Gyp Hill, located in Brooks County, Texas, a continuous core was taken from the surface through the cap rock and about 6 m (20 ft) into underlying salt. The upper 90 m (300 ft) of the core consist of bladed and equigranular gypsum crystals; common solution-enlarged fracture and vug porosity occur between crystals. Minor amounts (<1 percent) of anhydrite and carbonate are present as inclusions in the gypsum.

About 90 m (300 ft) deep, there is a transition downward from coarsely crystalline gypsum to gypsum-cemented anhydrite (fig. 24). The lower part of the cap rock (90 m to 273 m, 300 to 895 ft) consists of anhydrite crystals surrounded by varying amounts of poikilotopic gypsum cement (fig. 25) and chaotic masses of fine-grained anhydrite (fig. 26). Porosity and permeability are low throughout most of this interval (table 1). However, immediately above the salt (268 to 273 m, 880 to 895 ft) there is very little gypsum cement, and porosity is as high as 20 percent (fig. 27).

Cap rock formation at Gyp Hill apparently occurs by dissolution of salt and accumulation of insoluble material. Salt samples contain 13 to 42 percent anhydrite crystals (fig. 28) and less than 1 percent carbonate. Salt dissolution at the salt-cap rock boundary concentrates this residue into a porous sandstone composed of anhydrite crystals. Porosity is occluded a short distance above the salt (table 1) by precipitation of gypsum cement and by compaction and crushing of some anhydrite crystals caused by overburden pressure (fig. 26). The interface between cap rock and salt at Gyp Hill Dome exhibits moderate permeability (45 md); therefore, salt solution can continue to occur. The fact that the cap rock represents an accumulation of anhydrite indicates that there has been significant dissolution of the dome.
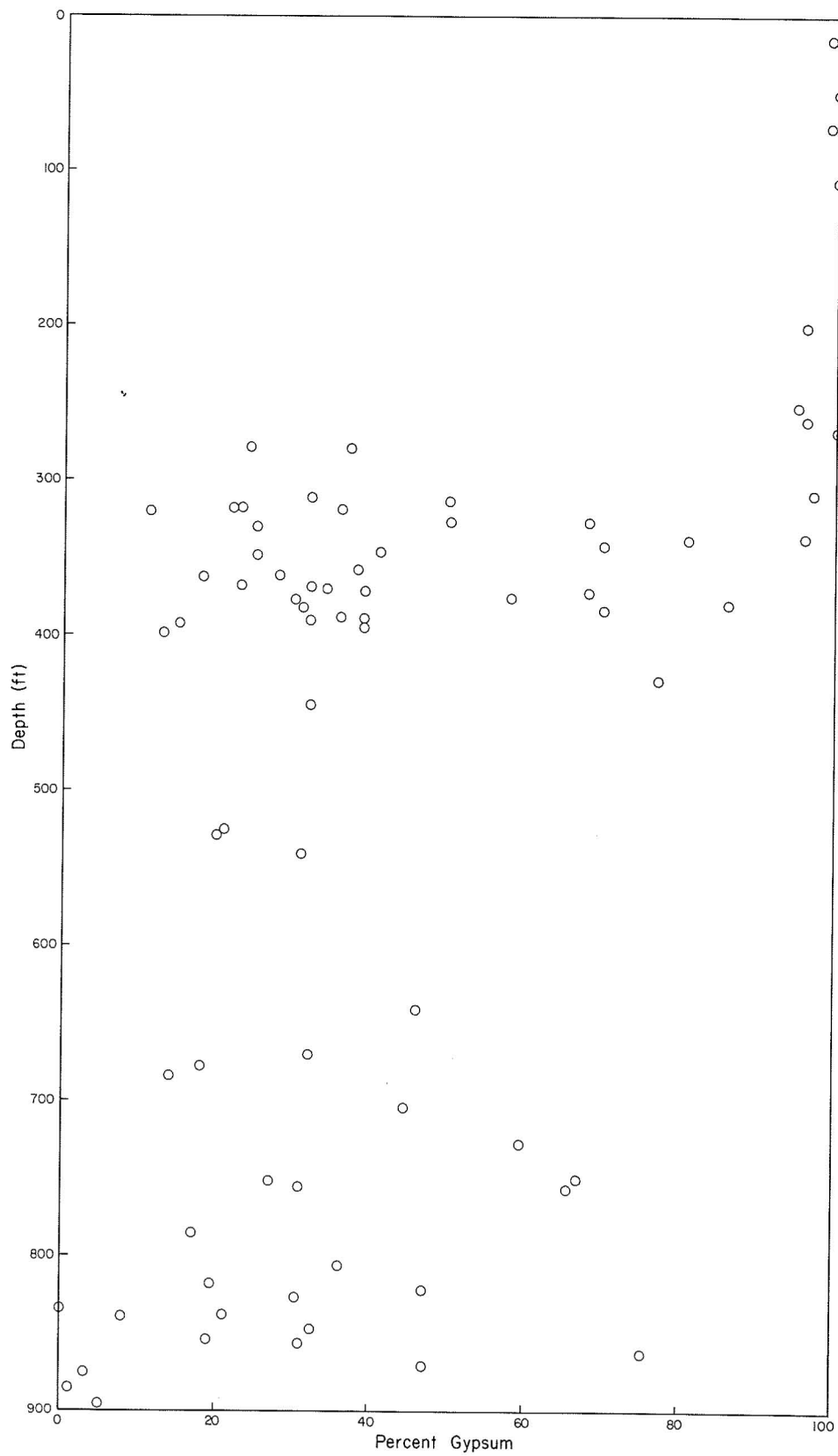
Figure 24. Percent gypsum versus depth in Gyp Hill cap rock. The non-gypsum fraction of the cap rock consists of anhydrite and rare calcite and pyrite.
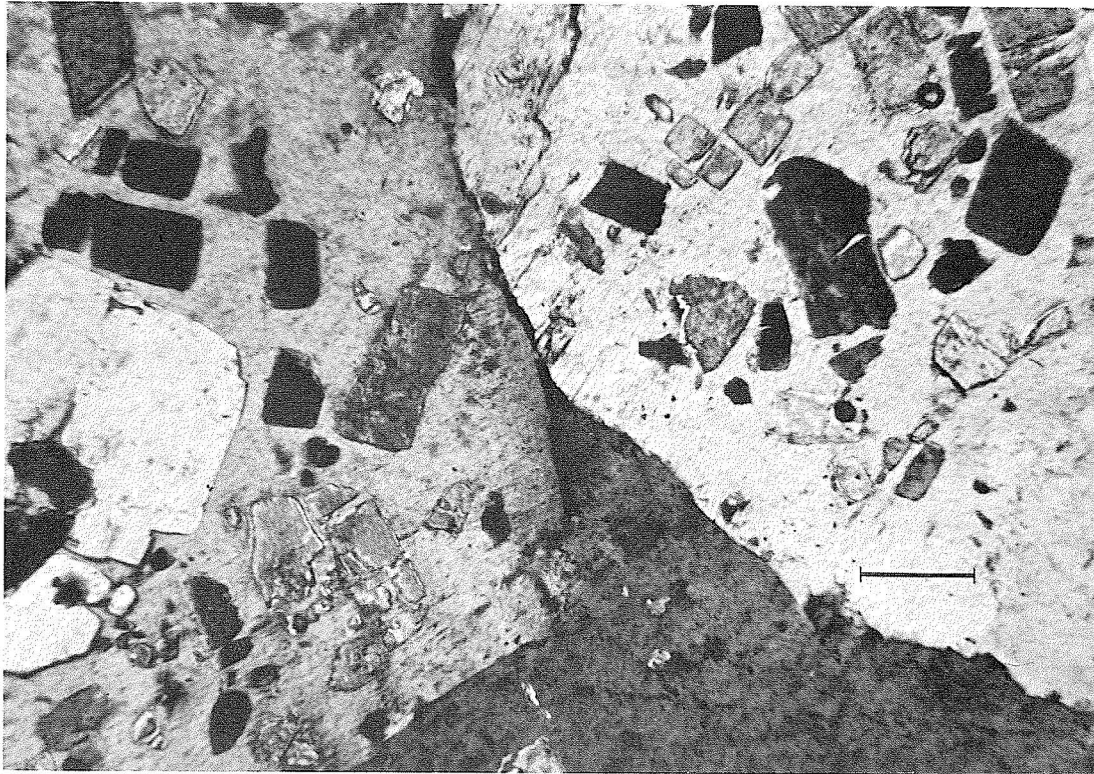
Figure 25. Rectangular anhydrite crystals surrounded by poikilotopic gypsum cement from 262.7 m (862 ft). Scale bar = 0.3 mm.

Figure 26. Rectangular anhydrite crystals surrounded by chaotic mass of fine-grained anhydrite. Depth is 160.0 m (525 ft). Scale bar = 0.3 mm.
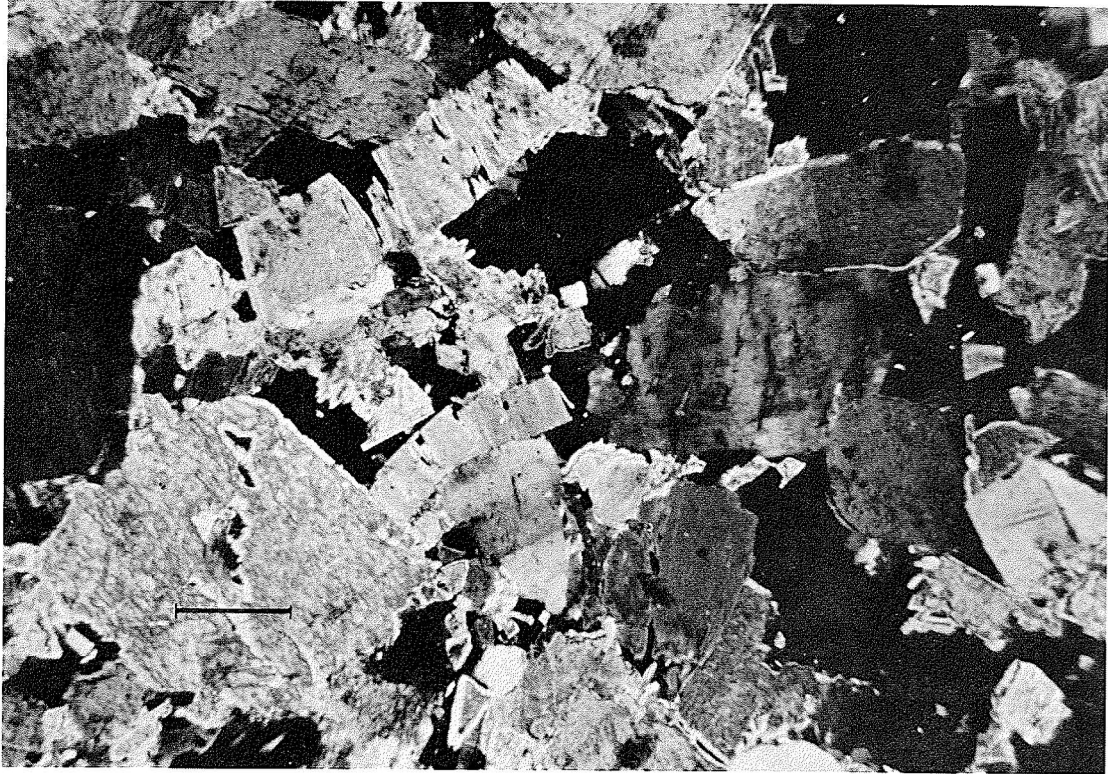
Figure 27. Porous anhydrite sand immediately above the salt at a depth of 272.8 m (895 ft). Porosity (black patches) is 20 percent in this sample. Scale bar = 0.3 mm.
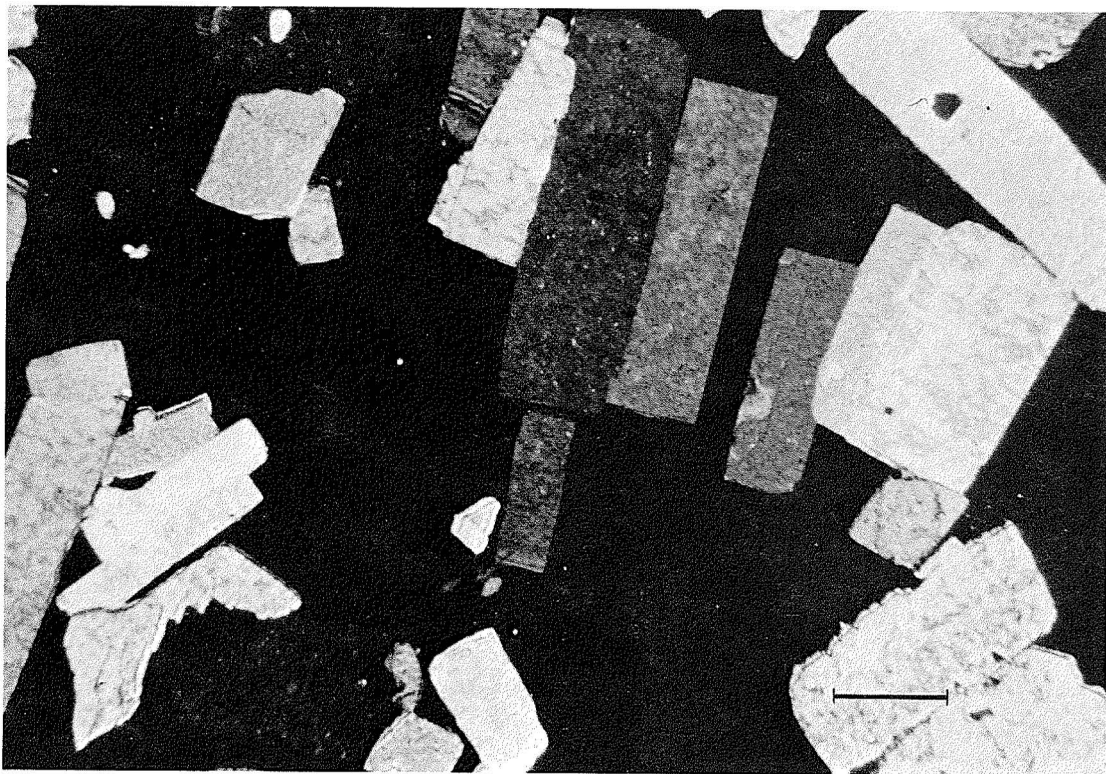
Figure 28. Rectangular anhydrite crystals in salt (black mineral). Depth is 278.9 m (915 ft), which is 6.1 m (20 ft) into the salt. Scale bar = 0.3 mm.

Table 1. Physical characteristics of Gyp Hill cap rock.

Depth (ft)	Permeability (md)	Porosity (%)	Density (g/cm^3)
50	0.01	1.6	2.35
123	0.01	3.0	2.35
152	0.01	1.4	2.58
171	0.01	2.0	2.34
230	0.01	2.5	2.33
272	0.01	1.2	2.43
284	0.01	3.4	2.81
310	0.01	1.3	2.35
340	0.01	1.5	2.81
370	0.01	1.3	2.77
400	0.01	2.6	2.50
428	0.01	1.6	2.65
500	0.01	5.1	3.00
600	0.01	2.6	2.97
690	0.01	3.1	2.97
740	0.01	3.3	2.92
794	0.01	1.6	2.78
815	0.01	2.2	2.95
835	0.01	1.6	2.82
855	0.01	3.6	2.97
875	0.01	4.4	2.88
890	45.00	20.0	2.99

IMPACTS OF SALT-BRINING ON PALESTINE SALT DOME

Graham E. Fogg and Charles W. Kreitler

Fifteen karstic collapse structures over the Palestine Salt Dome have been attributed to extensive brine production during the period 1904 to 1937. Three collapses have formed since 1937, one as recently as 1978. Palestine Dome is considered unsuitable as a nuclear waste repository because of the potential for additional collapses and because of the long-term impairment of the hydrologic security of the dome.

The Palestine Salt and Coal Company used brine wells to mine salt from Palestine Salt Dome during the period 1904 to 1937 (Powers, 1926; Avera, 1976). Hopkins (1917) mapped topography over the dome and locations of 16 brine wells drilled between 1900 and 1917 (fig. 29). Powers (1926) described the procedure used to mine salt:

> Wells are drilled to the caprock at 120 to 160 feet, casing is set, and then the well is deepened 100 to 250 feet in the salt. Water from a water sand under the caprock flows into the wells, dissolves the salt, and the brine is forced by compressed air to the plant.

Hopkins (1917) states:

> The main factor controlling the location of salt wells is the presence of a good caprock which serves as a seat for the casing and also holds up the overlying strata until a large cavity is dissolved out underneath it. When the supporting salt is sufficiently removed this rock, being undermined, caves in, with the overlying formations forming a large sink hole.

As of October 1979, 16 collapse structures had been found. Several of these are circular (in many cases water-filled) depressions that exhibit diameters of 8 to 32 m (27 to 105 ft) and depths of 0.6 to 4.5 m (2 to more than 15 ft) (fig. 30). Hightower (1958) mapped 13 sinks (fig. 31) and assumed that each marked the location of a former brine well. Sink 8 does not appear on Hightower's map but nonetheless must have occurred during the brining operations because it can be identified on aerial photographs dating as far back as 1932.

At least three collapses have occurred since brining ceased in 1937. Comparison of aerial photos of Palestine Dome in 1932, 1940, 1956, 1960, and 1976 (table 2) to the surface geology map of Hightower (1958) indicates that sink 14 (fig. 31) formed between 1956 and 1958, and sink 5 formed between 1960 and 1976. Mrs. Morris, the landowner, states that sink 5 occurred within minutes after her daughter drove an automobile over the site in 1972. Additionally, in 1978 the land surface suddenly

collapsed underneath a foundation support of Mrs. Morris' trailer home (see fig. 31) and left a depression measuring approximately 1.2 m (4 ft) wide and 0.6 m (2 ft) deep. It is not known whether these collapses mark brine well locations, because no record exists of all such locations and because dissolution caused by brining could occur both near the well bore and randomly at some distance.

Locations of actual brine wells drilled before 1917 were mapped by Hopkins (1917) (fig. 29) and further demonstrate the potential for the occurrence of additional collapses. Hopkins mapped nine productive brine wells on the northeast side of Duggey's Lake in the vicinity of sink 14, yet there are only three sinks in this area (fig. 31). Thus, at least six more collapses could occur in this area. Similarly, Hopkins found three wells just east of the southwestern neck of the lake, where no sinks have been found. This area is characterized by rapid erosion upslope and sedimentation along the lakeshore. Therefore, any collapse features that may have occurred could have been obliterated by these processes. Similarly, erosion may have been precipitated by land surface collapse and consequent lowering of the base level of the local stream.

Some brine wells were drilled into the present lakebed. Aerial photographs indicate that at least one sinkhole was engulfed by the lake when, in the 1940's, the lake level was raised by the construction of a concrete spillway at its outlet. In a search for additional collapses in the lakebed, several bathymetric and shallow seismic reflection surveys were run across the lake in conjunction with the U.S. Geological Survey. The bathymetry showed the lakebed to be fairly uniform and to reach a maximum depth of 1.8 or 2.1 m (6 or 7 ft). Although no depressions were observed, they may be present underneath a thick muck layer that covers the lakebed. The seismic survey was unable to penetrate the muck layer.

Chemical analyses (table 3) of water samples from water-filled sinkholes, Mrs. Morris shallow dug well, and Duggey's Lake show some general trends in ground-water chemistry and flow over the Palestine Dome. Mrs. Morris' well and most of the sinkholes contain low-TDS water typical of shallow ground water in the region. Duggey's Lake and sinks relatively near the lake contain brackish water. The implied hydrologic picture is that of recharge in the hills that surround the lake, downward movement of water to the dome, dissolution, and then discharge of saline waters into the lake and into some of the sinks near the lake.

Duggey's Lake contains brackish water derived apparently from upward discharge from aquifers overlying the dome. Evidence that such upward discharge exists is provided by local residents and by Dumble (1891), who state that (before lake

47

impoundment in the early 1900's) the lake basin was often swampy and contained salt incrustations. The brining operations could be an additional cause of the high lake salinity, since salt from brine previously discharged into the soil may still be washing into the lake via surface runoff.

Most sinkholes contain fresh water, an indication that they either are isolated from or supply recharge to deeper aquifers (table 3). It is plausible that many sinkholes are isolated (or perched) ponds because they all contain a 0.6 to 1.2 m (2 to 4 ft) thickness of muck. Water from sites 1, 3, 6, and 8 contains relatively high salinities. The high salinity at site 1 is probably caused by its proximity to a salt flat adjacent to the lake spillway. The salt flat apparently is sustained by occasional brackish water discharge over the spillway and possibly by seepage of lake water underneath the spillway.

High salinities at sites 3, 6, and 8 suggest that these sinks receive upward discharge of saline water. In sink 8, a brine well, its casing intact, is open to a depth of at least 30.5 m (100 ft). Since the top of the cap rock is approximately 37 to 49 m (120 to 160 ft) deep at site 8, the well provides a conduit for direct hydraulic exchange between the cap rock and the sink. It is reasonable to assume that this has caused the water in the sinkhole to be even higher in dissolved solids than water in the lake (table 3). Mixing along the well bore is apparently enhanced by seasonal fluctuations in the water level in the sinkhole. During wet periods, the well casing in the sink is completely submerged, thus permitting recharge of fresh water. During dry periods, on the other hand, the water level in the sink drops below the top of the casing, continues to drop below the water level in the well, and thus provides a potential for vertical, upward discharge of saline water.

The continued occurrence of sudden land subsidence over Palestine Dome appears to be the result of continued salt dissolution caused by (1) efficient pathways for ground-water flow created by abandoned brine wells and solution cavities and (2) a hydrologic scenario that provides for recharge and salt dissolution and discharge over the dome. Moreover, it is impossible to predict where future land collapses and accelerated rates of salt dissolution will occur. Hydrologic considerations indicate that Palestine Dome is an unsuitable candidate for a nuclear waste repository.

As a result of these findings, the Office of Nuclear Waste Isolation, has officially recommended that Palestine Dome be eliminated from consideration as a potential repository (Patchick, 1980).
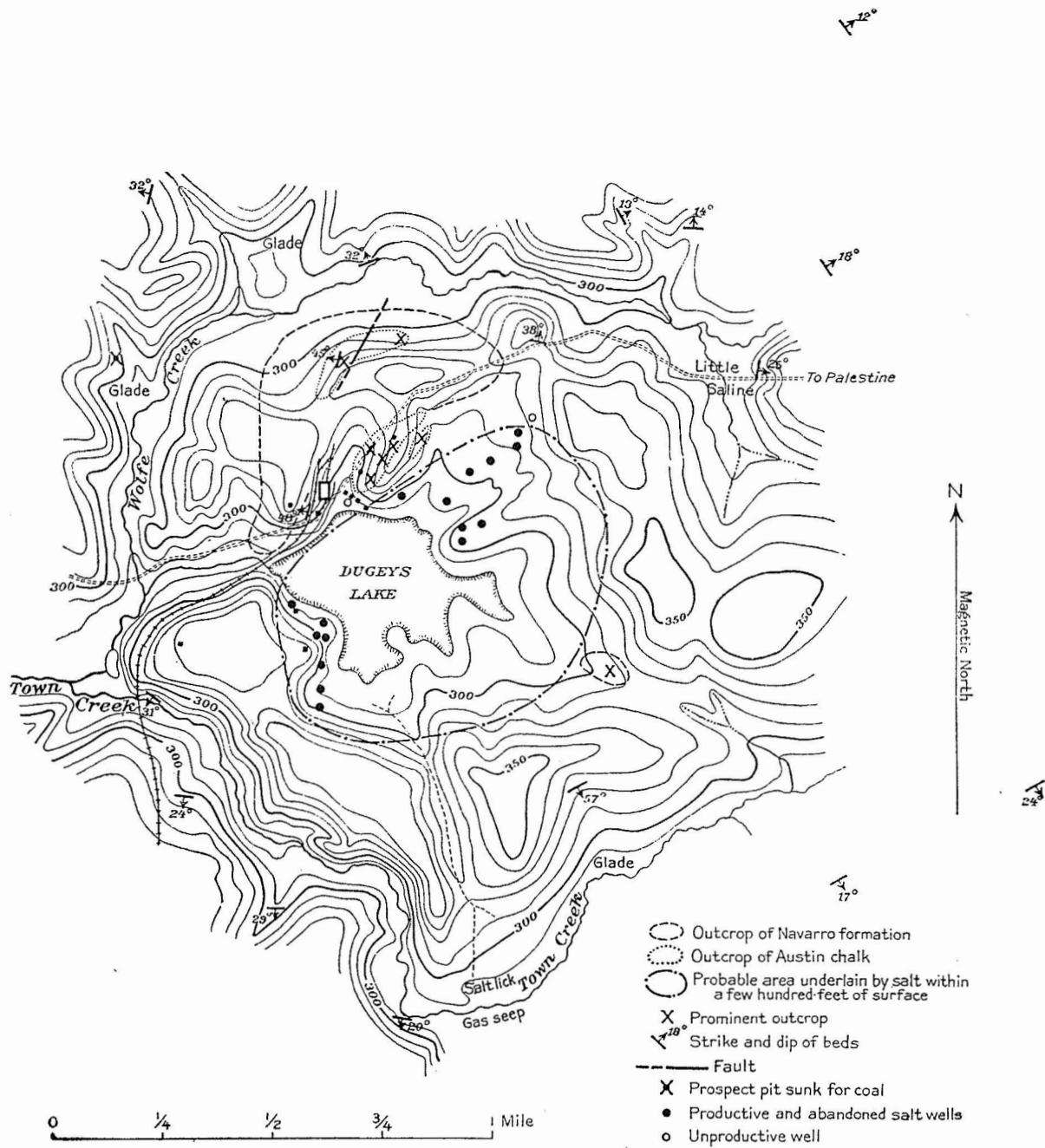
Figure 29. Sketch map of surface features over Palestine Salt Dome with locations of brine wells drilled between 1900 and 1917 (from Hopkins, 1917).

49

A

Figure 30. Photos of solution collapses at Palestine Salt Dome: (A) collapses 5 and 6; (B) collapse 15.

B
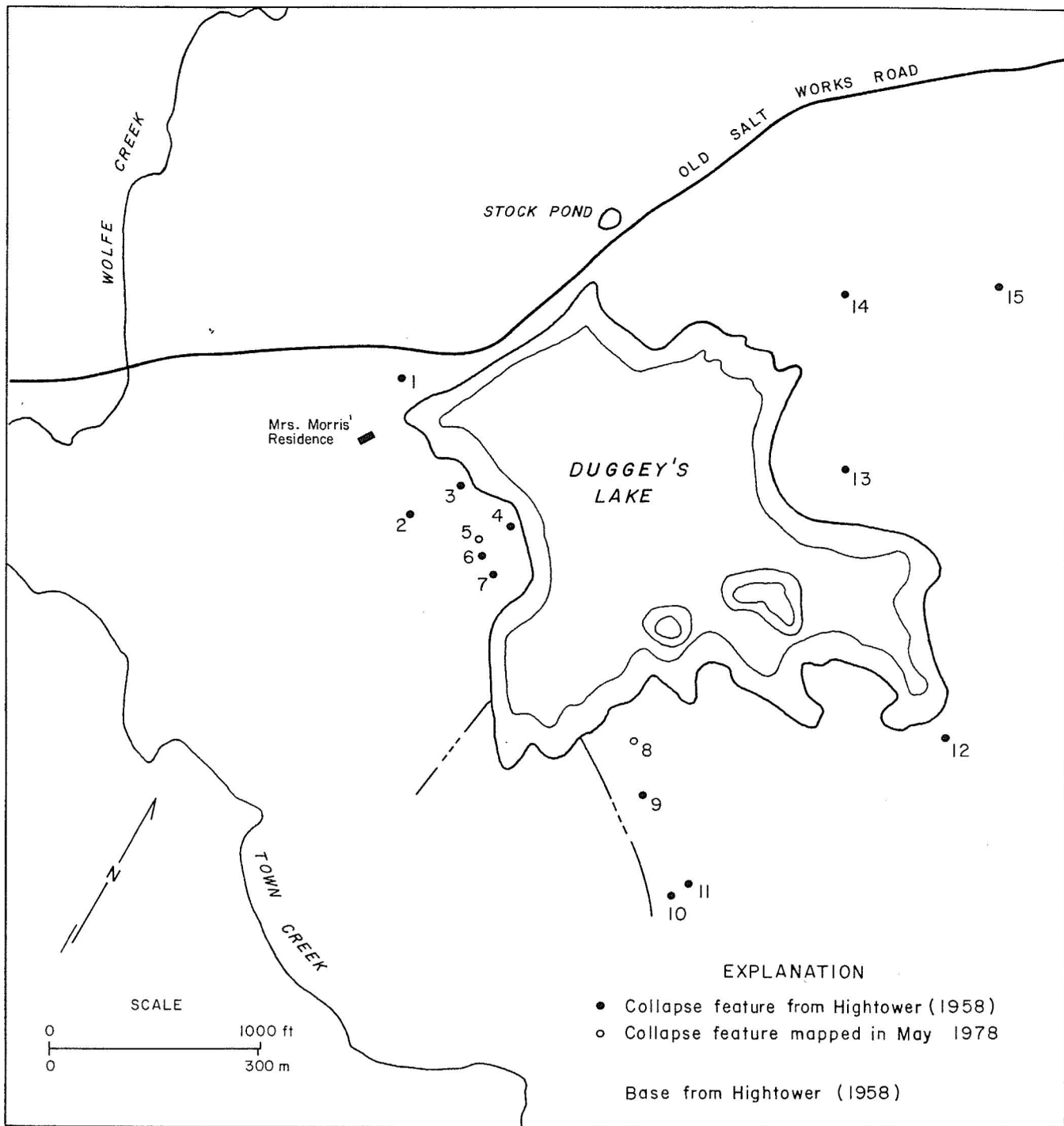
Figure 31. Locations of sinkholes overlying Palestine Salt Dome in October 1979.

Table 2. List of black-and-white aerial photos used in analysis of
sinkholes on Palestine Salt Dome.

Date	Identification code	Scale	Source agency	Holding agency
1932	—	1:18,000	Tobin Surveys, Inc.	Tobin Surveys, Inc.
1940	CKQ-3-101	1:20,000	Texas Highway Dept.	TNRIS[*]
1956	—	1:25,000	Tobin Surveys, Inc.	Tobin Surveys, Inc.
1960	CKQ-GAA-169	1:20,000	Texas Highway Dept.	TNRIS
	CKQ-GAA-170	1:20,000	Texas Highway Dept.	TNRIS
1976	4-252 GS-VEBT	1:25,500	USGS	USGS
	4-253 GS-VEBT	1:25,500	USGS	USGS

[*]Texas Natural Resource Information System

Table 3. Water chemistry, Duggey's Lake area (Palestine Salt Dome) (mg/l). Samples were collected between May 31, 1978, and June 2, 1978.

ION	1	6	5	3	7	8	9	15	13	14	12	Duggey's Lake	Morris Well
HCO_3^{-}	204.0	202.0	106.0	172.0	78.0	114.0	78.0	58.0	68.0	44.0	66.0	116.0	66.0
Cl^{-}	425.0	68.0	28.6	343.0	31.4	1450.0	23.0	10.6	13.4	9.5	44.3	1347.0	22.8
$SO_4^{=}$	104.0	13.5	13.2	42.0	1.5	30.0	1.5	7.2	4.5	18.0	78.0	37.8	13.5
Na^{+}	377.0	152.0	35.8	307.0	31.4	757.0	38.4	24.7	27.3	18.4	55.9	842.0	31.4
K^{+}	14.6	69.0	20.7	5.4	41.7	7.3	8.3	5.5	7.0	9.5	11.6	13.2	4.5
Ca^{+2}	90.5	31.4	25.0	59.5	15.2	342.0	23.4	21.8	17.0	12.2	24.7	160.0	24.2
Mg^{+2}	9.0	4.8	2.8	4.5	2.2	46.0	2.4	1.7	1.8	1.9	4.7	9.9	2.4
Mn^{+2}	0.01	0.01	0.05	0.01	0.08	1.93	0.02	0.01	0.01	0.02	0.29	0.39	0.06
Li^{+}	0.06	0.01	0.01	0.01	0.01	0.01	0.01	0.01	0.01	0.01	0.01	0.01	0.01
B	1.25	1.05	1.10	1.10	1.20	1.00	0.95	1.10	0.5	0.5	0.5	0.5	—
SiO_2	5.27	5.66	3.01	1.76	4.45	1.76	2.58	3.01	0.47	3.71	5.08	3.36	89.84
Sr^{+2}	0.5	0.2	0.1	0.3	0.1	1.4	0.2	0.1	0.1	0.1	0.1	0.8	0.1
F^{-}	na	0.13	0.0	na	na	na	0.1	0.1	na	na	na	na	0.1
TDS (total dissolved solids)	1231.2	547.8	236.3	936.6	206.7	2752.4	178.6	133.7	139.6	134.6	290.8	2530.5	254.8
pH	8.2	7.9	7.4	8.1	8.2	8.2	7.7	7.0	7.0	7.0	7.0	8.65	6.3

54

REGIONAL AQUIFER HYDRAULICS, EAST TEXAS BASIN

Graham E. Fogg

Ground-water circulation in the Carrizo-Wilcox aquifer is controlled predominantly by topography and structure. Fluid movement is generally downward, because of the structural dip and the leakage from overlying formations. Discharge to the Trinity and Sabine Rivers occurs via upward leakage across the Reklaw aquitard.

The regional aquifer hydraulics defines basinwide ground-water circulation patterns and provides an appropriate perspective for site-specific work. Geologic units considered to be potentially important to salt dome dissolution and transport of contaminants away from the domes are (upward) the Woodbine Group, Nacatoch Sand, Wilcox Group, Carrizo Formation, and Queen City Formation (see "Stratigraphic Framework"). Formations below the Woodbine are considered to be too deep and too low in permeability to threaten a repository shallower than 900 m (3,000 ft). The Wilcox and Carrizo units, both major fresh-water aquifers, are the shallowest aquifers in contact with the domes and are consequently the most critical. Work in regional hydraulics has focused on the Wilcox-Carrizo system and its fluid interactions with the overlying Queen City Formation, which is also an important aquifer.

The Woodbine and Nacatoch units are separated from the Wilcox Group by from 1 ft to several thousand feet of aquitards (and possibly aquicludes), and thus they are not easily recharged and discharged. This, together with the low permeability and transmissivity of these deeper units (relative to the Wilcox), imposes ground-water flow rates that are much lower than those for the Wilcox Group. The net result is that the Woodbine and Nacatoch aquifers have limited capacity to dissolve the domes or to transport dissolved solids into the biosphere. The Nacatoch Sand, in fact, probably poses no threat since it is thin and apparently low in permeability over most of the basin. The hydrogeology of these units (geology, pressure, and salinity data) is, nevertheless, being studied (see "Salinity of Formation Water").

On a regional scale, according to hydraulic head and geologic data, the Wilcox and Carrizo aquifers are hydraulically connected. Consequently, they have been combined as the Wilcox-Carrizo system for mapping of potentiometric surfaces (figs. 32, 33, and 34). The regional structural configuration of the Wilcox-Carrizo aquifer is complicated by the Sabine Uplift, which caused local counter-regional dips (fig. 35). Variations in lateral transmissivity in the Wilcox-Carrizo aquifer are governed by distributions of fluvial-deltaic sands and muds, which were deposited by a dendritic system of north-south oriented, high-percent-sand channels (fig. 36).

Ground-water circulation patterns in the Wilcox-Carrizo are controlled principally by topography and structure. In outcrop areas, flow lines closely follow topographic gradients as water moves away from watershed divides, which are major recharge areas, and toward stream valleys, which are major discharge areas (figs. 32, 33, and 35). Ground water leaves the outcrop area by discharge to streams and wells, evapotranspiration, and downdip subsurface movement, where the system is confined by the overlying Reklaw aquitard. Lateral, subsurface discharge from the confined part of the basin (figs. 32 and 34) follows the structural dip (fig. 35) as ground water moves toward the Texas-Louisiana border in the northern half of the basin and toward the Gulf of Mexico in the southern half of the basin. The ground-water divide is located in southern Smith County.

Natural recharge and discharge occur into and out of the confined part of the Wilcox-Carrizo aquifer by vertical leakage across the Reklaw aquitard between the Wilcox-Carrizo and the overlying Queen City aquifer. Evidence to document the leakage between the systems is as follows:

(1) Ground-water flow lines in the confined Wilcox-Carrizo aquifer tend to veer away from watershed divides toward stream valleys and thus imply recharge along the divides and discharge along the valleys. This is especially evident in Anderson County, where heads indicate an extensive recharge mound underlying the Trinity-Neches watershed divide (figs. 32, 33, and 34).

(2) Vertical head gradients indicate downward leakage (recharge) over all areas of the basin (fig. 37), except along the Trinity and Sabine river valleys, where presence of flowing wells (fig. 34) and Wilcox-Carrizo heads above streambed elevations (fig. 38) indicate upward leakage (discharge). In figure 34, the head differentials between the Queen City and Wilcox-Carrizo aquifers generally increase in magnitude toward watershed divides; this indicates that downward leakage increases accordingly and probably causes Wilcox-Carrizo heads to be higher underneath the divides. Figure 35 shows that the Wilcox-Carrizo does not discharge to the Neches River, which is the reason that heads and flow lines in figures 32 and 34 appear relatively unaffected by the river.

(3) In the Reklaw Formation, many silt and clay beds, which make the unit low in permeability, are lenticular but may become sandy in many areas, an indication that the Reklaw could leak significantly. In the northern half of the basin, net clay was not mapped because of limited success in distinguishing the Reklaw from the lenticular sands, silts, and clays of the Carrizo and Queen City aquifers (fig. 39).

56

Vertical movement within the Wilcox-Carrizo aquifer has been studied using pressure-versus-depth plots constructed from well-construction and water-level data. A plot of data for the entire basin (fig. 40) shows that the vertical flow component generally is directed downward. This is the result of leakage from above and/or flow parallel to (downward) the structural dip. Similar plots of data taken exclusively near streambeds should show upward movement in areas where heads are above streambeds (fig. 40).

Wilcox sand-filled channels do not appear to affect regional flow significantly, except perhaps in the northern half of the basin where flow lines converge on two relatively isolated channels trending through Gregg County (figs. 32, 34, and 35). This convergence also may be caused by historically high levels of pumpage in the Gregg County area. Other areas in figure 32 where pumpage has caused noticeable drawdowns are the City of Henderson (in Rusk County) and Nacogdoches and Angelina Counties.

Hydraulic head values for the Queen City aquifer follow closely the rolling topography above this unit, and the values are, therefore, irregular. As a result, it was not practical to produce a contour map of potentiometric surface from the data available; therefore, the heads are displayed as mean values in figure 41. The figure demonstrates a nearly random scattering of localized recharge and discharge areas over the aquifer.
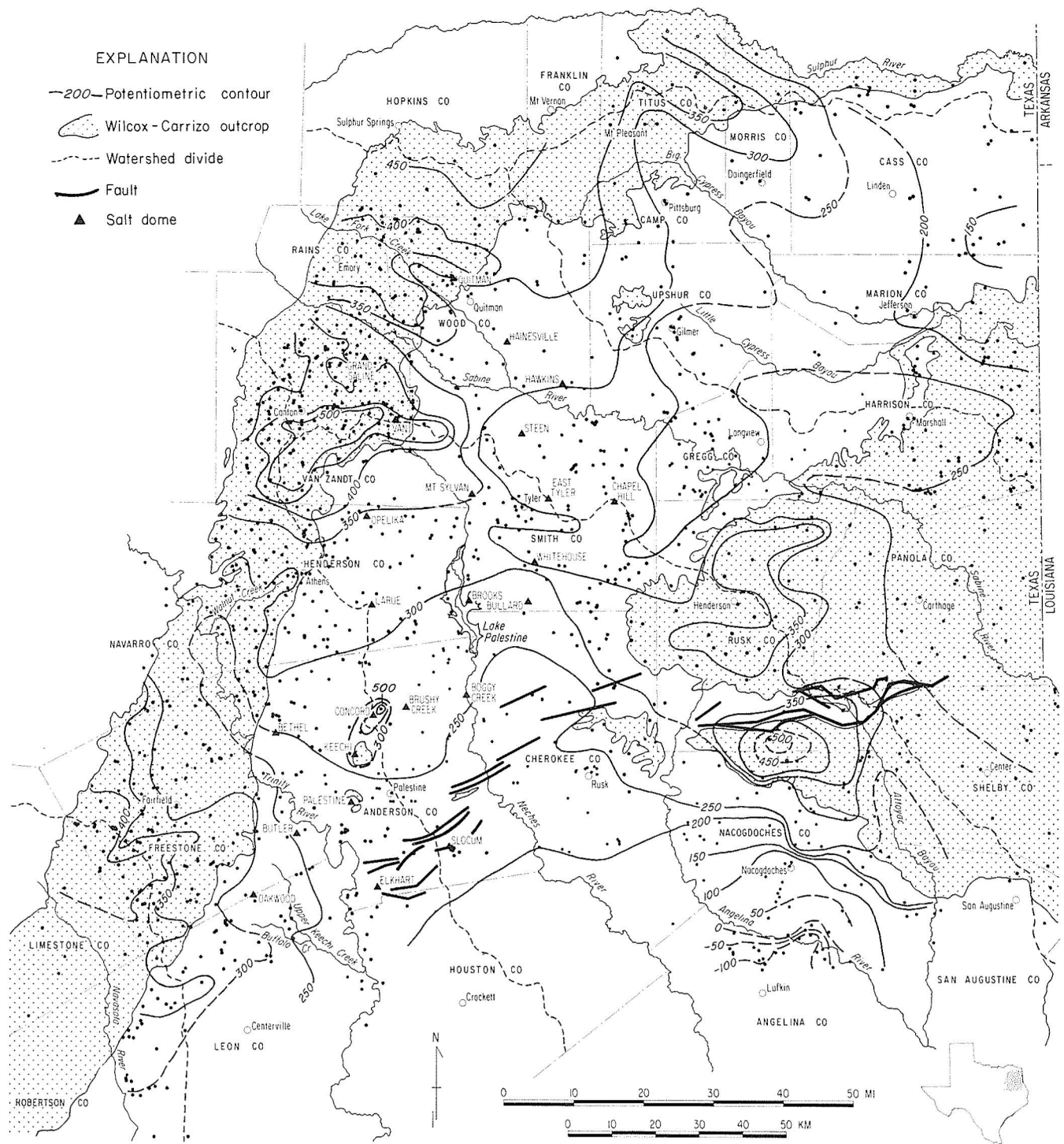
Figure 32. Potentiometric surface map of the Wilcox-Carrizo aquifer system. The water-level data are from 1936-1976; however, most of the data are selected from measurements made during 1962-1971 on the basis of historical water-level changes.
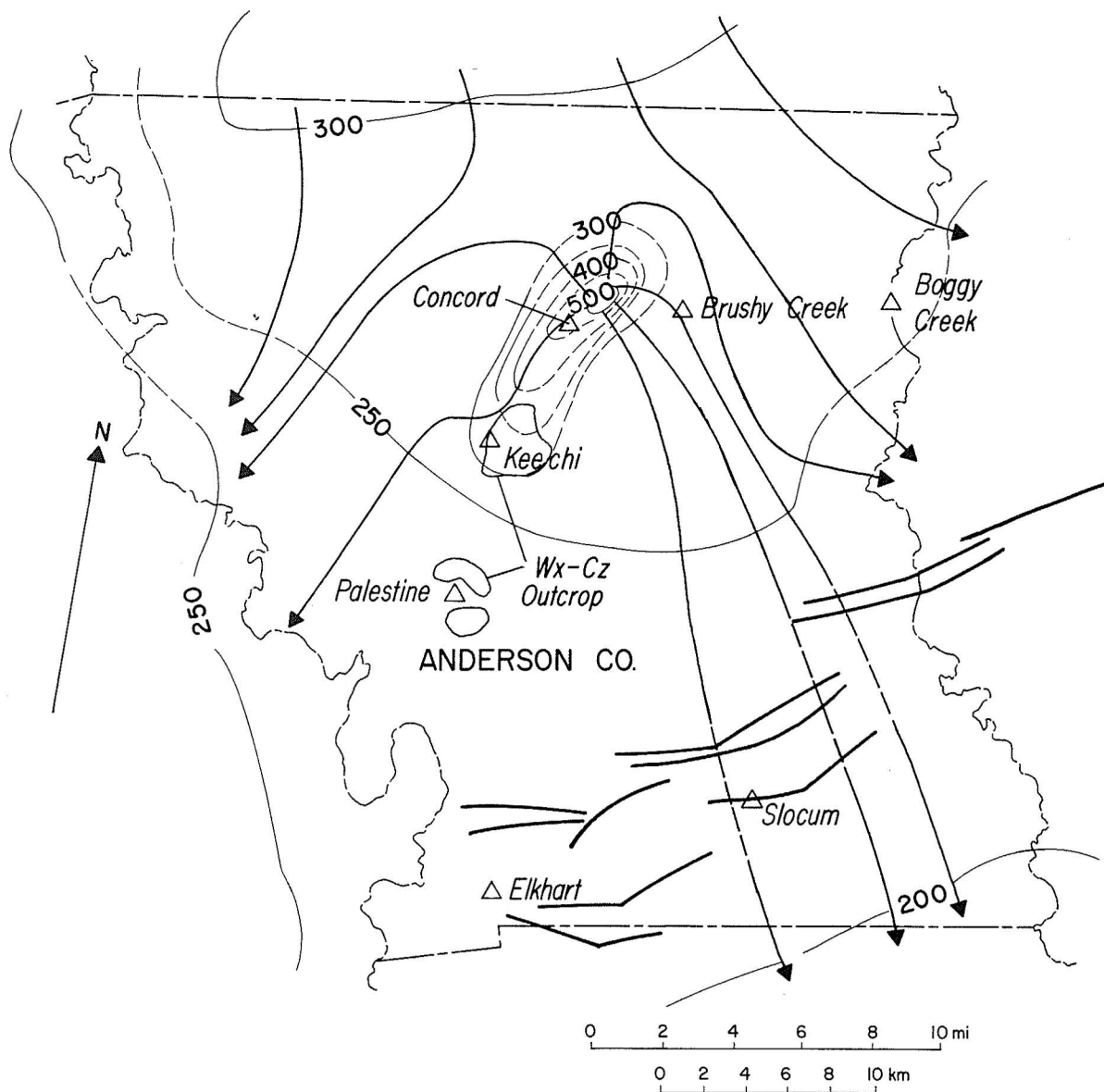
Figure 33. Detail of Wilcox-Carrizo ground-water flow in Anderson County.
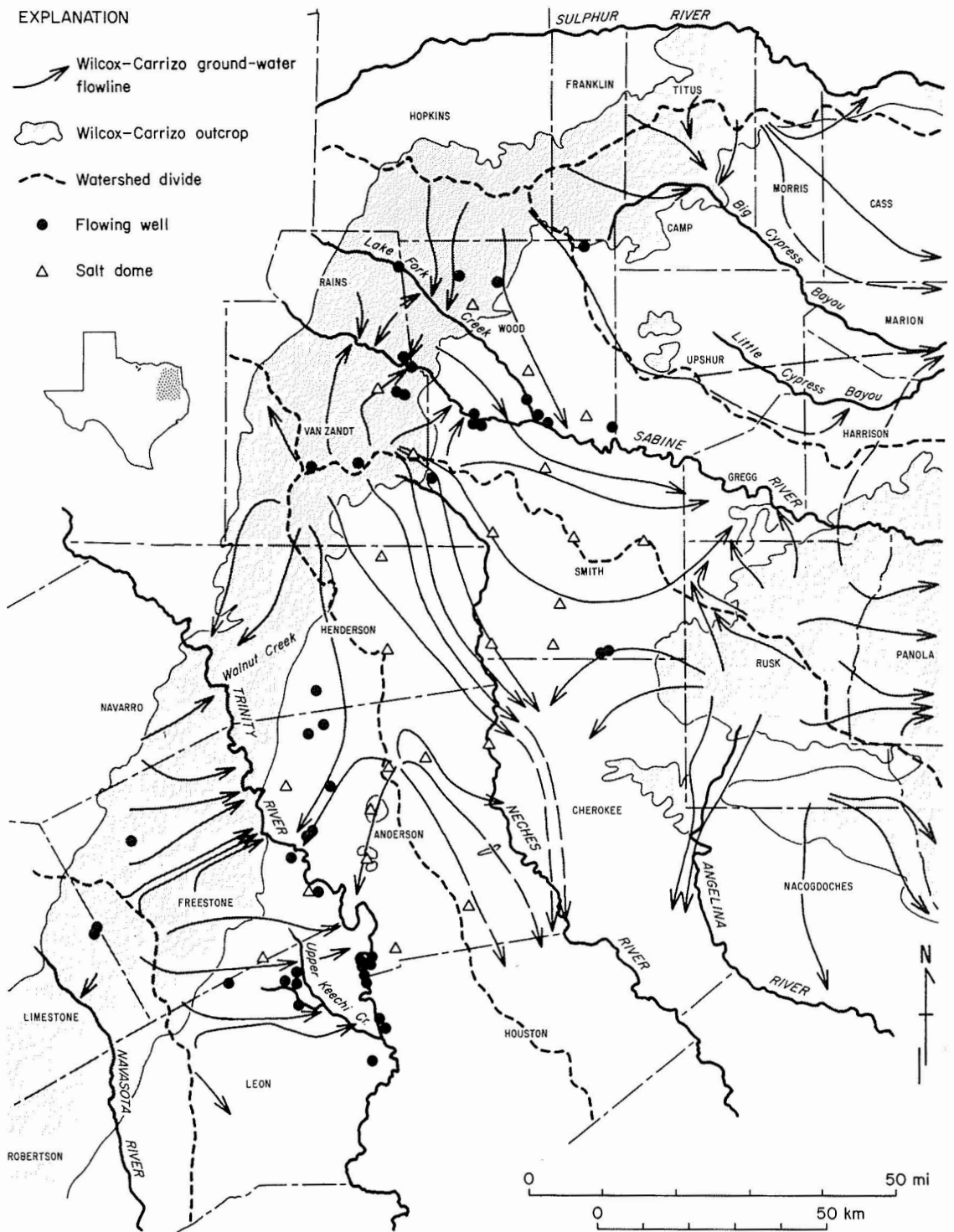
Figure 34. Ground-water flow lines in the Wilcox-Carrizo aquifer system drawn from figure 32. In both the outcrop and the confined parts, ground water tends to flow away from watershed divides and toward rivers.

60
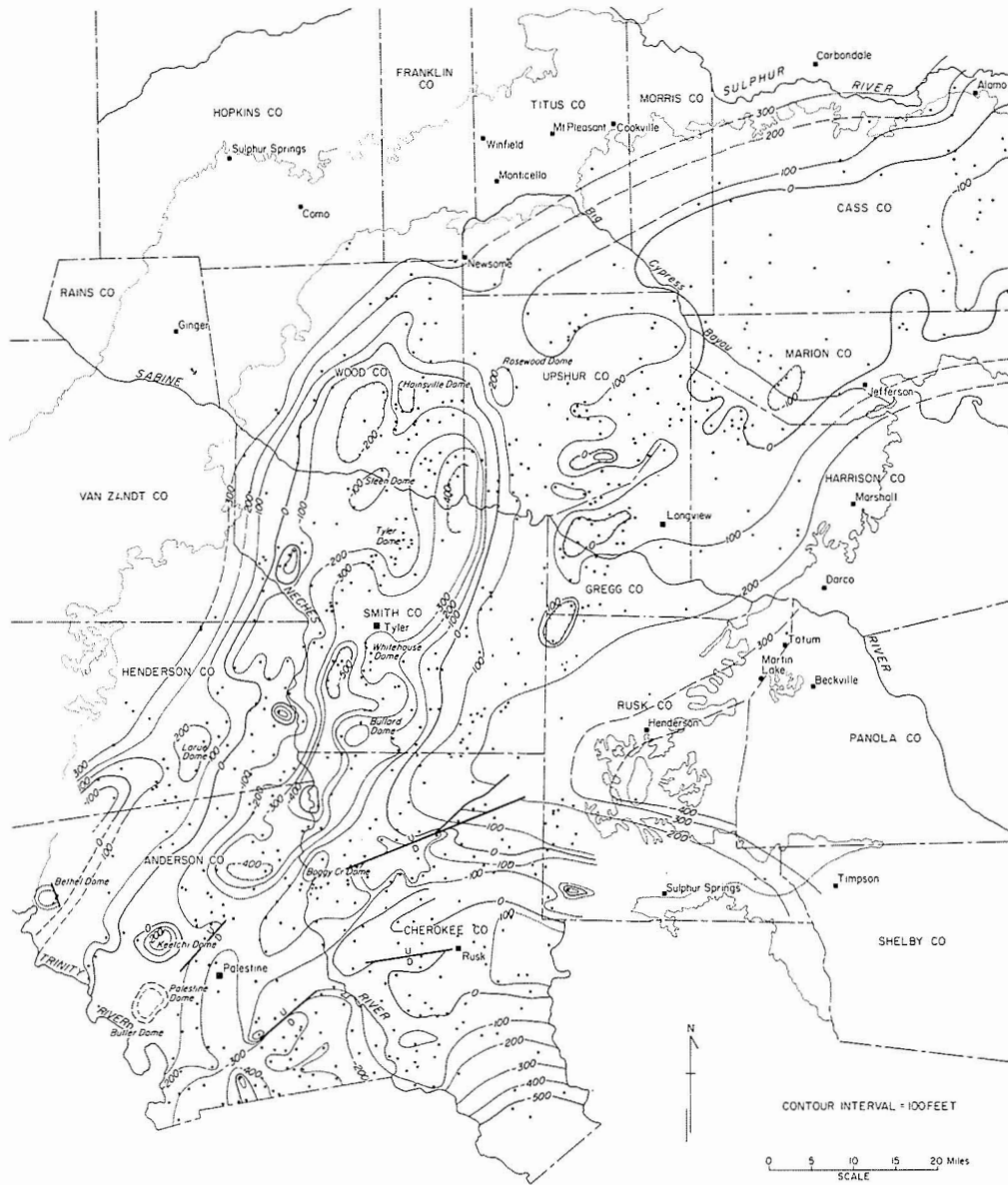
Figure 35. Structure contour map on top of Wilcox Group (from Kaiser, personal communication, 1979).

Figure 36. Percent sand map of Wilcox Group (from Kaiser and others, 1978).

Figure 37. Head differentials between Queen City and Wilcox-Carrizo aquifer systems. Widespread positive values indicate downward leakage from the Queen City to the Wilcox-Carrizo everywhere except along stream valleys, where data are insufficient. In many areas, differentials increase toward watershed divides owing to topographic effects.

63

Figure 38.   Profiles showing elevations of Wilcox-Carrizo water levels above major streambeds.   Heads above the streambeds indicate the presence of vertical upward leakage through the Reklaw aquitard.   Heads along the Neches River document that it receives no discharge from the Wilcox-Carrizo system.

Figure 39. Net clay thickness of Reklaw aquitard. Leakage across the unit may be enhanced where it thins or becomes discontinuous. The clays tend to be discontinuous in the area of the map and become even more so in the northern half of the basin.
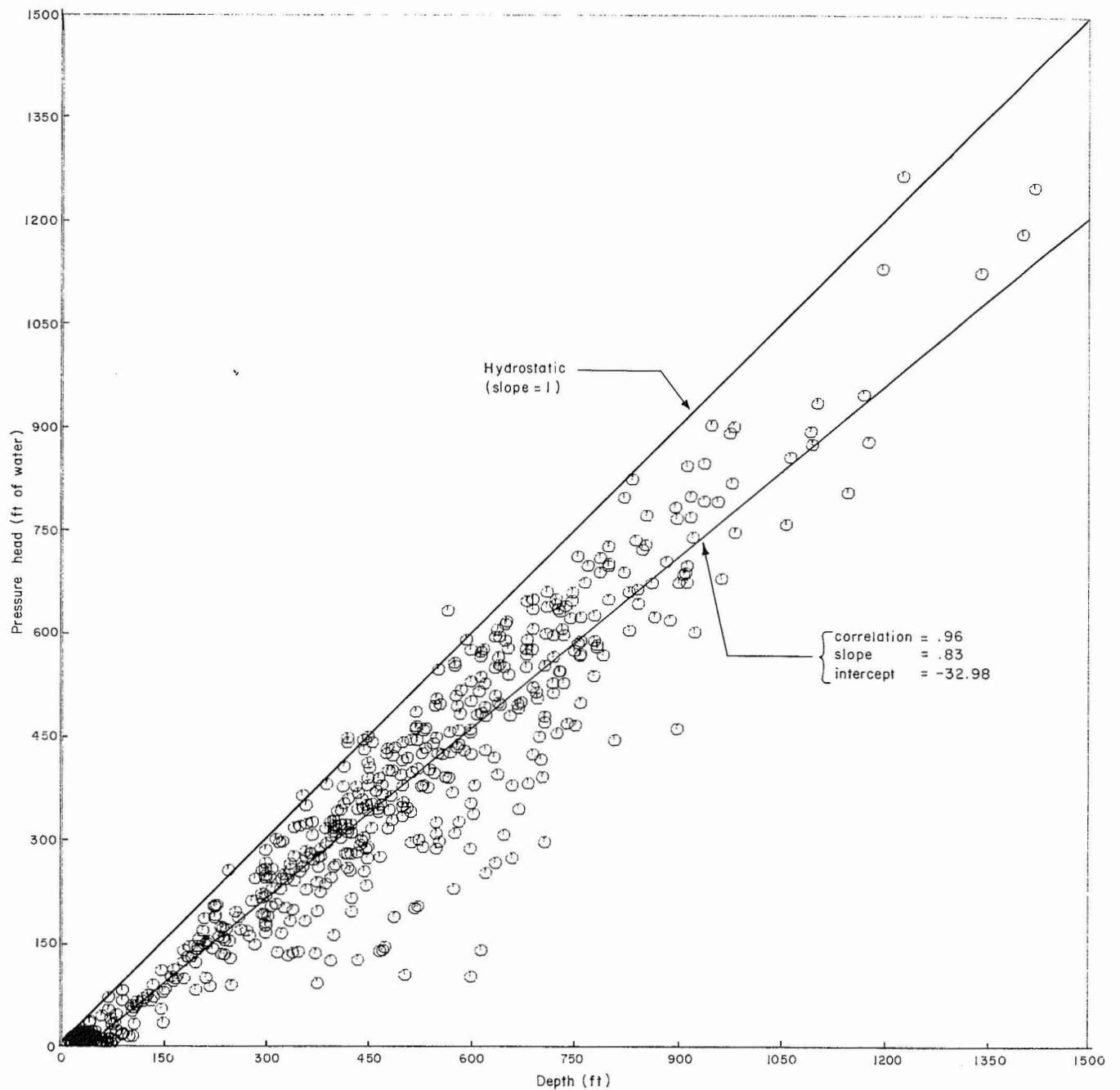
Figure 40.   Basinward pressure-versus-depth relationship for the Wilcox-Carrizo aquifers.   The less-than-hydrostatic slope (.83) indicates a component of downward flow over most of the region. This relationship should be reversed beneath the Sabine and Trinity Rivers, an indication of upward movement.

66

SCALE

0   5   10   15   20   25 Miles

0   5   10   15   20   25 Kilometers

N

ANDERSON
COUNTY

EXPLANATION

o   Well tapping Queen City aquifer

250   Mean Queen City water level

---- Watershed divide

+   Indicates presence of flowing wells
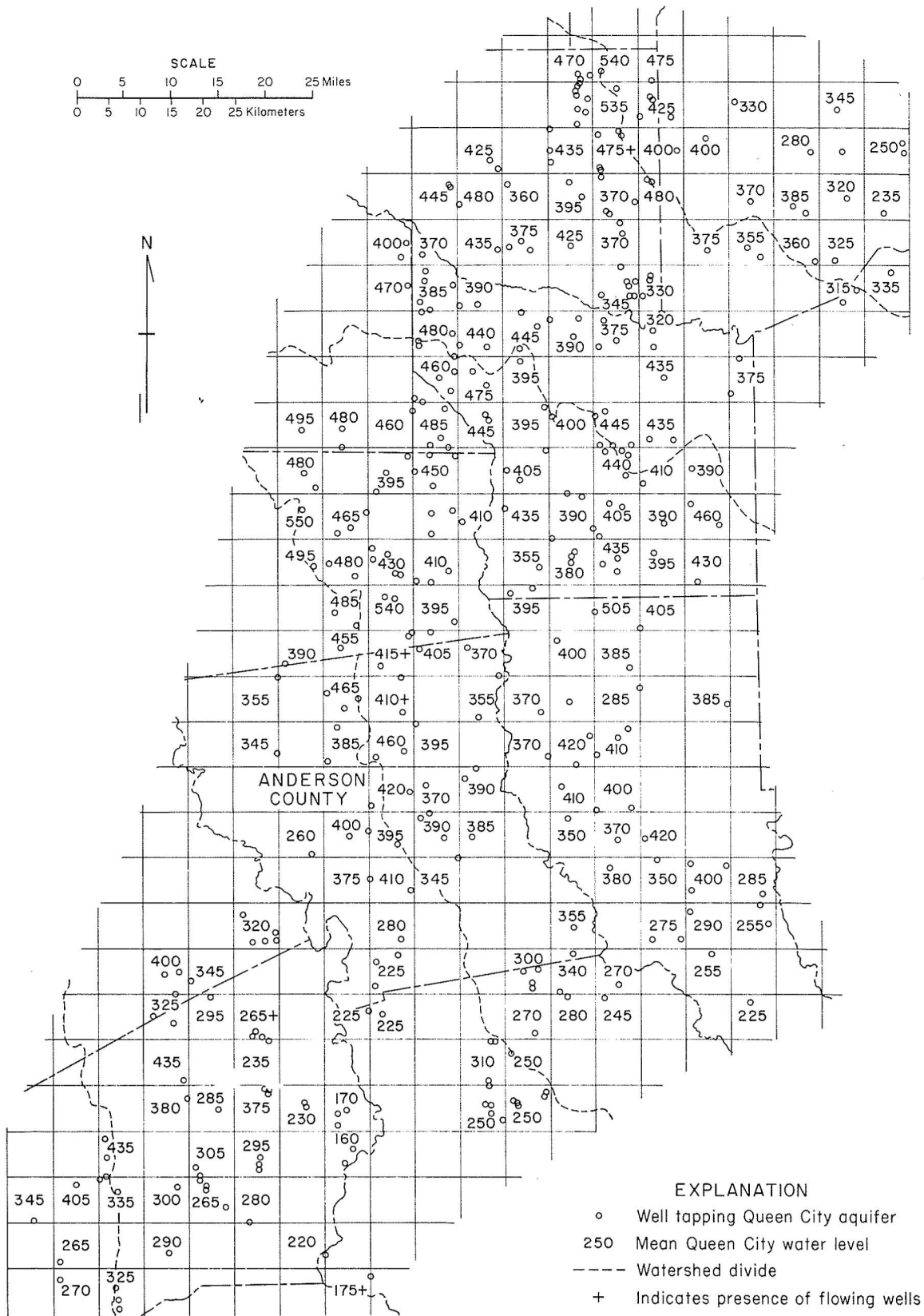
Figure 41. Potentiometric surface map for the Queen City aquifer. The irregular heads are caused by irregular topography. Closely spaced recharge and discharge areas are scattered throughout the aquifer.

SALINITY OF FORMATION WATERS

Graham E. Fogg

Estimates of the salinities of formation water in the Woodbine, Nacatoch, and Wilcox stratigraphic units have been accomplished using electric log interpretation (SP and resistivity). These estimates provide general information on salt dome dissolution in the East Texas Basin.

Estimates of salinities of formation water in the Woodbine, Nacatoch, and Wilcox units were made from electric logs (SP and resistivity). These estimates provide general information on the occurrence of salt dome dissolution in the East Texas Basin.

Maximum salinity in sands of the Woodbine Formation was mapped from SP values using methods outlined by Keys and MacCary (1971) (fig. 42). The map demonstrates a variable distribution of maximum salinity values ranging from 30,000 to 300,000 ppm. A vague trend of increasing salinities toward the central axis of the basin corresponds to a salinity map in figure 42 of the Woodbine constructed by Core Laboratories (1972). Because of the scatter and the sparsity of laboratory water analyses, no means exists of detecting salt dome dissolution by the Woodbine aquifer system. A similar analysis of the Nacatoch Formation showed the unit to be either missing, very thin, or tightly cemented everywhere except in the northern part of the basin. The thin Nacatoch aquifer poses a relatively minor threat to the stability of the domes under study.

Salinity estimates for the Wilcox Group were made using an empirical relationship between electric log resistivity and total dissolved solids (TDS). A graph (fig. 43) displays formation resistivities (Ro) in sands tapped by water wells versus corresponding TDS values determined in the lab from the well discharge waters. Although the graph is thought to be fairly accurate (±500 mg/l), it should be considered preliminary until further calibrated and verified by geophysical logs and water samples obtained from the current drilling program.

A map of percent thickness of fresh water (less than 1,000 mg/l) in the Wilcox aquifer (fig. 44) indicates three sources of salinity: (1) upward leakage of deep, saline water along faults, (2) incomplete flushing of saline water in muddy areas of the Wilcox Group, and (3) salt dome dissolution. Upward leakage along faults may be occurring in the Mount Enterprise-Elkhart Graben in southern Anderson and Cherokee and northern Houston Counties, where salinities increase abruptly. High salinities from salt dome dissolution could be confused with high salinities resulting from upward flow

along numerous faults associated with the domes. The lack of high salinities around domes depicted in figure 44, however, suggests that the domes are neither dissolving significantly nor creating pathways for upward leakage.

Incomplete flushing of saline water in muddy areas of the Wilcox Group is suggested by a good correlation between saline zones (fig. 44) and muddy zones on the sand-percent map (fig. 36; see "Regional Aquifer Hydraulics, East Texas Basin") such as in Upshur County, southeast of Mount Sylvan Dome and east of Whitehouse and Bullard Domes. The saline intervals near the three domes are not caused solely by dome dissolution, because salinities decrease and fresh-water thicknesses increase toward the domes. The original sources of saline water in the muddy sediments may be from salt dome dissolution during the geologic past (such dissolution could be slower today owing to cap rock development) or from marine waters that submerged the Wilcox at least twice since it was deposited 40 million years ago. The continued presence of saline water in and around the muddy facies is possibly enhanced by ground-water velocities that are probably as low as 15 to 9,150 cm/million years (0.5 to 200 ft/million years). These rates were calculated using maximum and minimum hydraulic gradients of 6.3×10^{-3} and 1.0×10^{-3} measured in sands surrounding the muds (fig. 32; see "Regional Aquifer Hydraulics, East Texas Basins"), and estimated clay hydraulic conductivities of 3×10^{-5} and 3×10^{-3} cm/day (10^{-4} and 10^{-6} ft/day).

There is little evidence of past or present salt dome dissolution in figure 46. Only around Oakwood Dome, a distinct plume appears directly related to dissolution. However, this plume contains mostly brackish water (<3,000 ppm) and does not seem to indicate a significant rate of salt removal (see "Hydrologic Stability of Oakwood Dome"). Without exception, the maximum concentrations of dissolved solids in the Wilcox were found in muddy sands at the bottom of the aquifer. In nearly every case these concentrations are around 5,000 ppm ($\pm$1,000 ppm), and in a few isolated areas appear to reach 10,000 ppm. Additional details of salinity distributions around the salt domes are shown in cross section in "Evolution of East Texas Salt Domes" (figs. 12, 13, 14, 16, 17, and 18). The sections indicate a general lack of anomalous salinities around the domes, in agreement with figure 44.

Although salinities in the Carrizo and Queen City aquifers were not mapped, none of the electric logs observed throughout the basin indicated brackish or saline water in these units, except near the Mount Enterprise-Elkhart Graben Fault Zone. This agrees with the regional aquifer hydraulics, which indicates predominantly vertical downward movement in the Eocene aquifer units.

Figure 42. Maximum salinity in the Woodbine Sand as estimated from SP curves. The broad scattering of data could be due to limited circulation in the unit, fluid injection, and/or errors induced by the method of estimation.
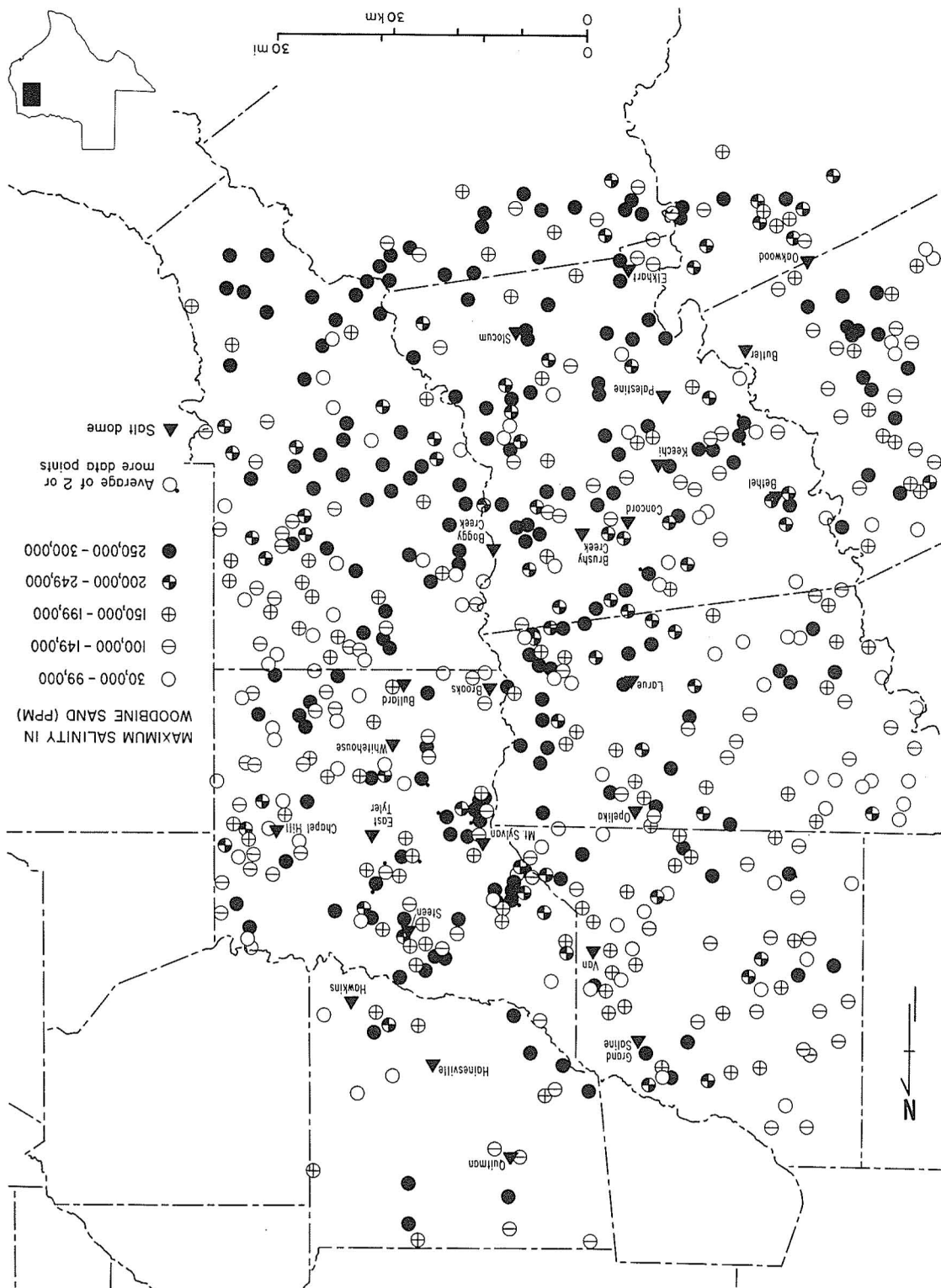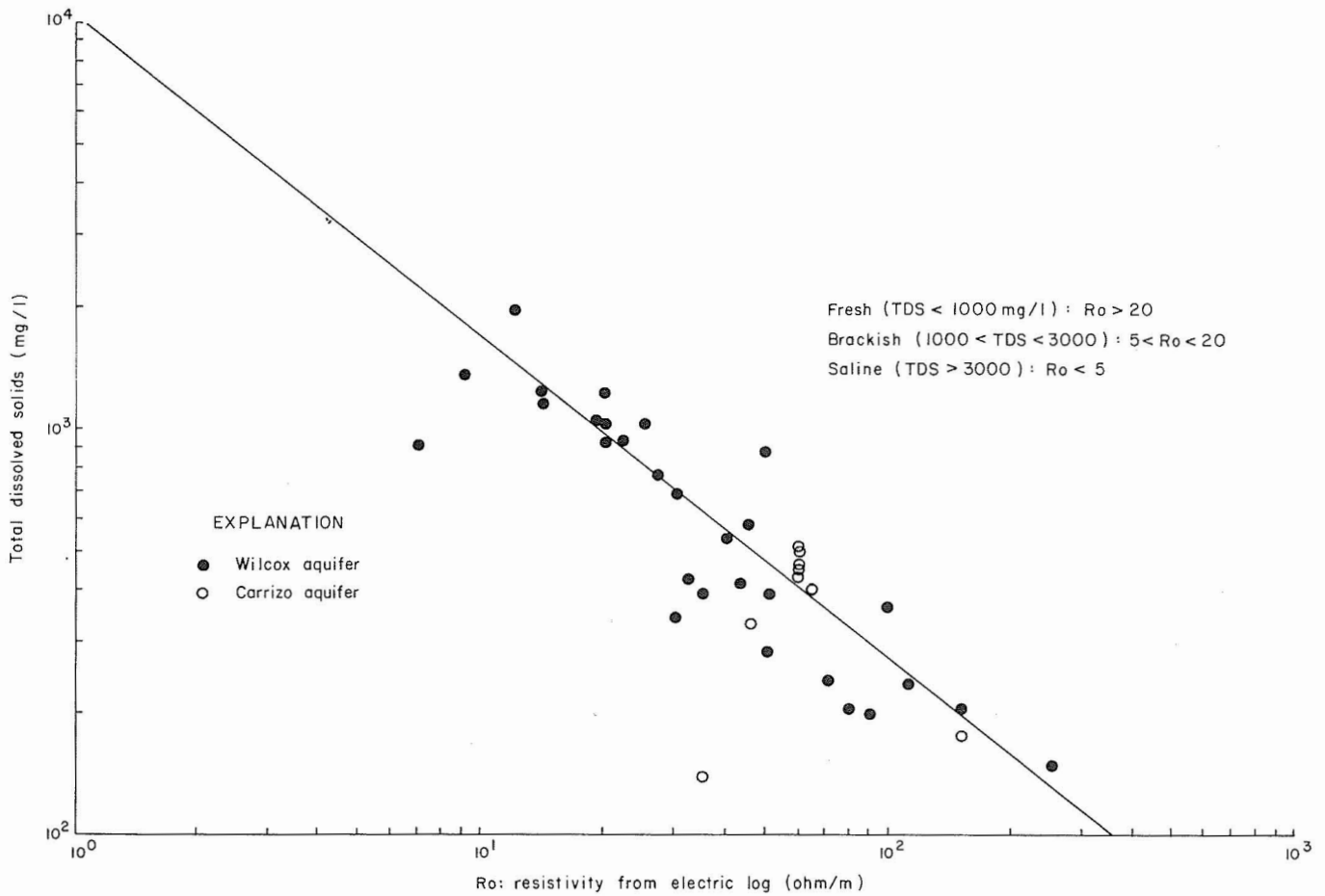
Figure 43. Relationship between formation resistivity (Ro) and TDS concentration of formation water. The straight line was eye-fit rather than calculated by linear regression, since several values of Ro were of uncertain accuracy and had to be weighed subjectively.
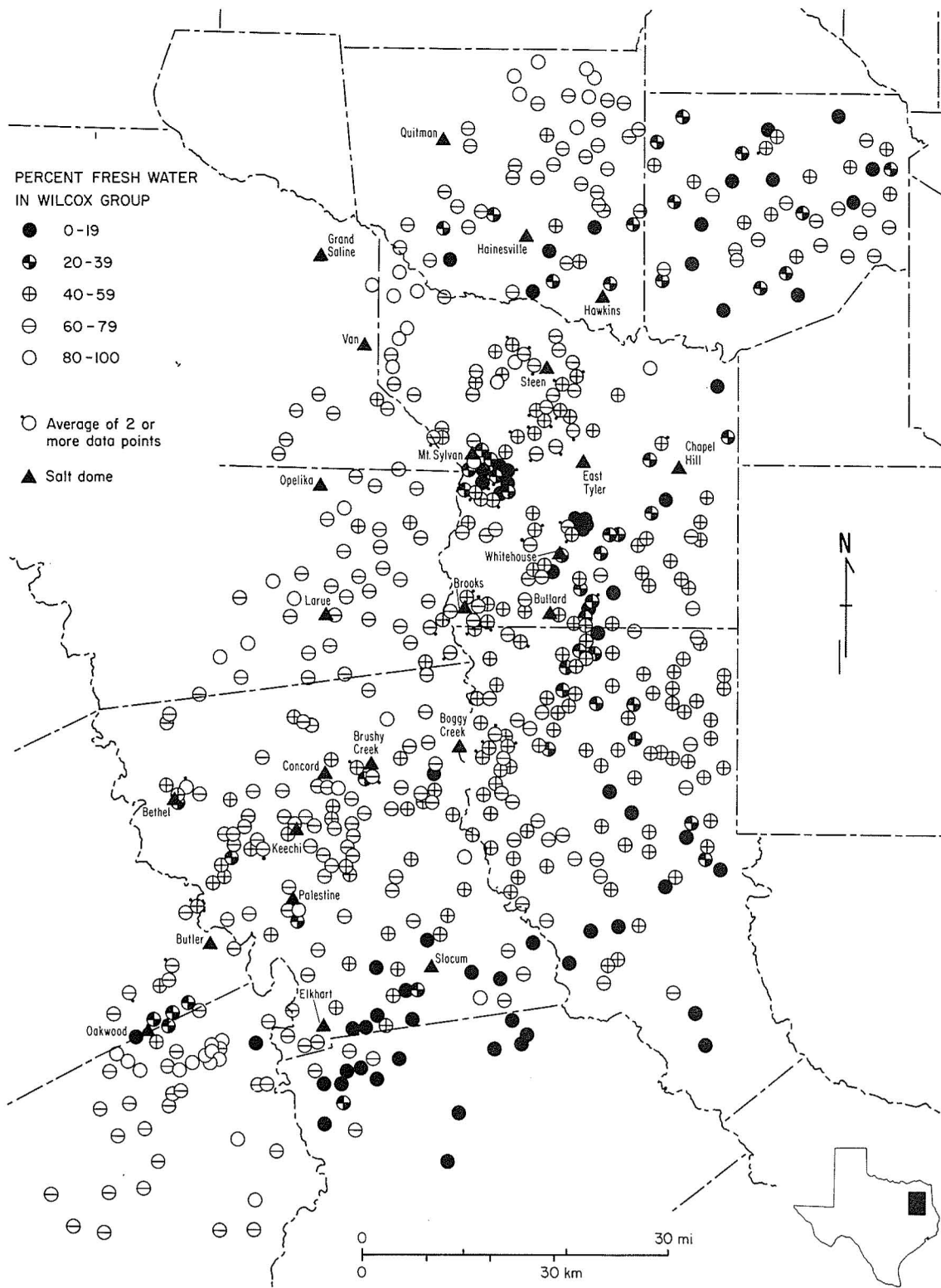
Figure 44. Percent of Wilcox thickness containing fresh water (<1.000 mg/l) as estimated from the resistivity curve of electric logs.

GEOCHEMISTRY OF GROUND WATER IN THE WILCOX AQUIFER

Charles W. Kreitler and Graham E. Fogg

Ground-water chemistry trends in the Wilcox aquifer clarify the potential for the transport of radionuclides, the general flow paths, and the significance of carbon-14 age dates of the ground waters.

The Wilcox aquifer is the most continuous geologic unit containing fresh ground water in the East Texas Basin. If a breach occurred in a salt dome repository and radionuclides leaked to an aquifer, it would be in the Wilcox system. The geochemistry of the ground water in the Wilcox aquifer indicates the ability of the aquifer to retard radionuclide migration. Anomalous geochemical zones in the aquifer, which may represent recharge and discharge or relative flow rates, support interpretations of regional flow of ground water. Absolute age dating of Wilcox ground waters is complemented by regional geochemical data.

The results of over 800 complete water chemistry analyses were obtained from the Texas Natural Resource Information System (TNRIS). These data were evaluated by means of a computer program, WATEQ, which analyzes the cation-anion balances. Next, the interrelationships between different chemical and aquifer parameters were evaluated by a statistical program (SPSS). The following correlations were observed:

(1) Shallow ground waters in the recharge zone exhibit lower pH, higher calcium, higher magnesium, higher silica, higher sulfate, and lower bicarbonate content relative to deeper artesian waters.

(2) Deeper artesian ground waters have high pH, low calcium, low magnesium, low silica, low sulfate, and high bicarbonate values.

(3) A sodium bicarbonate-rich water is generated as ground water moves farther from the recharge zone (fig. 45). Sodium replaces calcium and magnesium by cation exchange on clays. This continual displacement of calcium permits undersaturation of calcite and, therefore, subsequent dissolution of more calcite. Calcite dissolution operates predominantly in a closed system; no external source of acidity causes the dissolution. This is indicated by the continual rise in pH away from the recharge area.

(4) The pH of ground water changes from 5 to 7 in the recharge zone to 8 to 9 in downdip sections (fig. 46).

(5) Silica concentration decreases with depth. The source of the silica in the shallow ground waters and the mechanism for silica loss are not known (fig. 47).

(6) Sulfate concentration decreases with depth (fig. 48). Loss of sulfate is probably by reduction. Sulfate reduction indicates low Eh values in the ground water.

Ground-water chemistry indicates a trend from an oxidizing, low-pH ground water in the recharge zone to a reducing, high-pH ground water in the artesian section. Migration of radionuclides is dependent on pH and Eh conditions (Bondietti, 1978; Relyea and others, 1978).

The outcropping Wilcox aquifer generally contains neutral to acid water (fig. 46). These low-pH waters also are found at the ground-water divide in the Tyler area and in the Keechi Dome area. Regional ground-water flow studies have postulated that these sites are recharge areas, an interpretation substantiated in part by the water chemistry.
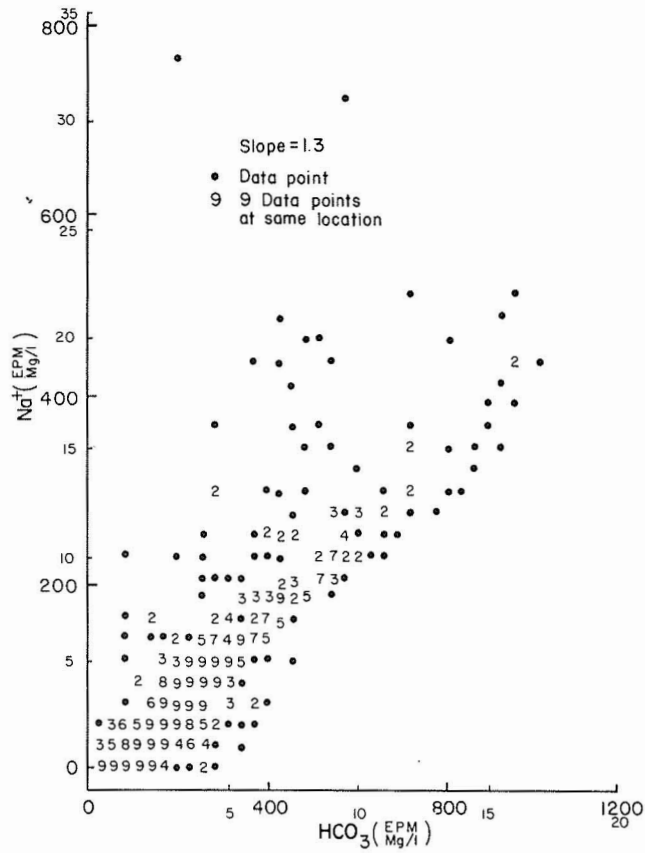
Figure 45. Correlation of sodium and bicarbonate in Wilcox ground-water concentration increases downdip from recharge zone.
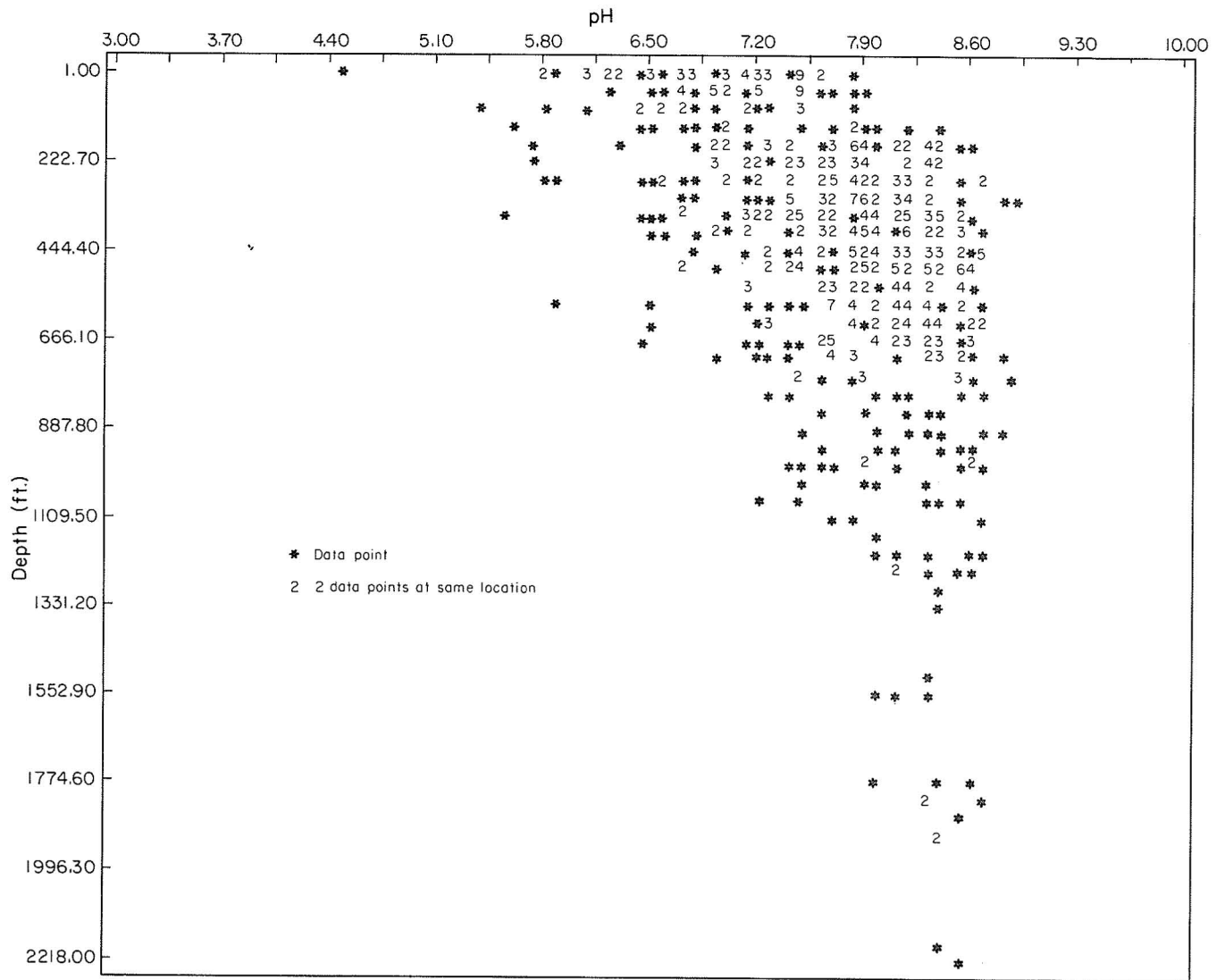
Figure 46. Increase in pH values with depth, resulting from calcite dissolution and cation exchange in a predominantly closed system.

SiO$_2$ (mmoles/ liter)

Depth (ft.)

* data point

9 9 data points at same location
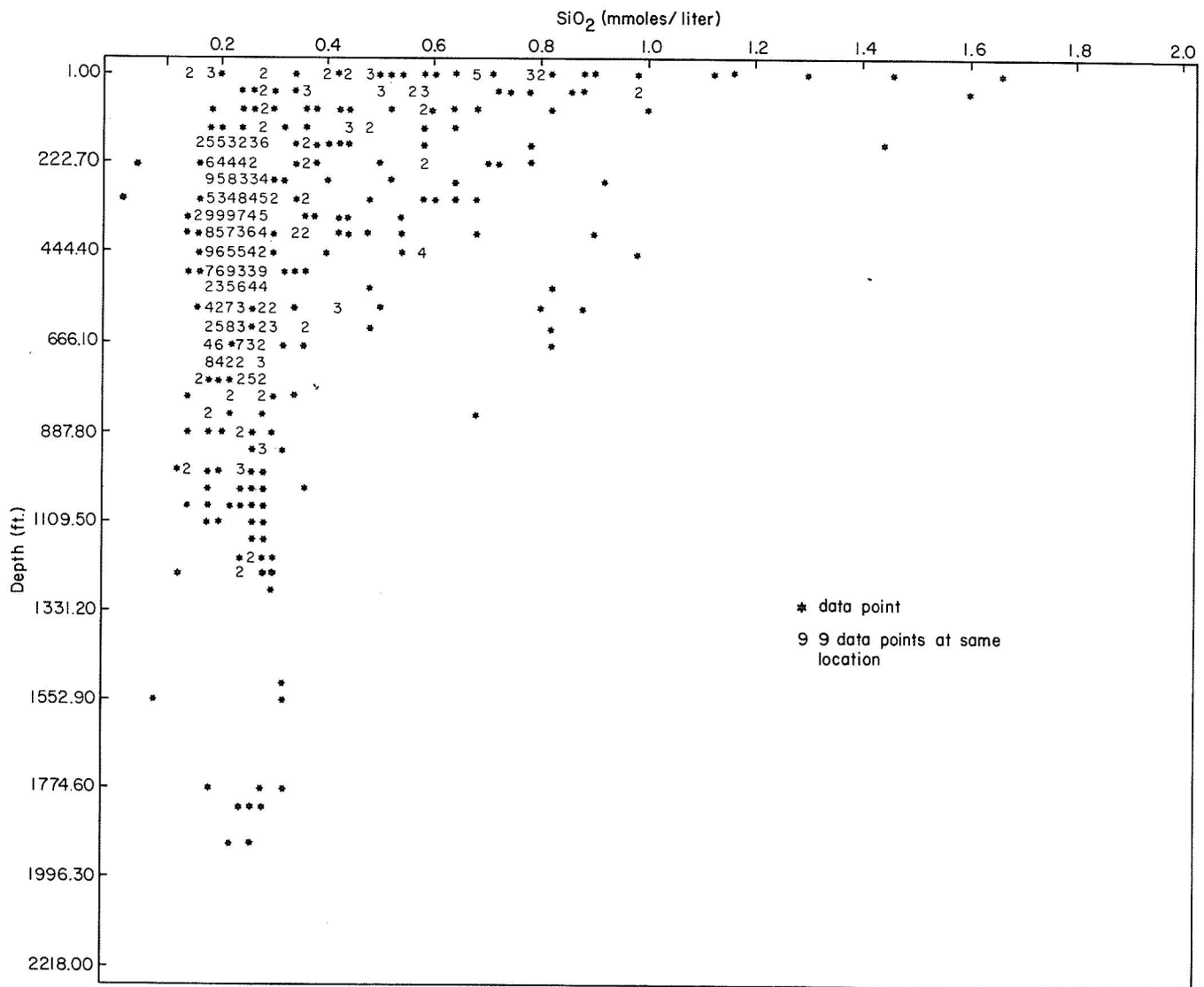
Figure 47. Decrease in silica concentrations with depth.

SO$_4$ (epm)

```
             1.5      4.5      7.5     10.5     13.5     16.5     19.5     22.5     25.5     28.5
  1.00 -9998654522  3    2   *  *        *    * *      *               *          *              *          *
       58665*    22 2** *    *2   *      *        2              * *                                        *
       35*2 *    *  *   **        *2                  *                      *
       342** **2 *
       6863823** *    *          *
222.70 7976** *  *       *
       596772**         *
       97983       *  *
       999*35    *
       799633
444.40 6998*    *  *      *
       99342***     *
       7933 2*        2
       2994**                   **
       5944* *
666.10 7963*              *
       3944                              *
       464**      * *
       242
       *22
887.80  232 **       *
       * ***2
       27*
        2 2*
       22*         *
1109.50  3 *
       2*  *     *
       ** 2   *
1331.20 *
       *
       *
1552.90 2     *
1774.60 2*
       3
       *
       2
1996.30
       *
2218.00 *
```

Depth (ft.)

*   data point

9   9 data points at same location
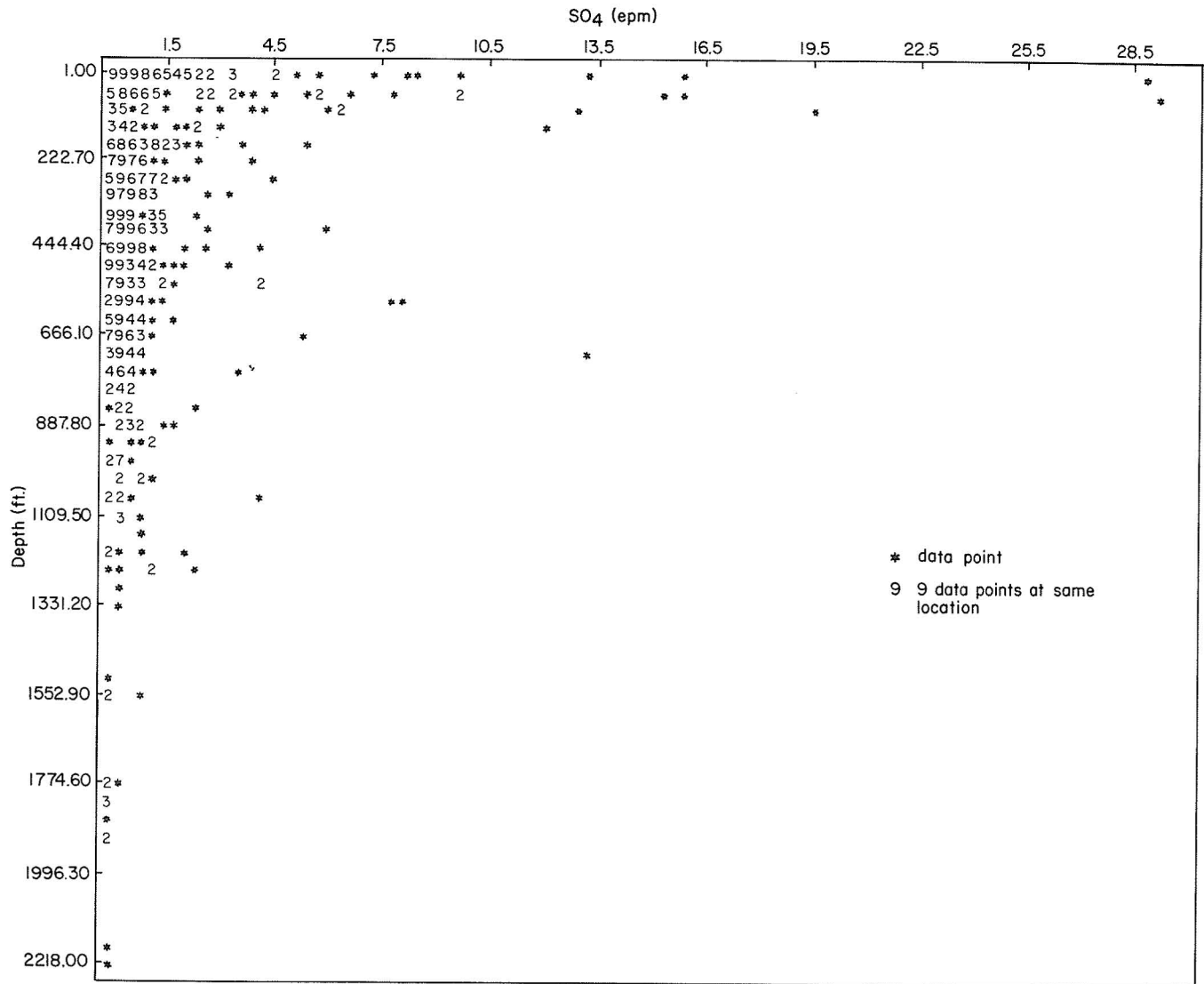
Figure 48. Sulfate reduction with depth. Loss of sulfate implies greater reducing conditions at greater depths.

CARBON-14 DATING OF WILCOX AQUIFER GROUND WATER

Charles W. Kreitler and David Pass

Ground-water age dating in the Wilcox aquifers by carbon-14 indicates progressively older waters down the structural and potentiometric dip. Uncorrected ages vary from approximately 10,000 to 30,000 years old.

Specific questions involving ground-water flow in the Wilcox aquifer are as follows: (1) Are flow velocities in the shallow part of the aquifer significantly higher than in the deeper aquifer? (2) Is there significant leakage from the overlying Queen City Formation into the Wilcox aquifer? (3) Because strata are uplifted around many salt domes, are dome areas recharge zones within the artesian part of the aquifer? (4) Does saline water leak upward from deeper formations along the flank of the domes? These questions can be resolved partly by using carbon-14 absolute age dating of the bicarbonate ion in ground waters.

Maximum measurable age of a carbon sample by conventional carbon-14 techniques is approximately 50,000 years. Bicarbonate ion in ground-water samples results from (1) the generation of carbon dioxide in the soil zone of the recharge area, and (2) the dissolution of carbonate minerals or the decomposition of organics in the aquifer. Carbon-14 is added to the ground-water bicarbonate ions only by carbon dioxide from the soil zone. Other potential sources are probably significantly older than several half lives of carbon-14 and, therefore, represent "dead" carbon. In calculating the age of bicarbonate in ground water by carbon-14, a correction factor must be included to account for dead carbon. Carbon-14 dates presented in the following section are uncorrected values. A correction factor has yet to be determined; corrected values will be presented at a later time.

Nine water samples from the western outcrop of the Wilcox Group to the Elkhart Graben have been analyzed (fig. 49). Wells along the Wilcox outcrop are relatively shallow, whereas wells in the artesian section are the deepest wells penetrating the Wilcox. Samples were collected from approximately the same stratigraphic horizon from outcrop to the deepest part of the Wilcox aquifer. Table 4 lists information about the wells sampled for these analyses.

From the recharge zone into the deepest part of the basin, the waters become progressively older from approximately 10,000 years in outcrop (locations 1 and 2) to approximately 28,000 years south of the Elkhart Graben (location 9). The water sample from the Keechi Dome area (location 5), where the Wilcox Group crops out

because of doming and where evidence exists of substantial leakage through the Reklaw aquitard, is significantly younger than shallow ground waters near the regional Wilcox outcrop belt.

Shallow ground waters sampled in the outcrop of the Wilcox aquifer are older (approximately 10,000 years) than expected. Sample locations probably represent discharge zones rather than recharge zones of the outcrop (locations 1 and 2). These "old" ages are additional evidence for topographic control of ground-water flow in the Wilcox system.
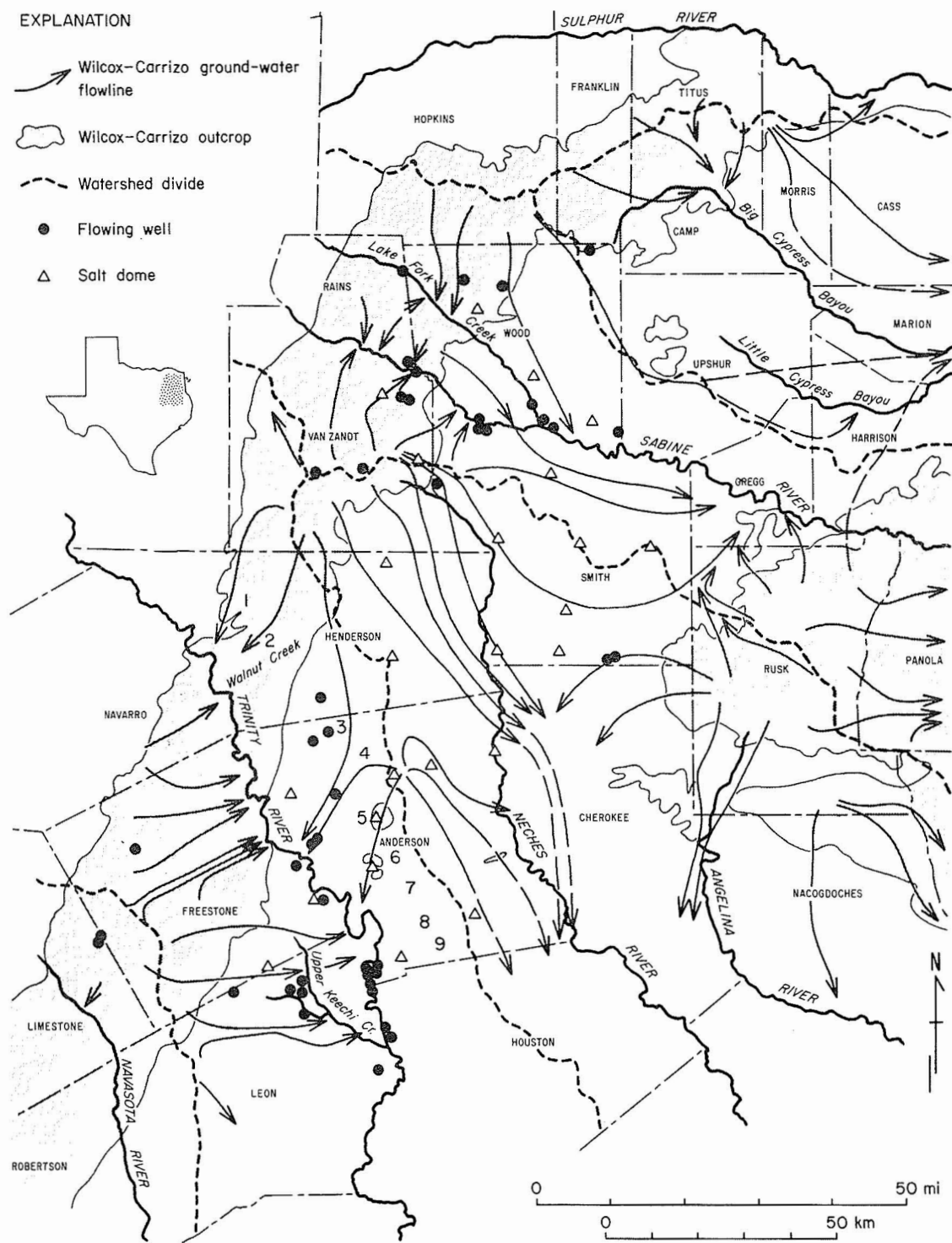
Figure 49. Location of ground-water samples from Wilcox aquifer used for carbon-14 age dating. Numbers 1 through 9 indicate locations. Table 4 provides additional information on samples.

81

Table 4. Carbon-14 data on profile from Wilcox outcrop through Keechi Dome to southern edge of East Texas Basin (sample locations on figure 49).

Number on map	State well no.	Aquifer	Screened interval (below land surface)	C^{14} age (uncorrected)	Comments
1	34-49-103	Wilcox	196-260	$11,030 \pm 290$	Shallow outcrop, but may be in discharge zone
2	34-49-806	Wilcox	395-445	$9,120 \pm 100$	Shallow outcrop, but may be in discharge zone
3	38-02-302	Wilcox	1,154-1,192	$21,260 \pm 340$	Near a gas field
4	38-03-701	Wilcox	1,070-1,085 1,105-1,141	$17,860 \pm 190$	Upgradient from Keechi Dome
5	38-11-102	Wilcox	746-756 819-829	$11,230 \pm 480$	Flank of Keechi Dome
6	38-11-603	Wilcox	1,485-1,540	$18,840 \pm 290$	Downgradient from Keechi Dome
7	38-19-303	Wilcox	1,614-1,700	$19,100 \pm 600$	South of Palestine, Texas
8	38-20-604	Wilcox	1,675-1,720 1,753-1,822	$23,420 \pm 1,050$	Just north of Elkhart Graben
9	38-21-705	Wilcox	1,695-1,795	$27,890 \pm 2,890$	Just south of Elkhart Graben

82

PETROGRAPHY AND DIAGENESIS OF WILCOX SANDSTONES

Shirley Dutton

Drill cuttings of Wilcox sandstones from 40 wells show a wide variation in mineral composition. Diagenetic features include calcite cement and rare clay rims and leached feldspars.

Drill cuttings of Wilcox sandstones from depths of 15 to 849 m (50 to 2,875 ft) were sampled from 40 wells in the East Texas Basin (table 5, fig. 50). Porosity, texture, and grain relationships are difficult to observe in cuttings, but mineralogic composition can be determined. Cements can often be recognized in larger fragments.

Wilcox sandstones exhibit a wide variation in composition, ranging between quartzarenite, litharenite, and arkose (fig. 51). Most samples contain about 75 percent quartz and more rock fragments than feldspar. Orthoclase feldspars are more abundant than plagioclase. Some samples contain abundant shale clasts, which may be Wilcox shale that was mixed with the sand during drilling. Carbonate rock fragments and glauconite are locally abundant. Metamorphic and igneous rock fragments constitute about 3 percent of the framework grains.

Minor diagenesis has occurred in these shallow sandstones. Micritic and sparry calcite cements are present in several cutting samples. One indurated sample was available from the Navarro no. 1 Greenwood well in Anderson County. Sand grains are cemented by clay rims, and glauconite composes up to 28 percent of the framework composition. Leached feldspars are present in this sample and in several samples from cuttings.

Similar diagenetic changes have been observed in shallow Frio (Oligocene) sandstones of the Gulf Coast (Bebout, Loucks, and Gregory, 1978). Leached feldspars, clay rims, and sparry calcite cement all formed near the surface and in the shallow subsurface.
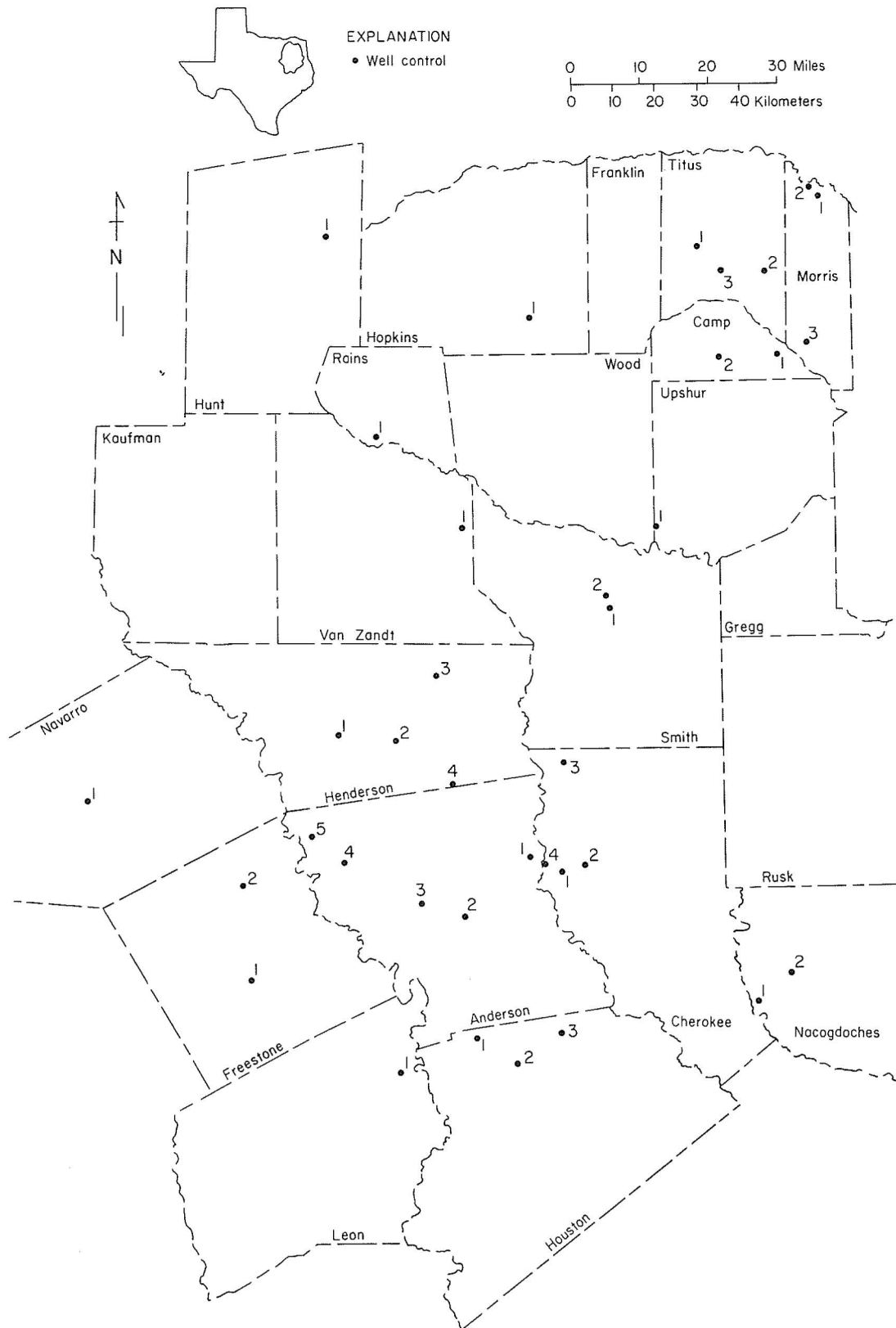
Figure 50. Location of wells in the East Texas Basin sampled for cuttings of Wilcox sandstones. Location numbers refer to table 5.
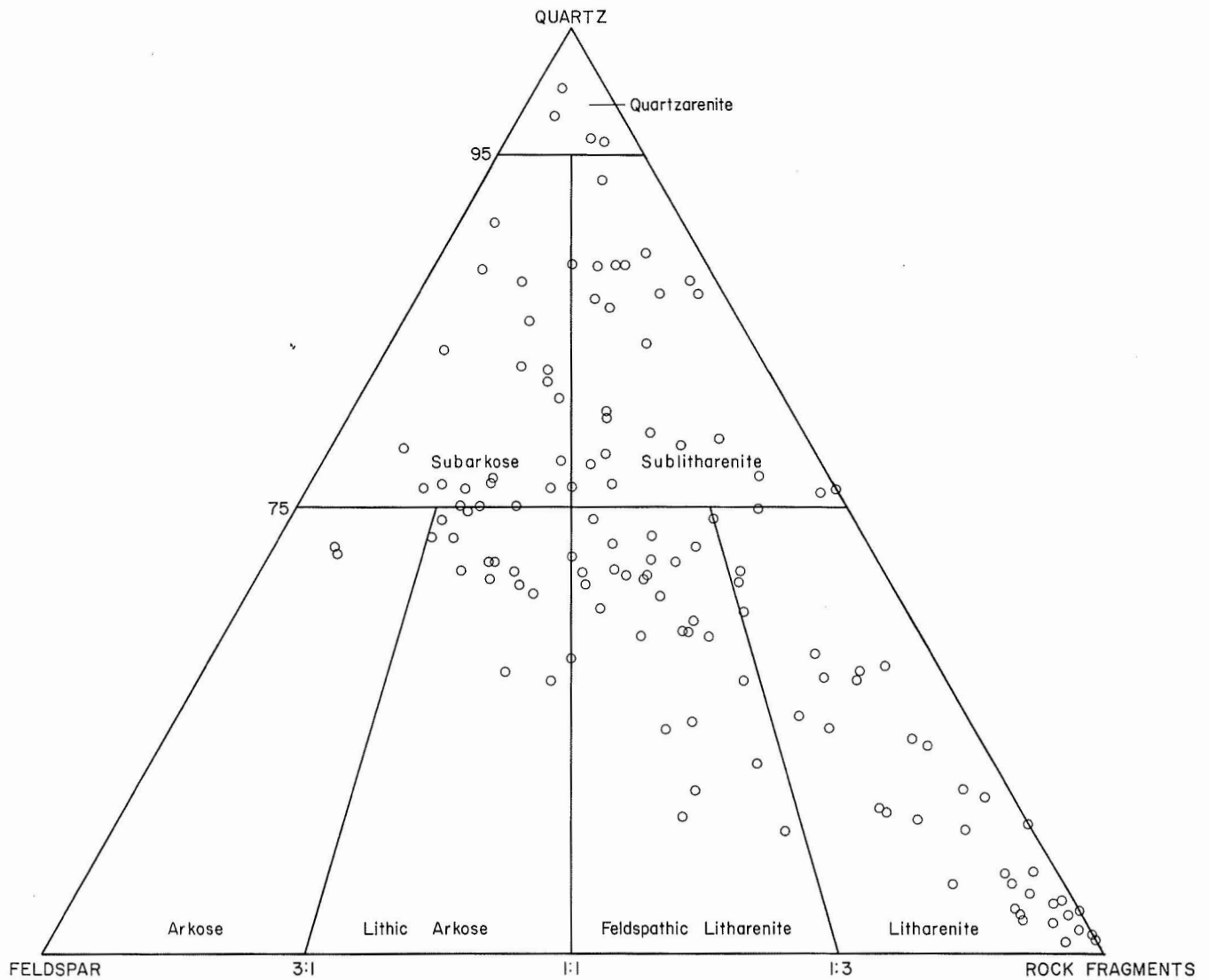
Figure 51. Classification of sandstones from the Wilcox Group using Folk's (1974) classification system.

Table 5. Wells sampled for cuttings of Wilcox sandstones.

County	BEG number	Operator	Well name
Anderson	1	Humble	#1 Lucy Ruff
	2	Layne-Texas	#3 City of Palestine Water Well
	3	Navarro	#1 Greenwood
	4	Texas Co.	#1 Durden
	5	Tidewater-Seaboard	#1 Rampy
Camp	1	Tidewater	#1 Roberts
	2	Stephens & Peveto	#1 Smith
Cherokee	1	American Liberty	#1 Cobb-Holman
	2	Grelling	#1 Batton
	3	Humble	#1B Stephens
	4	Humble	#1 Carter
	5	Humble	#1 New Birmingham
Freestone	1	Byars & Peveto	#1 Riley
	2	Humble	#1 Bonner
Henderson	1	LaRue	#1 Robbins
	2	Stanolind	#1 Dupree
	3	Lone Star Prod.	#1 Allyn Est. "B"
	4	Edson Petr.	#1 Miller
Hopkins	1	Donnie Petr. Co.	#1 Welborn
Houston	1	Jack Frost	#1 Adams
	2	American Liberty	#1 J. A. Bean
	3	Shell	#1 G. E. Dorsey
Hunt	1	Stanolind	#1 Bickley
	2	Humble	#1 Norman
Leon	1	Lone Star Prod.	#1-C Shell-Page
Morris	1	B. Fields	#1 Pruitt
	2	Selby	#1 Browne
	3	C. B. Zuber et al.	#1 G. A. Conner
Nacogdoches	1	Fain et al.	#1 Yates
		Douglas Exploration	#1 Hayter
Navarro	1	Bateman et al.	#1 S. P. Love
Rains	1	Humble	#1 Mainard
Smith	1	Humble	#1 Shamburger
	2	Skelly	#1 Chisum
Titus	1	W. M. Coates	#1 Ben Lackey
	2	Humble	#1 Stevens
	3	Humble	#1 Searcy

Table 5 (continued).

County	BEG number	Operator	Well name
Upshur	1	Carpenter	#1 White
Van Zandt	1	Ellison	#1 Furrh

SURFACE GEOLOGY AND SHALLOW BOREHOLE INVESTIGATIONS OF OAKWOOD DOME--PRELIMINARY STUDIES

Edward W. Collins and David K. Hobday

On Oakwood Dome, Claiborne (Eocene) strata constitute a complex facies association that may indicate that structural uplift was contemporaneous with sedimentation over the dome. Quaternary deposits apparently were not displaced by dome movement, but data are limited. Geomorphic anomalies may reflect recent differential movement.

Claiborne strata are exposed in typical domal configuration over Oakwood Dome (fig. 52). Structural dips of Claiborne units are up to 20 degrees. Superimposed Quaternary terrace deposits appear unaffected by domal structure. A representative north-south cross section of the Claiborne Group (fig. 53) displays about 80 m (262 ft) of domal uplift on the top of the Carrizo Formation. Core descriptions from borehole OK-115 (fig. 55) were summarized on the illustration for lithologic characterization, and paleoenvironmental interpretations were based on studies of cores and local outcrops, on correlation with exposures studied in adjacent areas of Leon, Freestone, and Anderson Counties, and on regional subsurface mapping by Guevara and Garcia (1972).

The Carrizo Formation crops out in stream channels over the central Oakwood Dome area. Sands in the lower part of the formation are interpreted to be upper alluvial plain deposits, whereas the finer grained upper part reflects a lower alluvial plain environment with extensive floodbasins. Thinning of approximately 10 m (30 ft) from borehole OK-115 to borehole OK-102 may indicate domal uplift concurrent with deposition.

The Newby Member of the overlying Reklaw Formation contains abundant glauconite and an open shelf fauna, but a trace fossils assemblage is characteristic of shallow water. Preliminary indications are that the shallowest water may have been situated directly over the dome. The Marquez Member of the Reklaw Formation represents restricted marginal marine conditions. Crevasse splays and small bayhead deltas were sites of coarser grained clastic sedimentation.

The Queen City Formation comprises coarsening-upward, shoal-water, Guadalupe-type delta sequences and polymodally crossbedded marginal marine sand shoals. The basal sand unit thins toward the dome and is a possible indication of the effects of positive topographic expression on sedimentation.

Quaternary terrace deposits crop out over the southern half of Oakwood Dome. They vary from silty clay to poorly sorted sand and gravel. A series of shallow boreholes permits delineation of thickness and lateral extent of these deposits. Although the erosional base of the Quaternary displays minor variations in elevation, the resulting cross sections (figs. 54, 55, and 56) indicate that there is no discernible warping or faulting of the Quaternary deposits.

Three normal faults are visible in outcrop, but these cut only Claiborne strata, which are downthrown away from the dome. Additional fracture zones are common, and a prominent pattern of radial lineaments is probably fault controlled. None of the faults can be shown to displace Quaternary strata, but because of poor exposures and erosional modification of the terrace surface, displacement cannot be entirely discounted.

Certain parts of the dome have been subjected to modern incision; elsewhere on the dome are small, asymmetrical Holocene terraces. These patterns of trenching and aggradation could be a response to minor dome movement. Borehole OK-105 in a floodplain area encountered 10.7 m (35 ft) of modern alluvium. Three hundred meters (1,000 ft) upstream from this locality, Eocene bedrock is exposed. Approximately 1 km (3,400 ft) south of borehole OK-105, ground level resistivity showed that the modern alluvium is 3 m (10 ft) thick. These data suggest thicker sediment accumulation over the dome, which may be explained by climatic variations influencing drainage or change of base level related to solution and collapse of the dome.

Figure 52. Surface geology of Oakwood Dome showing borehole locations.
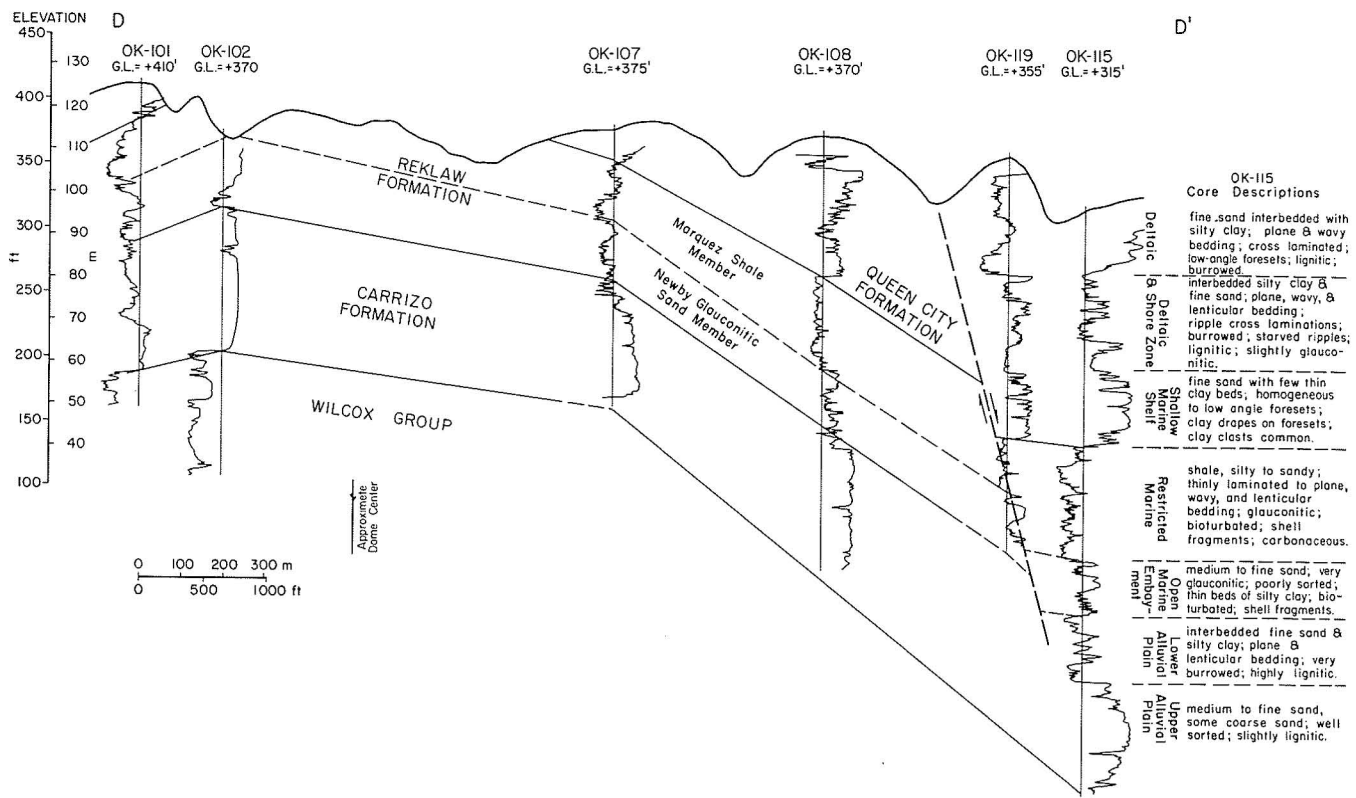
Figure 53. North-south cross section through Claiborne Group over Oakwood Dome.
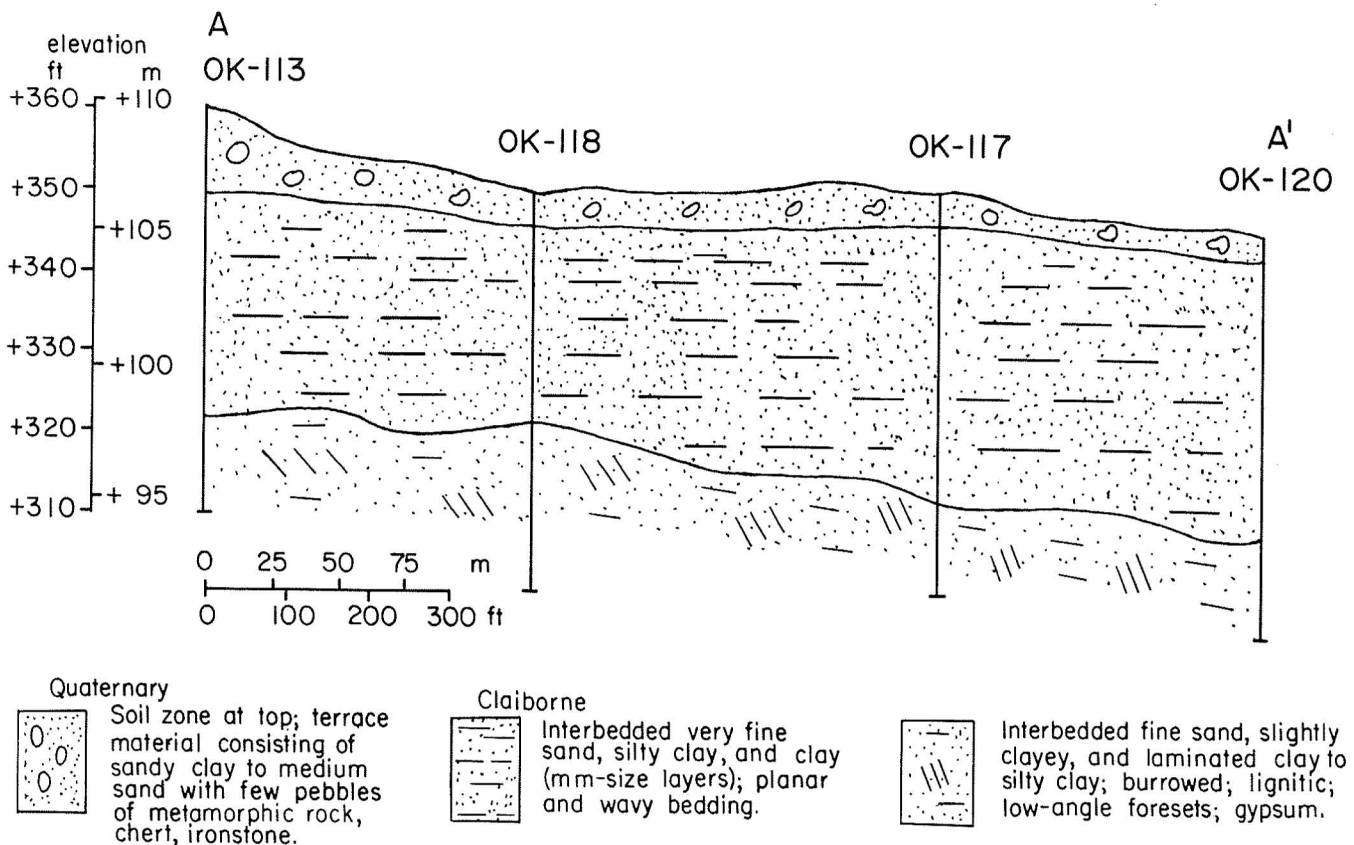
Figure 54. Cross section A-A' through Quaternary deposits.
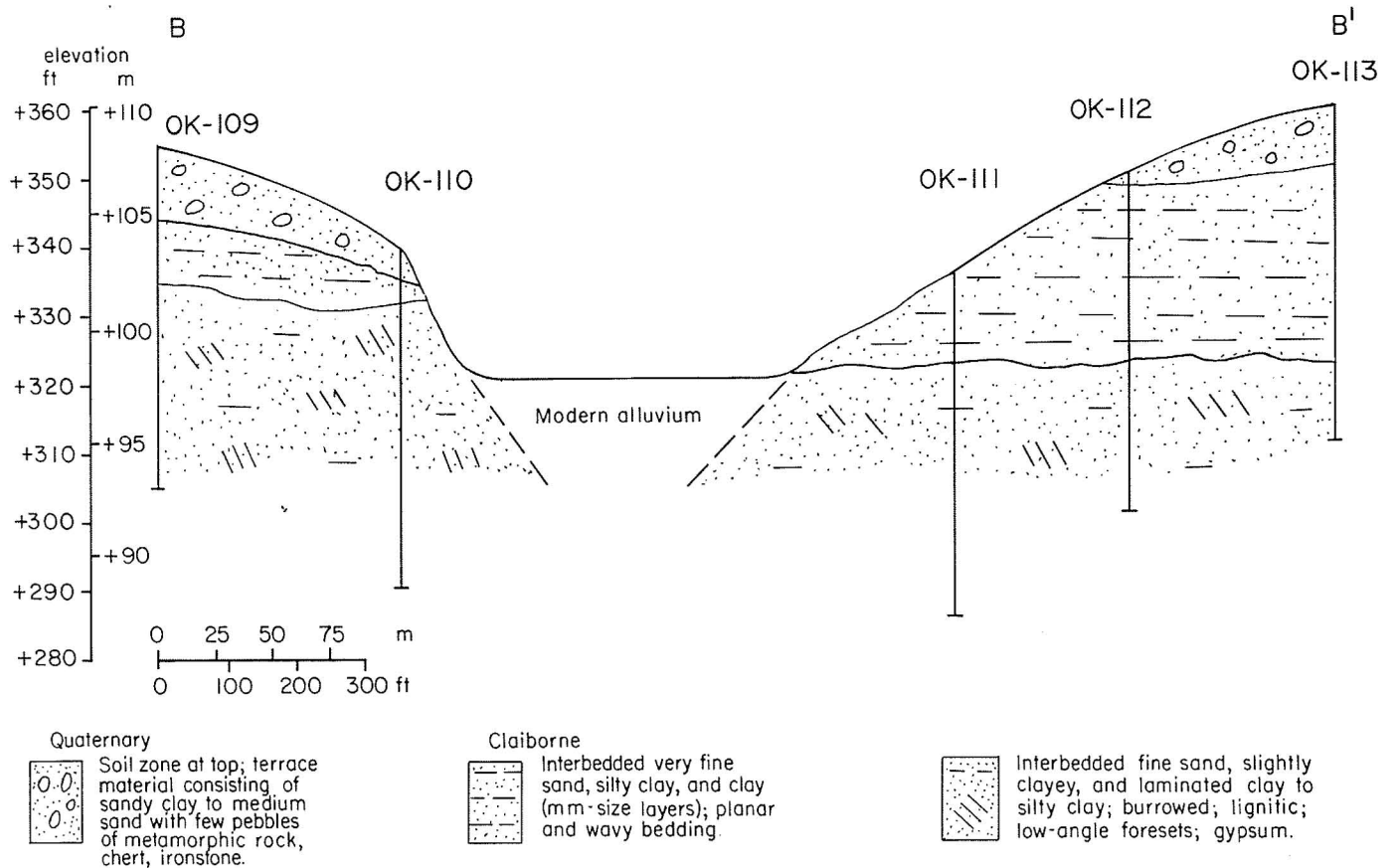
Figure 55. Cross section B-B' through Quaternary deposits.
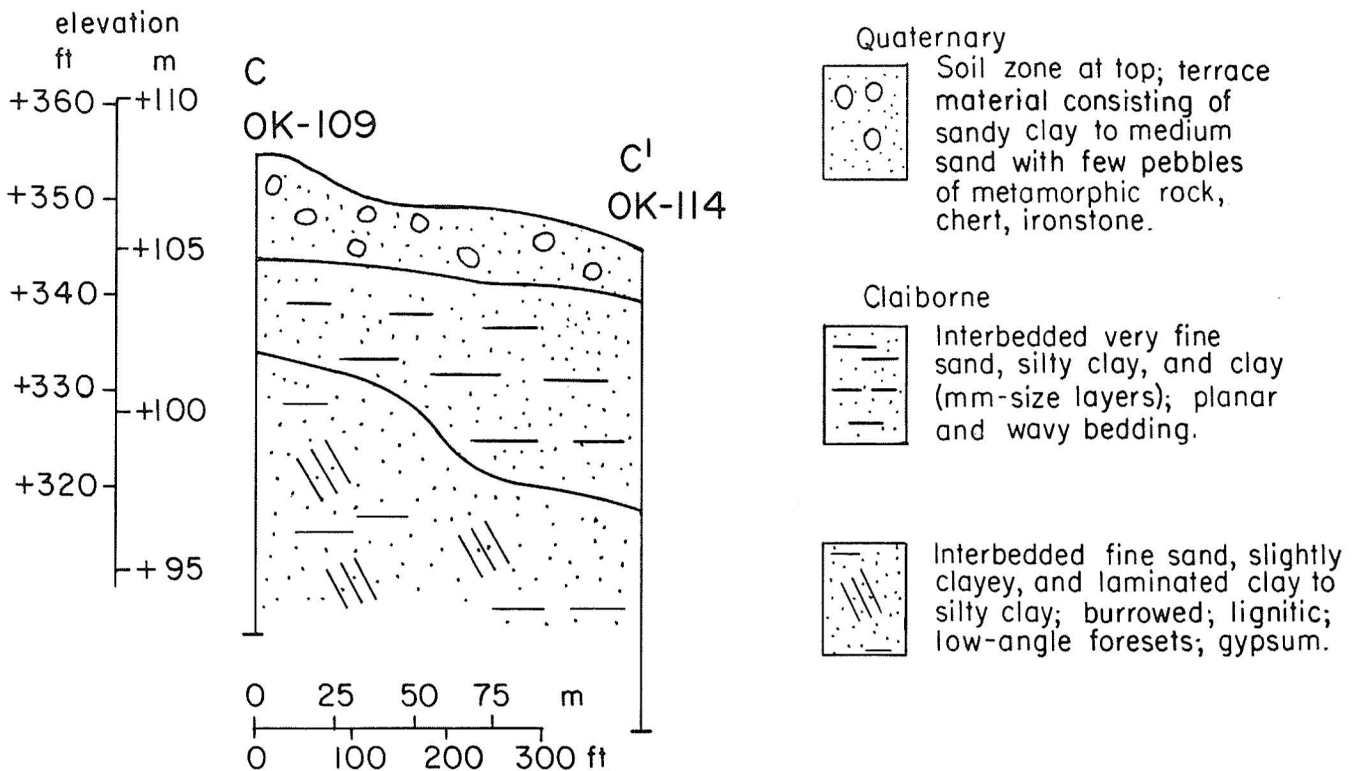
Figure 56. Cross section C-C' through Quaternary deposits.

92

ANALYSIS OF SELECTED STREAM DRAINAGE SYSTEMS IN THE EAST TEXAS BASIN

Owen Dix

The study of link length distributions from drainage basins in the East Texas Salt Dome Basin indicates that four of six salt domes studied are overlain by mature drainage. Two of the domes (Oakwood and Grand Saline) display anomalous link length distributions, an indication that surface movement above these domes has been more recent.

This study was designed to determine whether stream drainage patterns above selected salt domes have been affected by recent movement involving either uplift, graben formation, or solution collapse. East Texas is geologically and structurally suitable for stream drainage analysis since the sediments are flat-lying, the relief is subdued, and the Tertiary formations are similarly resistant to erosion. A number of characteristic drainage patterns are directly related to relief, which is in turn determined by structure, lithology, and vertical movements. These characteristics include drainage density and various link length and link frequency distributions. A link is the fundamental unit of a channel network, and was defined by Shreve (1966) as a section of channel between a source and a junction (exterior link) or between two junctions (interior link).

With a mirror stereoscope, active stream channels were traced from low-altitude aerial photographs (scales ranging from 1:16,900 to 1:25,500). Oakwood, Palestine, Keechi, Grand Saline, Hainesville, and Van Salt Domes were selected for this study. For comparative purposes, 10 non-dome drainage basins were also selected. Each of the non-dome basins is developed on a single stratigraphic unit (either the Wilcox Group, the Queen City Formation, or the Sparta Formation). Drainage patterns over the six domes range from centripetal-annular (Oakwood and Palestine Domes) to subdendritic (Keechi, Hainesville, and Van Domes). Grand Saline displays a centripetal pattern, and the non-dome basins all have dendritic drainage.

Drainage densities over the six salt domes vary from 2.9 km/km^2 (Van Dome) to 5.7 km/km^2 (Oakwood Dome) and generally increase with increasing relief (fig. 57). Mean drainage density for the 10 non-dome basins is 4.1 km/km^2; those basins located on the Queen City Formation tend to have a higher density (4.5 km/km^2) than basins located on the Wilcox Group (4.1 km/km^2) and the Sparta Formation (3.5 km/km^2).

Emphasis was placed on exterior links since these are the most sensitive to variations in the environment (Abrahams and Campbell, 1976). Exterior links have

been subdivided into source (S) and tributary-source (TS) links (Mock, 1971). An S link is an exterior link that combines with a second exterior link, and a TS link is an exterior link that joins an interior link (fig. 58). Abrahams and Campbell (1976) have concluded that these two link types have significantly different length distributions in natural drainage systems. Application of the Chi-square and the Kolmogorov non-parametric statistical tests to the East Texas data indicates that S and TS link distributions are statistically different (at the 0.05 level of significance) over some of the domes studied, and that these link distributions vary according to relief and drainage density as follows:

(1) S and TS links from drainage basins with high drainage densities and relief ratios tend to have the same length distributions. Drainage over Grand Saline and Oakwood Domes falls into this category (fig. 59), as does drainage from one of the non-dome basins. Short links are abundant, and both distributions exhibit high kurtosis. Drainage of this type is thought to be relatively youthful and has yet to undergo extensive stream abstraction. Composition of drainage over Grand Saline Dome may have been affected by the destruction of natural vegetation over a large proportion of the area. Over Oakwood Dome, oil field activities also may have influenced stream drainage.

(2) As relief is reduced, exterior links are abstracted (Abrahams, 1977), and drainage density decreases. This process generally commences at the center of the basin (Schumm, 1977, p. 64-66) and leads to unequal S and TS length distributions (figs. 59 and 60). This difference in length distributions has been attributed to a tendency for TS links to increase in length downstream in association with increased valley size (Abrahams and Campbell, 1976), but may also be controlled by the different topological positions occupied by S and TS links. The S link distribution is essentially the same as that for S links of type (1), but longer TS links are more abundant. Palestine, Keechi, and Hainesville Domes, together with 9 of the 10 non-dome basins fall into this category, which is typical of mature drainage basins.

(3) Where relief is very low, S and TS links again tend to have the same length distributions, but with a considerably greater mean length than type (1) above. This is because of maximum stream abstraction and the uniform size of stream valleys. Van Dome falls into this category (fig. 59). Progression from type (1) to type (3) is shown in figure 61. Figure 62 shows the inverse relationship between relief ratio and mean exterior link length.

These data, therefore, suggest that drainage over Oakwood and Grand Saline Domes is younger than that over the remaining four inland domes. Because of the low resistance to erosion of the East Texas Tertiary sediments, lithology and structure are

not thought to have controlled the nature of these drainage patterns (that is, the drainage is not superposed). This implies more recent surface movement above these two domes. Of the remaining inland domes, link distribution of the Palestine is most similar to the Oakwood type (fig. 59). Evidence of pre-existing topographic highs over Keechi and Hainesville Domes includes the drainage patterns and the presence of encircling areas of higher relief.
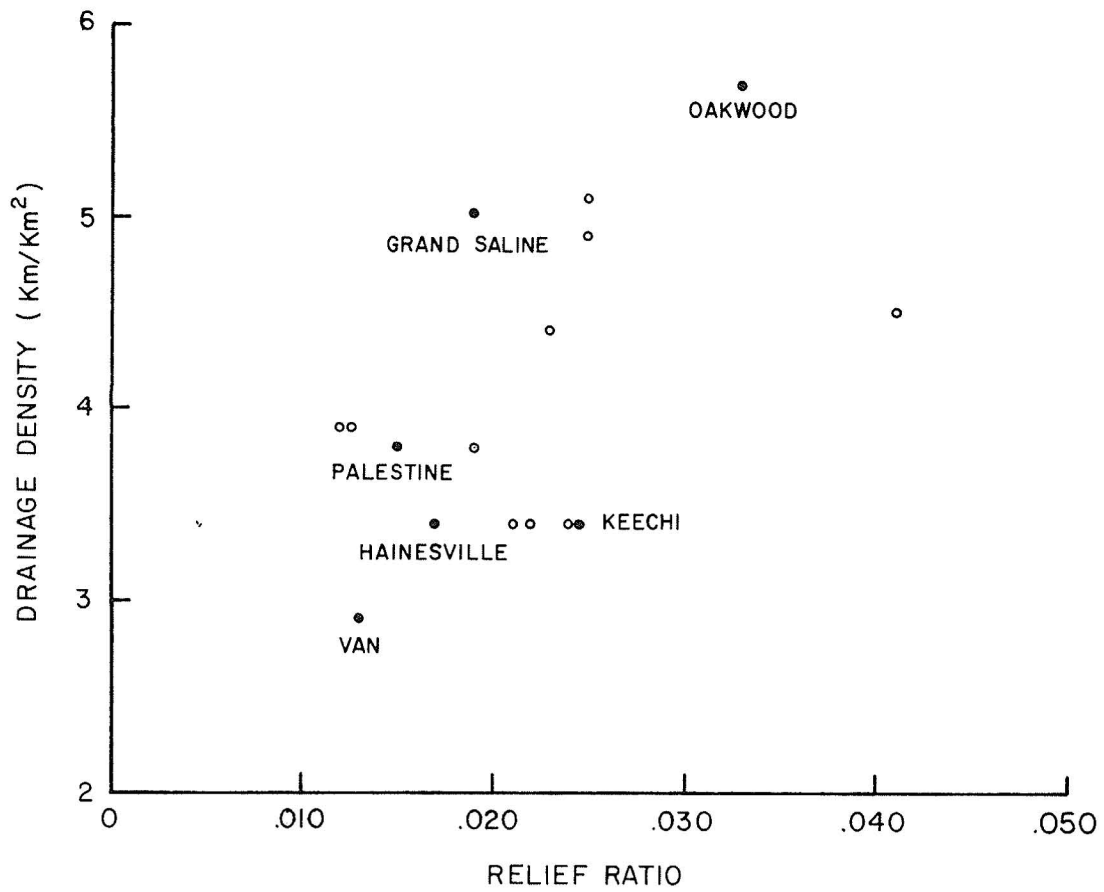
Figure 57. Relationship between relief and drainage density. Solid dots represent domes, and circles represent non-domes.
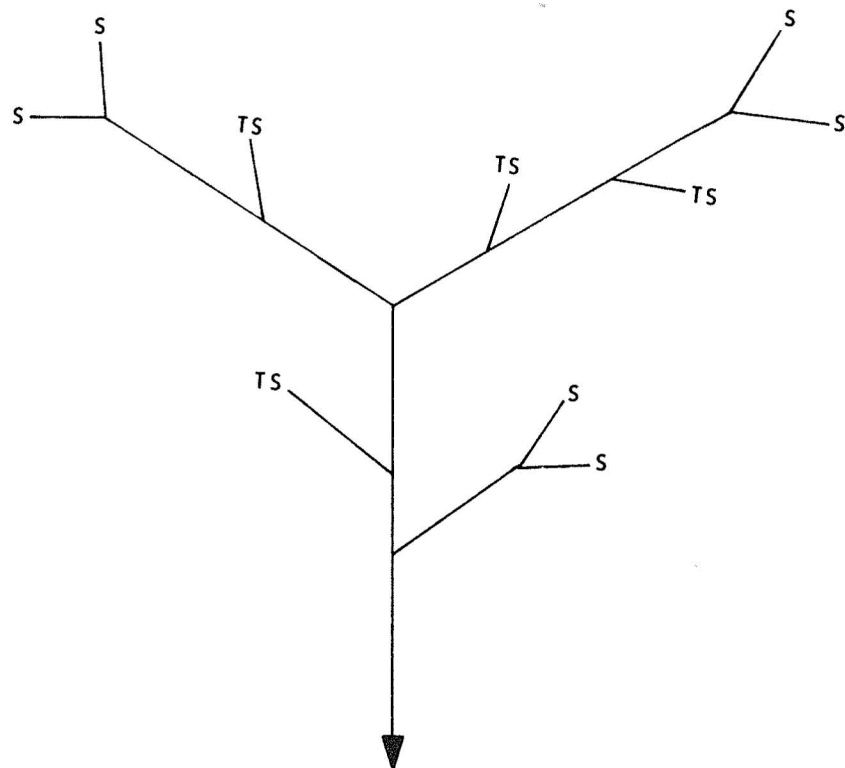
Figure 58. Diagram showing source (S) and tributary-source (TS) links.

96
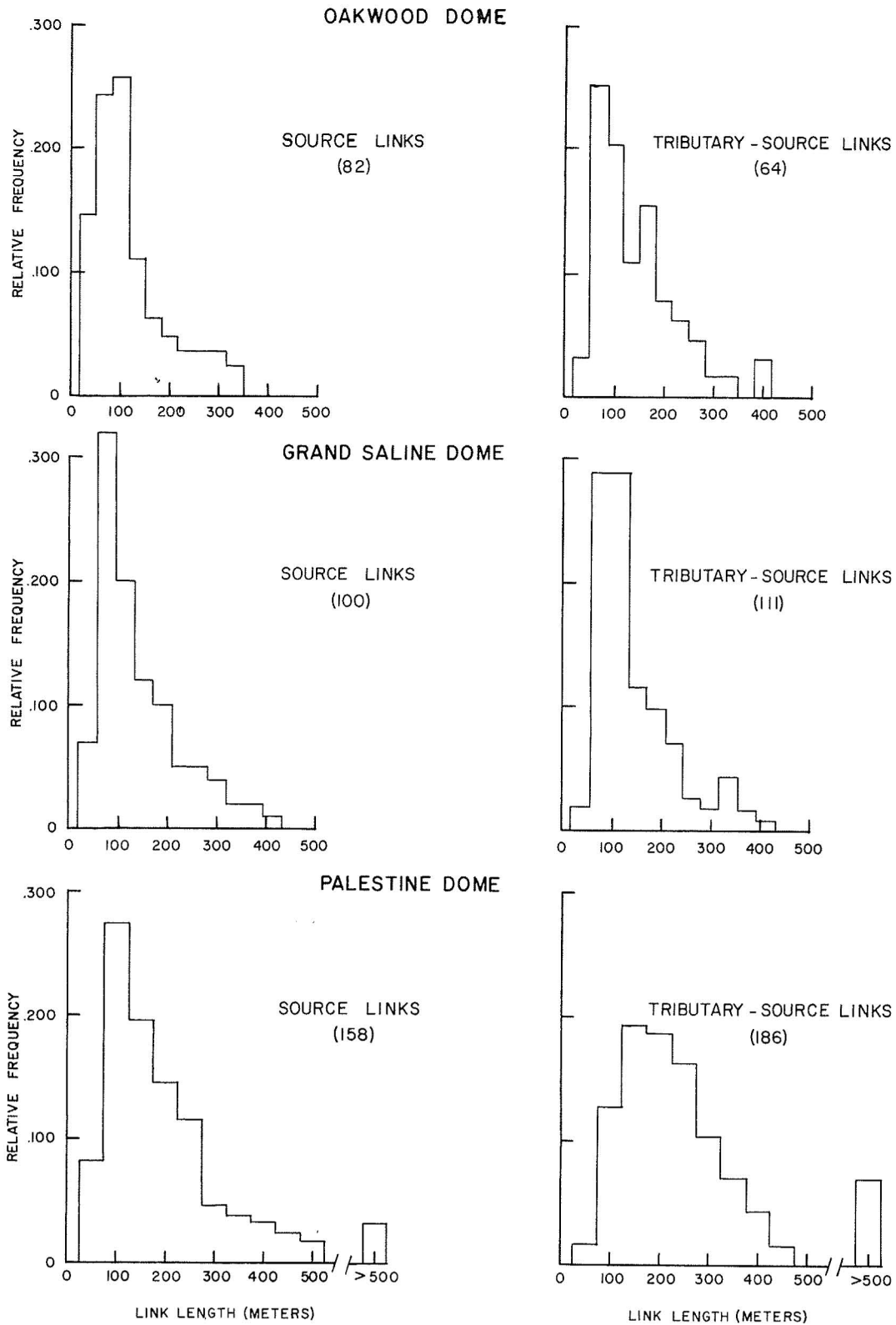
Figure 59. Source and tributary-source link length distributions for drainage basins overlying East Texas salt domes. Numbers in parentheses indicate population size.
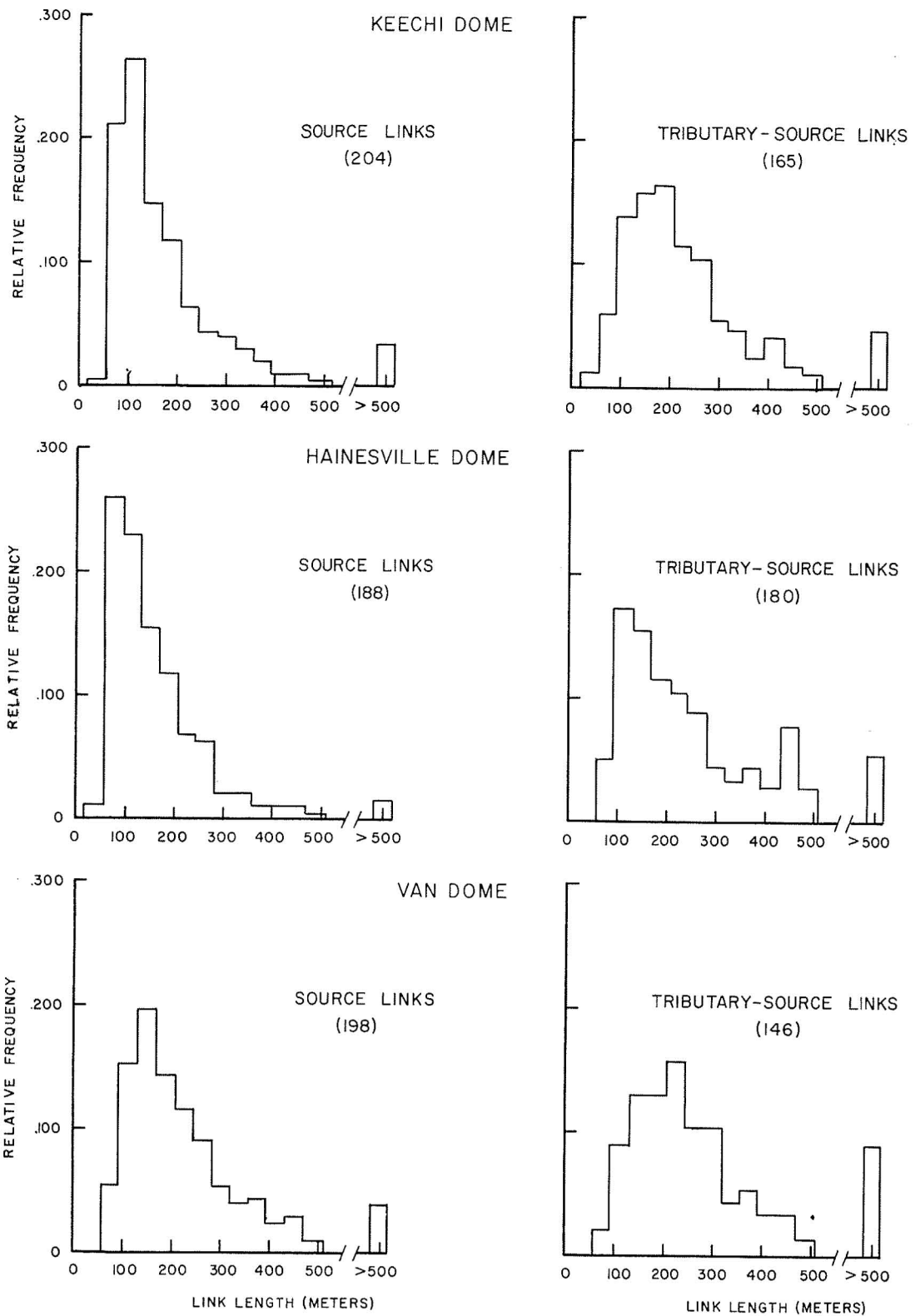
Figure 59 (continued).
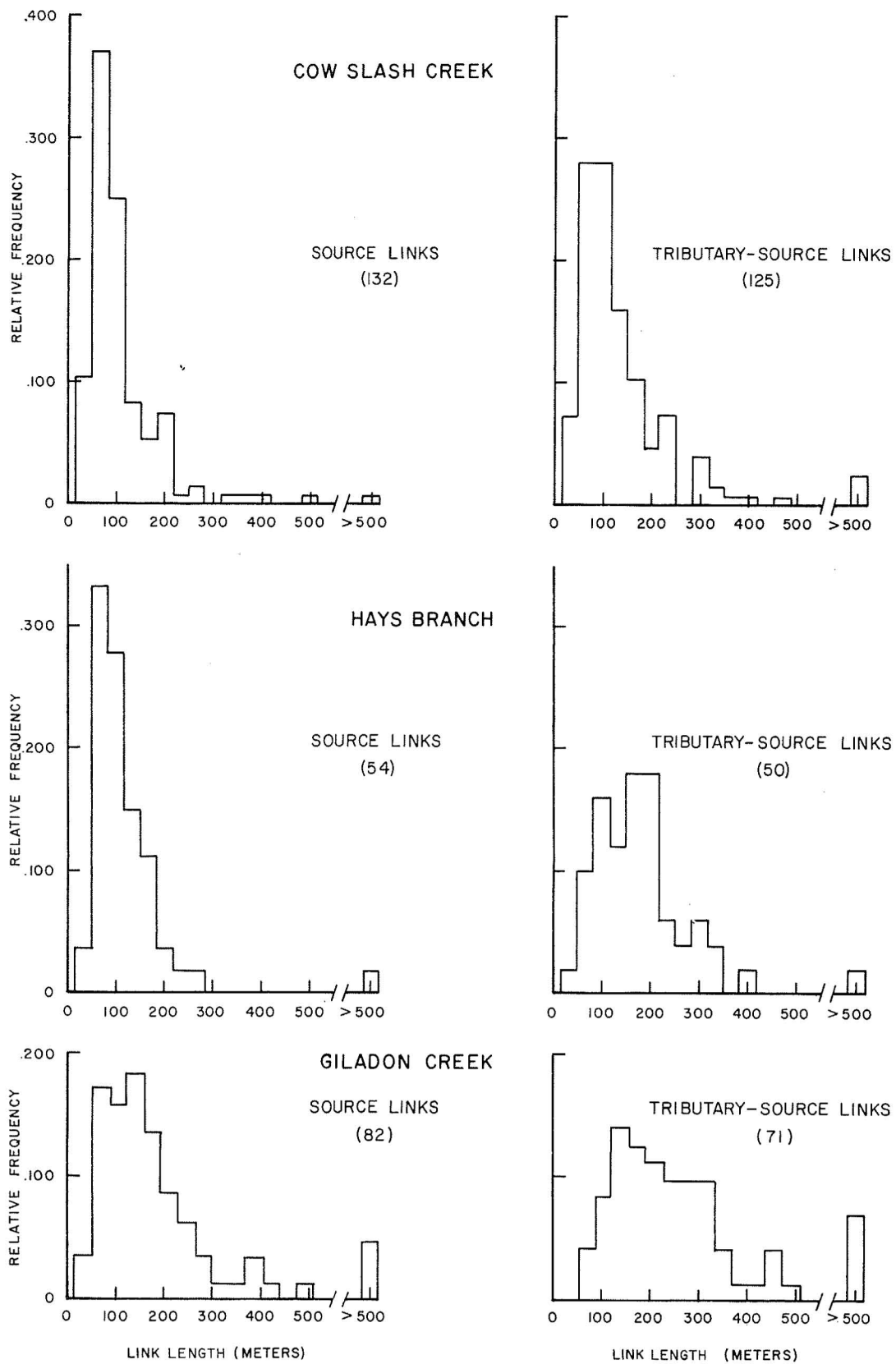
Figure 60. Source and tributary-source link length distributions for non-dome drainage basins in East Texas.
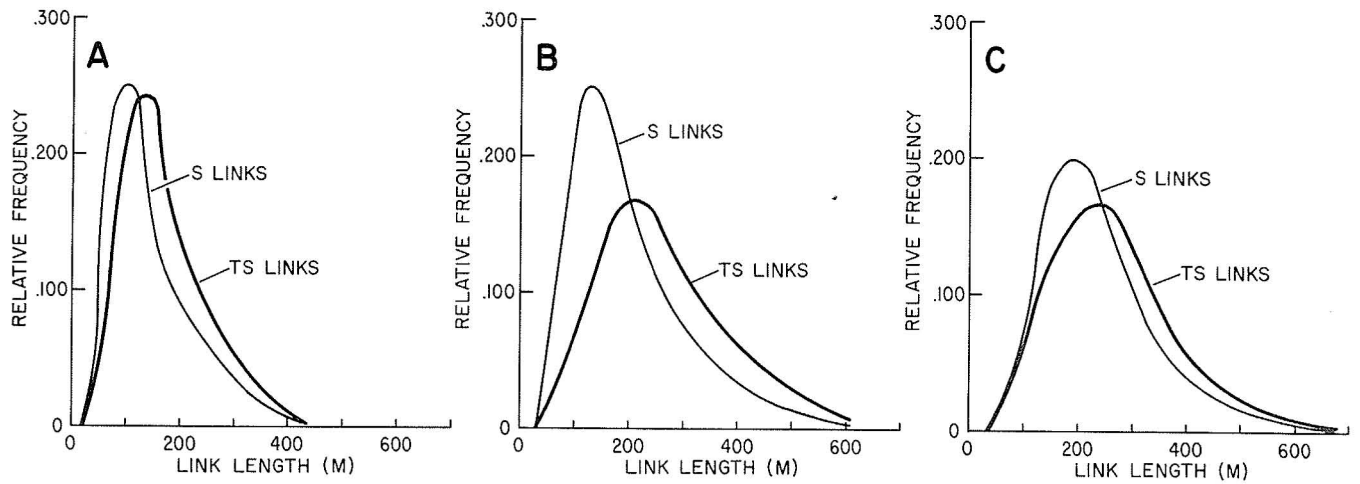
Figure 61. Variation of source and tributary-source links with drainage maturity: (A) high-relief; (B) moderate-relief; and (C) low-relief drainage.
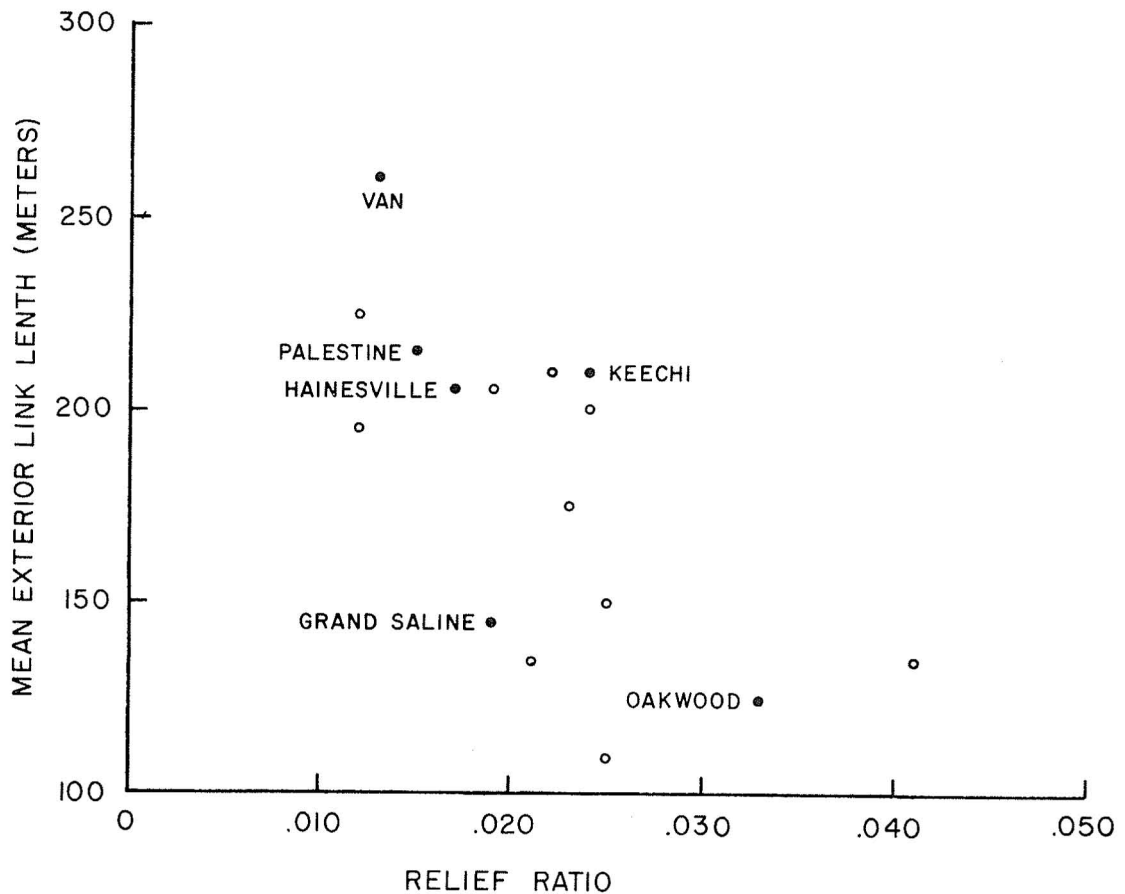
Figure 62. Inverse relationship between relief ratio and mean exterior link lengths.

STUDIES OF LINEAMENTS IN EAST TEXAS

Owen Dix

Low-altitude aerial photographs are being used to identify lineaments in the East Texas Salt Dome Basin. Regional lineament trends are inferred to be related to basement tectonics, whereas modifications to these trends in the vicinity of salt domes probably relate to salt dome structures. The age of such structures is critical.

Lineaments have been defined as rectilinear or curvilinear mappable surface features that reflect subsurface phenomena (O'Leary and others, 1976). Recent studies indicate a close relationship between basement tectonics and superficial structural patterns (Gay, 1973, p. 4; Frost, 1977). To investigate this relationship further, an area of approximately 15,400 km^2 (6,000 mi^2) in East Texas is being studied to determine regional lineament trends and the effects of salt dome tectonics on these trends (fig. 63).

Lineaments are marked on stereoscopically viewed, low-altitude, black-and-white aerial photographs. The lineaments are marked by features such as straight stream channels, changes in topography, and tonal changes. To date, 95 percent of the photographs have been marked and double checked; triple checking is nearing completion. Ultimately each lineament will be given a set of coordinates, and the data will be computerized. As this will be done only on completion of triple checking, an area covered by sixteen 2.3 m by 2.3 m (7.5 ft by 7.5 ft) quadrangles was selected for initial analysis (fig. 63). This study area was divided into a northern subarea containing no salt domes and a southern subarea containing Keechi, Palestine, Oakwood, Bethel, and Butler Domes.

Lineaments range in length from 0.4 to 4.9 km (1,360 to 16,660 ft), the mean being 0.9 km (3,060 ft). Since lineament length is considered important (Frost, 1977), the total length of lineaments within each 10° angular interval has been plotted on rose diagrams (fig. 64A). Mean length of lineaments tends to increase with the total number of lineaments in each 10° interval, which results in an enhancement of peaks when total lengths are plotted (Haman and Jurgens, 1976). Application of the Chi-square one-sample test (Siegel, 1956, p. 42-47) in the northern subarea revealed four statistically significant peaks located on bearings of 030°, 055°, 295°, and 330° (fig. 64B). These four peaks constitute two orthogonal sets (Gay, 1973, p. 3-6), which may represent the regional lineament pattern of the Northeast Texas Salt Dome Basin. The 055° trend, which is better represented here than in the southern subarea, may

have been enhanced by the Mexia-Talco Fault System located approximately 30 km (18.7 mi) to the northwest (fig. 63). It is interesting to note that these peaks agree well with lineament peaks in Precambrian and Paleozoic sediments of the San Saba area (020°, 060°, 295°, 330°) and the Palo Pinto area (030°, 060°, 295°, 345°), Central Texas (Brown, 1961).

A rose diagram for the southern subarea also shows four statistically significant peaks at azimuths of 025°, 060°, 295°, and 325° (fig. 64B). These peaks correspond well to those in the northern subarea, although they are not as pronounced. This is probably the result of interference by randomly and radially oriented boundary lineaments around the salt domes. Furthermore, east-west lineaments are noticeably more abundant in the southern subarea, the quadrangle containing Oakwood Dome having a pronounced peak at 085°. This may be related to the trend of the Elkhart-Mount Enterprise Fault Zone, which has a west-southwest trend east of Oakwood Dome. There is an increase in the number of lineaments around Palestine, Oakwood, and to a lesser extent Keechi Domes. Lineaments over Oakwood Dome tend to be oriented east-west, and the frequency of lineament intersections increases. Over Palestine Dome, the lineaments tend to be radially oriented. However, until data from the entire study area are available for analysis, no additional conclusions can be drawn.
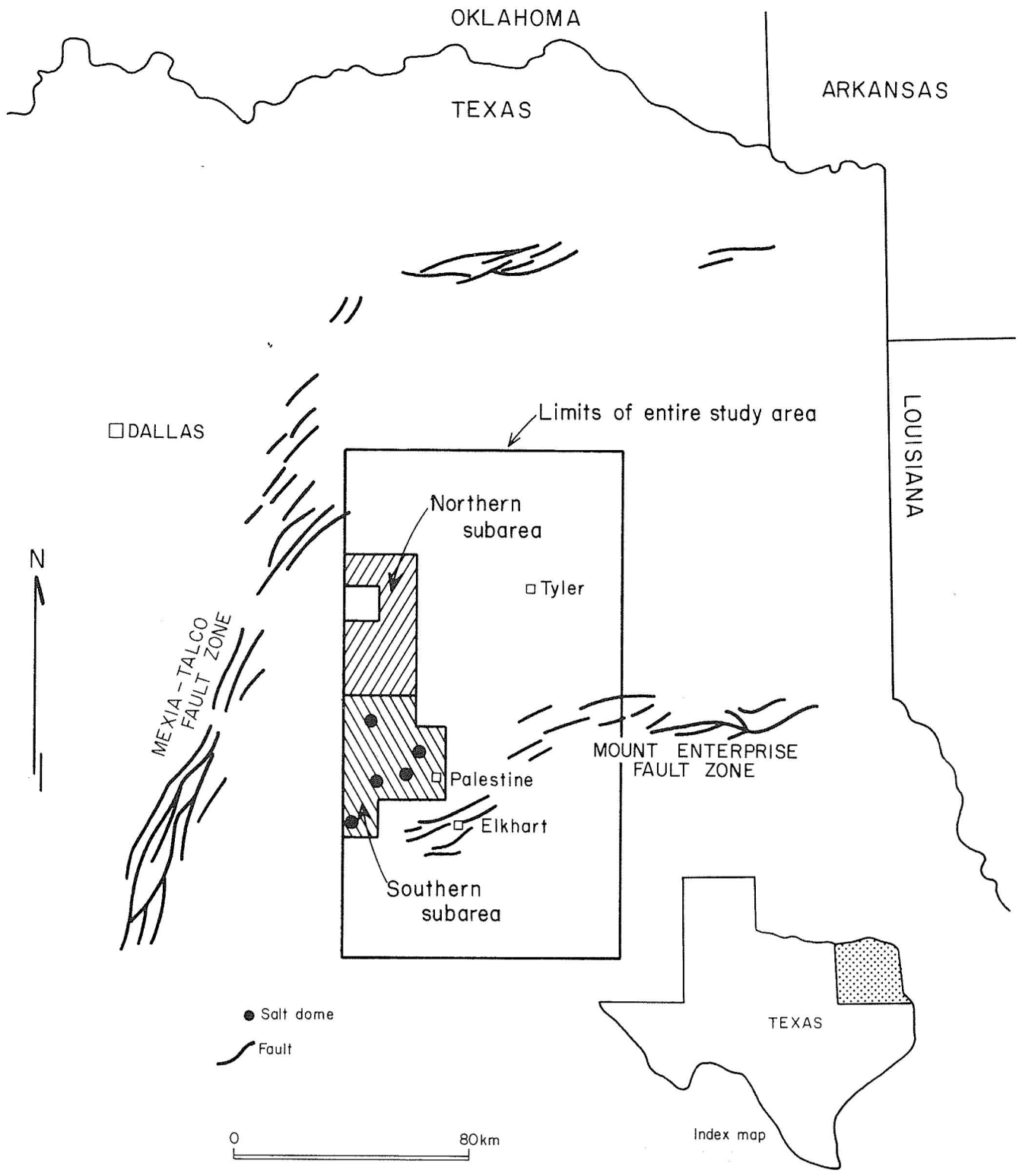
Figure 63. Location map of lineament study area.

A.

60km 40 20 0 20 40 60 km

484 LINEAMENTS

B.

60 km 40 20 0 20 40 60 km
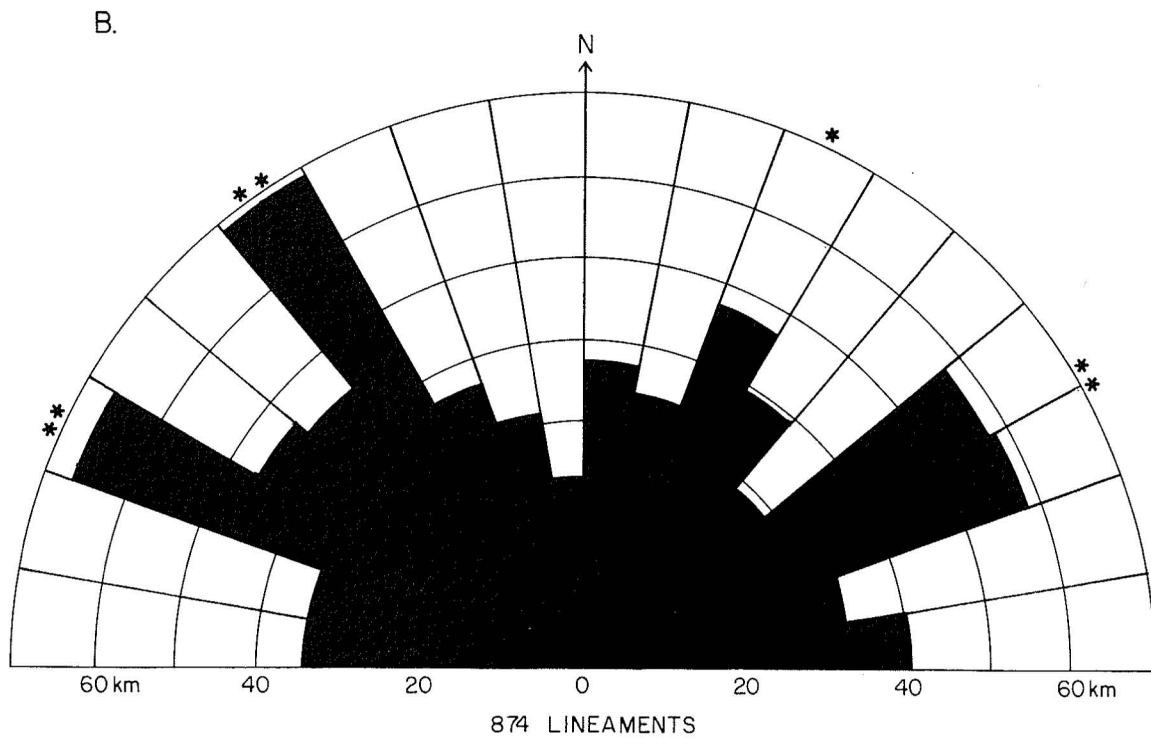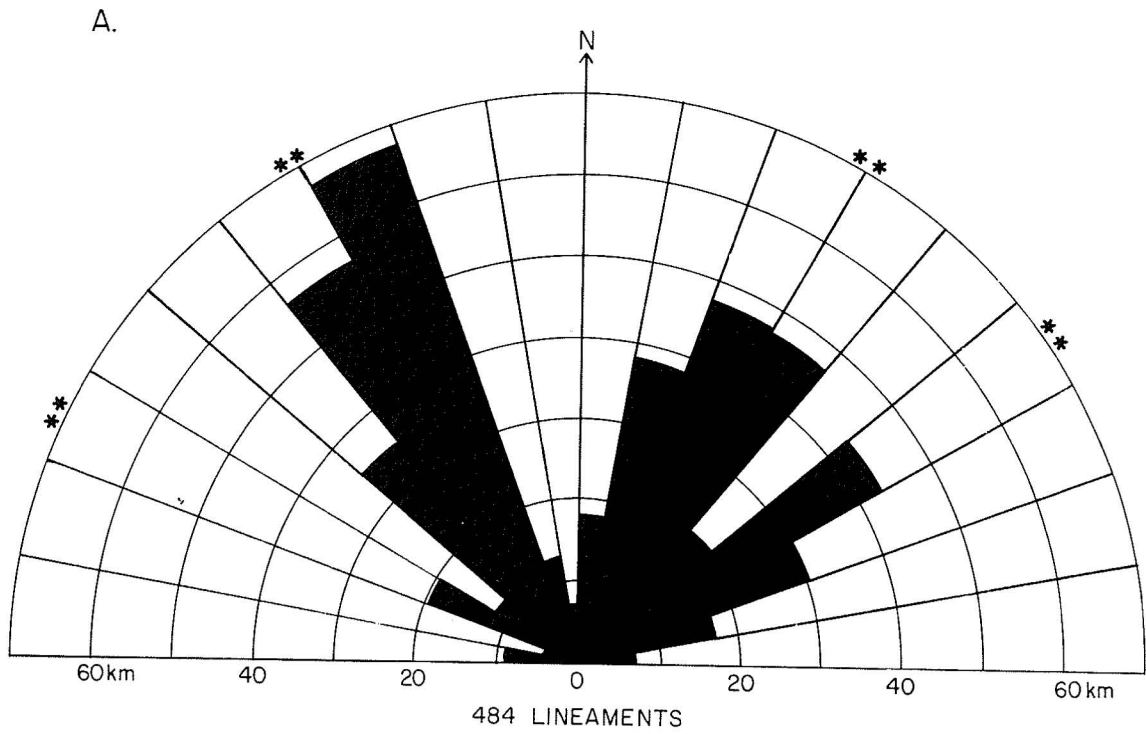
874 LINEAMENTS

Figure 64. Rose diagrams of lineaments using total lengths for each 10° sector: (A) northern subarea; (B) southern subarea. Asterisks represent peak significance; ** = 0.05 level of significance, * = 0.10 level of significance.

THE QUEEN CITY FORMATION

David K. Hobday and Edward W. Collins

The Queen City Formation of the East Texas Basin includes five distinct sedimentary facies: fluvial, deltaic, barrier, tidal delta, and tidal flat. Oakwood Dome may have had topographic expression during deposition and thereby influenced facies characteristics and distribution on a local scale.

Regional patterns of facies distribution were established for the Queen City Formation (figs. 65 and 66) to determine the extent to which salt domes may have influenced the depositional environment and thereby provided information concerning dome growth history. Previous facies studies of the Queen City Formation in the region were carried out by Guevara and Garcia (1972).

Five facies are characterized by distinct assemblages of physical and biogenic structures. In the northwest, an alluvial plain was traversed by rivers of fluctuating discharge and seasonally changing channel geometry, which included both braided and meandering components. Small fluvially dominated deltas developed along the western half of the embayment, prograding across the shallow Weches shelf. Eastward of the area of active deltaic sedimentation were low coastal barriers, which may have formed contemporaneously as strike-fed features, or by subsequent processes of delta destruction. Flood-tidal deltas were deposited on the landward sides of barrier inlets and were particularly widespread during initial phases of marine transgression near the end of Queen City deposition. Inner parts of the Queen City embayment experienced subdued wave activity and enhanced tidal processes and were covered by shallow subtidal sand shoals and broad tidal flats comprising alternating layers of sand and mud.

Although sufficient data are currently unavailable for a definite conclusion, local facies characteristics suggest that Oakwood Dome may have existed as a positive topographic feature during Queen City deposition. This pattern is also emerging in ongoing studies of the underlying Reklaw Formation.
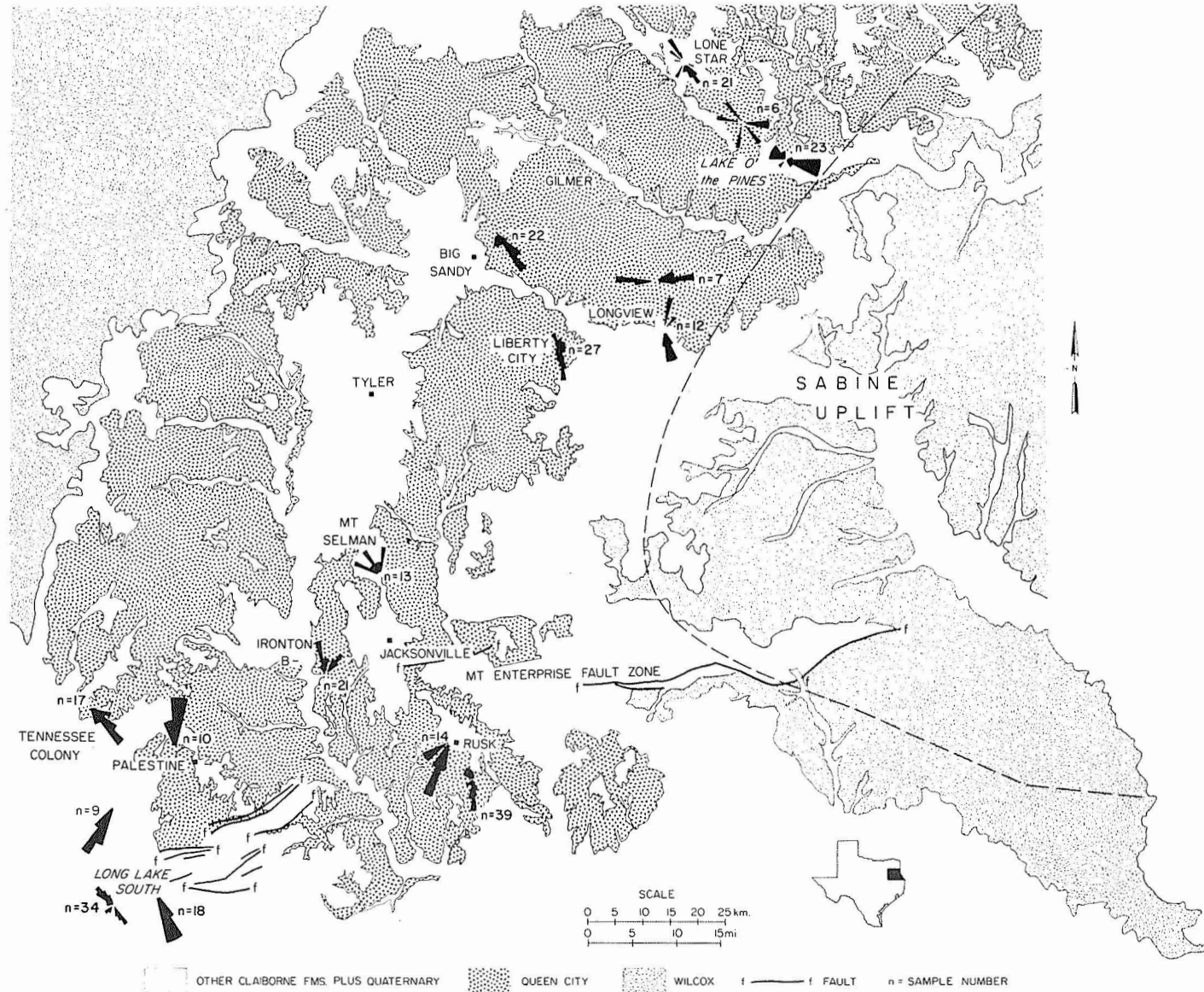
Figure 65. Outcrop area of the Queen City Formation in East Texas; paleocurrent patterns measured at major outcrops.
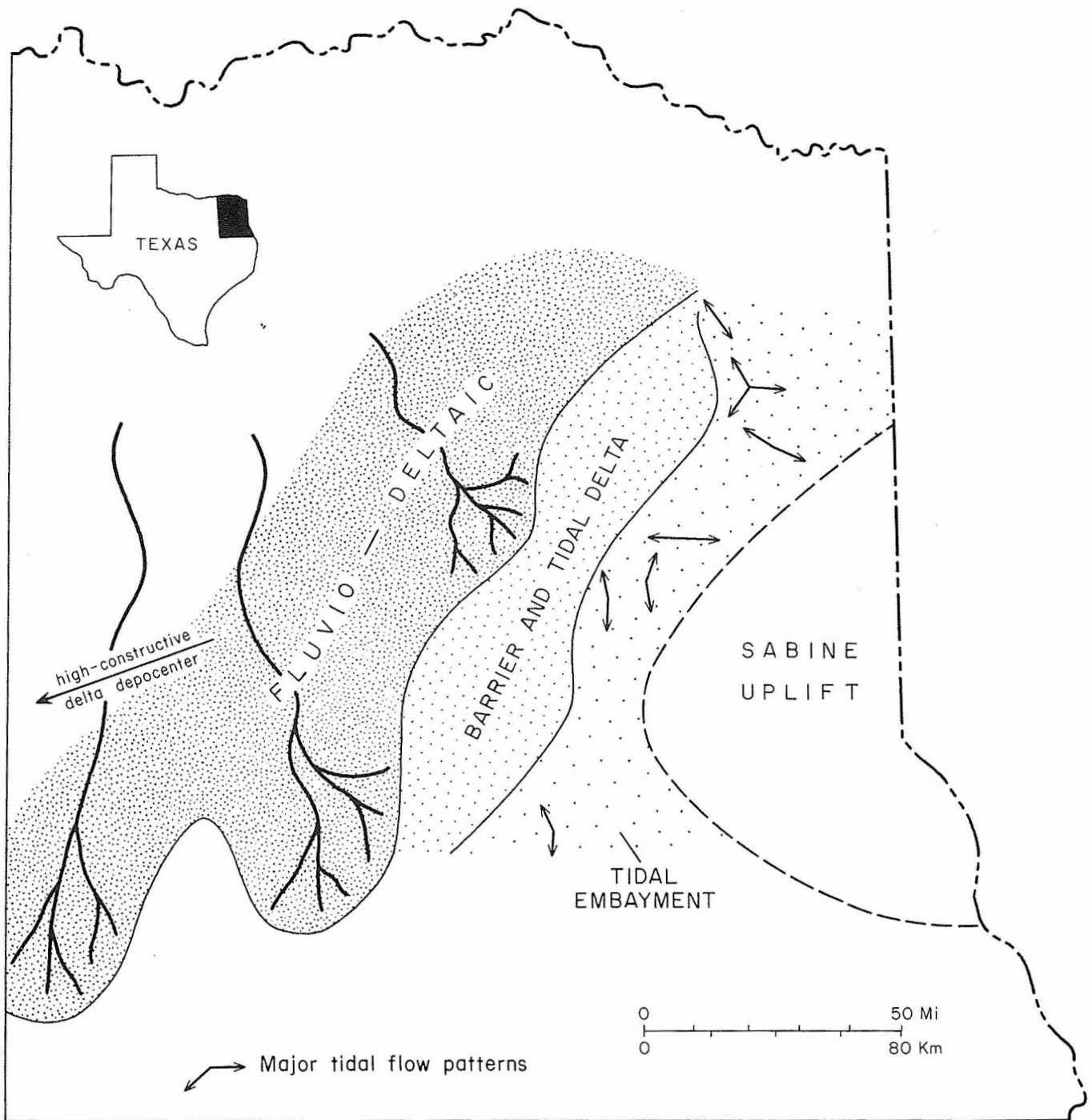
Figure 66. Schematic paleogeographic reconstruction of major Queen City facies in the East Texas Embayment.

ACKNOWLEDGMENTS

REFERENCES

Abrahams, A. D., 1977, The factor of relief in the evolution of channel networks in mature drainage basins: American Journal of Science, v. 277, p. 626-646.

Abrahams, A. D., and Campbell, R. N., 1976, Source and tributary-source link lengths in natural channel networks: Geological Society of America Bulletin, v. 87, p. 1016-1020.

Antoine, J. W., Bryant, W. B., and Jones, B. R., 1967, A hypothesis concerning the origin and development of salt structures in the Gulf of Mexico sedimentary basin: Gulf Coast Association of Geological Societies Transactions, v. XVII, p. 211-216.

Avera, C., 1976, Centennial notebook: Palestine, Texas, Royall National Bank.

Bebout, D. G., Loucks, R. G., and Gregory, A. R., 1978, Frio sandstone reservoirs in the deep subsurface along the Texas Gulf Coast: The University of Texas at Austin, Bureau of Economic Geology Report of Investigations 91, 93 p.

Bondietti, E., 1978, The effect of redox potentials on sorption of radionuclides to geologic media: Proceedings of the Task 4 Waste Isolation Safety Assessment Program, Battelle Pacific Northwest Laboratories, Second Contract Information Meeting, v. 1, EY-76-C-06-1830, p. 379-403.

Brown, C. W., 1961, Comparison of joints, faults, and airphoto linears: American Association of Petroleum Geologists Bulletin, v. 45, no. 11, p. 1888-1892.

Core Laboratories, Inc., 1972, A survey of the subsurface saline water of Texas, Volume 1: Texas Water Development Board, Report 157.

Dumble, E. T., 1891, Anderson County: Texas Geological Survey Second Annual Report, p. 304-305, 315-317.

Eaton, R. W., 1956, Resume of subsurface geology of northeast Texas with emphasis on salt structures: Gulf Coast Association of Geological Societies Transactions, v. V, p. 79-84.

Exploration Techniques, Inc., 1979, Report on gravity modelling for Keechi and Oakwood Domes: Report prepared for Law Engineering Testing Company, Houston, Texas.

Fogg, G. E., Simpson, E. S., and Neuman, S. P., 1979, Aquifer modeling by numerical methods applied to an Arizona groundwater basin: University of Arizona, Tucson, Technical Reports on Natural Resource Systems, Report No. 32.

Folk, R. L., 1974, Petrology of sedimentary rocks: Austin, Texas, Hemphill Publishing, 182 p.

Frost, R. T. C., 1977, Tectonic patterns in the Danish region (as deduced from a comparative analysis of magnetic, Landsat, bathymetric, and gravity lineaments): Geologie en Mijnbouw, v. 56, p. 351-362.

Gay, S. P., 1973, Pervasive orthogonal fracturing in Earth's continental crust: American Stereo Map Co., Salt Lake City, Utah, 124 p.

Granata, W. H., 1963, Cretaceous stratigraphy and structural development of the Sabine Uplift area, Texas and Louisiana, in Report on selected North Louisiana and South Arkansas oil and gas fields and regional geology: Shreveport Geological Society, Reference Volume V, 201 p.

Guevara, E. H., and Garcia, R., 1972, Depositional systems and oil-gas reservoirs in the Queen City Formation (Eocene) Texas: The University of Texas at Austin, Bureau of Economic Geology Geological Circular 72-4, 22 p. (Reprinted from Gulf Coast Association of Geological Societies Transactions, v. 22).

Haman, P. J., and Jurgens, K., 1976, The discovery of the Caroline Arch, Alberta, by lineament analysis: Utah Geological Association, Proceedings of the First International Conference on the New Basement Tectonics, Salt Lake City, Utah, June 3-7, 1974, p. 153-162.

Hightower, M. L., 1958, Structural geology of the Palestine Salt Dome, Anderson County, Texas: University of Texas, Austin, Master's thesis, 83 p.

Hopkins, O. B., 1917, The Palestine Salt Dome, Anderson County, Texas: U.S. Geological Survey Bulletin 661, Contributed to Economic Geology, pt. 2, Mineral Fuels, p. 253-270.

Kaiser, W. R., Johnston, J. E., and Back, W. N., 1978, Sand-body geometry and the occurrence of lignite in the Eocene of Texas: The University of Texas at Austin, Bureau of Economic Geology Geological Circular 78-4, 19 p.

Keys, W. C., and MacCary, L. M., 1971, Application of borehole geophysics to water resources investigations, techniques of water resources investigations of the U.S. Geological Survey: Washington, D.C., U.S. Government Printing Office.

Kreitler, C. W., Wermund, E. G., Guevara, E. H., Giles, A., and Fogg, G., 1978, Preliminary evaluation of salt domes in East Texas for the National Waste Terminal Storage Program: U.S. Department of Energy, 16 p.

Kupfer, D. H., 1970, Mechanism of intrusion of Gulf Coast salt, in Technology of Gulf Coast salt: Louisiana State University School of Geoscience, p. 25-66.

Lyons, R. L., 1957, Geology and geophysics of the Gulf of Mexico: Gulf Coast Association of Geological Societies Transactions, v. VII, p. 1-10.

McGookey, D., 1975, Gulf Cenozoic sediments and structure: an excellent example of extra-continental sedimentation: Gulf Coast Association of Geological Societies Transactions, v. XXV, p. 104-120.

Mock, S. J., 1971, A classification of channel links in stream networks: Water Resources Research, v. 7, p. 1558-1566.

Narasimhan, T. N., and Witherspoon, P. A., 1977, Numerical model for saturated-unsaturated flow in deformable porous media, volume 1, theory: Water Resources Research, v. 13(3), p. 657-664.

Narasimhan, T. N., and Witherspoon, P. A., 1978, Numerical model for saturated-unsaturated flow in deformable porous media, volume 3, applications: Water Resources Research, v. 14(6), p. 1017-1034.

Narasimhan, T. N., Neuman, S. P., and Witherspoon, P. A., 1977, Mixed explicit-implicit iterative finite element scheme for diffusion type problems, volume II, solution strategy and examples: International Journal of Numerical Methods Engineering, v. 11, p. 325-344.

Narasimhan, T. N., Neuman, S. P., and Witherspoon, P. A., 1978, Finite element method for subsurface hydrology using a mixed explicit-implicit scheme: Water Resources Research, v. 14(5), p. 863-877.

Netherland, Sewell, and Associates, 1976, Geologic study of the interior salt domes of Northeast Texas Salt Dome Basin to investigate their suitability for possible storage of radioactive waste material as of May, 1976: Report prepared for the Office of Waste Isolation, Energy Research and Development Administration, Union Carbide Corp., Nuclear Division, 57 p.

Neuman, S. P., in press, Statistical characterization of aquifer heterogeneities: an overview, in Recent trends in hydrogeology: Geological Society of America Special Paper.

Neuman, S. P., and Narasimhan, T. N., 1977, Mixed explicit-implicit iterative finite element scheme for diffusion type problems, volume I, theory: International Journal of Numerical Methods Engineering, v. 11, p. 309-323.

Nichols, P. H., 1964, The remaining frontiers for exploration in northeast Texas: Gulf Coast Association of Geological Societies Transactions, v. XXIV, p. 7-22.

Nichols, P. H., Peterson, G. E., and Wercestner, C. E., 1968, Summary of subsurface geology of northeast Texas, in Beebe, B. W., and Curtis, B. F., eds., Natural gases of North America: American Association of Petroleum Geologists Memoir 9, v. 2, p. 982-1004.

O'Leary, D. W., Friedman, J. D., and Pohn, H. A., 1976, Lineament, linear, lineation: some proposed new standards for old terms: Geological Society of America Bulletin 87, p. 1463-1469.

Patchick, P. F., 1980, The suitability of Palestine salt dome, Anderson County, Texas, for disposal of high-level radioactive waste: Office of Nuclear Waste Isolation, ONWI-74, 35 p.

Powers, S., 1926, Interior salt domes of Texas: American Association of Petroleum Geologists Bulletin, v. 10, p. 1-60.

Relyea, S. F., Ames, L. L., Serne, R. J., Fulton, R. W., and Washburne, C. D., 1978, Batch KD determinations with common minerals and representative ground-waters: Proceedings of the Task 4 Waste Isolation Safety Assessment Program, Battelle Pacific Northwest Laboratories, Second Contractors Information Meeting, PNL-SA-7352, v. 2, p. 259-330.

Schumm, S. A., 1977, The fluvial system: New York, John Wiley, 338 p.

Schwartz, F. W., 1977, Macroscopic dispersion in porous media: the controlling factors: Water Resources Research, v. 13 (4), p. 743-752.

Shreve, R. L., 1966, Statistical law of stream numbers: Journal of Geology, v. 74, p. 17-37.

Siegel, S., 1956, Non-parametric statistics for the behavior sciences: New York, McGraw-Hill, 312 p.

Trusheim, F., 1960, Mechanism of salt migration in northern Germany: American Association of Petroleum Geologists Bulletin, v. 44, p. 1519-1540.

Turk, Kehle, and Associates, 1978, Tectonic framework and history, Gulf of Mexico region: Report prepared for Law Engineering Testing Company, Marietta, Georgia, 28 p.

Vail, P. R., Mitchum, R. M., Jr., and Thompson, S., III, 1977, Global cycles of relative changes of sea level, in Payton, C. E., ed., Seismic stratigraphy - application to hydrocarbon exploration: American Association of Petroleum Geologists Memoir 26, p. 83-97.

Waters, J. A., McFarland, P. W., and Lea, J. W., 1955, Geologic framework of the Gulf Coastal Plain of Texas: American Association of Petroleum Geologists Bulletin, v. 39, p. 1821-1850.

Wood, M. L., and Walper, J. L., 1974, The evolution of the interior Mesozoic basins and the Gulf of Mexico: Gulf Coast Association of Geological Societies Transactions, v. XXIV, p. 31-41.